國 立 交 通 大 學

光電工程學系博士班

博士論文

主動陣列觸控面板與光感測器之畫素電路研究

Study on the Pixel Circuits of Active Matrix Touch Panel and Light Sensor

研 究 生：周祿盛

指導教授：戴亞翔　博士

中 華 民 國 一0二 年 七 月

主動陣列觸控面板與光感測器之畫素電路研究

Study on the Pixel Circuits of Active Matrix Touch Panel and Light Sensor

研 究 生：周祿盛　　Student: Lu-Sheng Chou

指導教授：戴亞翔　博士　　Advisor: Dr. Ya-Hsiang Tai

國 立 交 通 大 學

光電工程學系博士班

博士論文

A Dissertation

Submitted to Institute of Electro-Optical Engineering,

Department of Photonics, College of Electrical and Computer Engineering, National Chiao Tung University

in Partial Fulfillment of the Requirements

for the Degree of

Doctor of Philosophy

in

Electro-Optical Engineering

July 2013

Hsinchu, Taiwan, Republic of China

中華民國 一0二 年 七 月

主動式陣列觸控面板與光感測器之畫素電路研究

研究生：周祿盛　　指導教授：戴亞翔博士

國立交通大學

光電工程學系

摘要

本論文研究如何利用薄膜電晶體元件特性來開發整合觸控面板或光感測器於平面顯示器之相關課題，在元件研究的基礎下，考慮感測器或感測電路在實際情況下所會面臨的問題並提出改善方法。

在觸控感測部分，我們利用了原先在顯示器中造成設計困難的 RC 時間延遲原理，設計出新型觸控感測電路。此利用前後條掃描線所驅動的觸控感測畫素電路上，當人體觸控造成電容值增加時，將使得前後掃描線訊號的開電壓脈衝出現重疊的情況，在此重疊期間，感測電路將會導通並輸出一電晶體開電流等級之感測訊號。故此電路相較於其他主動式觸控感測電路具有大訊號易讀取的優點，對於後端讀取系統的需求度較低，可有效降低整體產品之成本。同時開關電流的訊號比也提供了感測電路對於元件變異性的高容忍度。而當感測電路未被讀取或觸摸時，感測訊號僅為電晶體的關電流等級，此低電流輸出可有效降低整個感測面板之功耗，達到節能的效果。本文詳盡討論各種可能利用 RC 時間延遲概念製成的觸控電路組成，並且嘗試以非晶矽與非晶矽銦鎵鋅氧化物之薄膜電晶體製作此感測電路，以證明此種感測電路技術可適用於不同材料之電晶體製程中。此外，

所提出之感測電路技術亦可適用於內嵌式或外貼式二種結構。對應不同的結構，電路之設計亦有所不同，為此我們提出該感測電路設計的流程，以利於此感測電路技術更快速且有效地應用於平面顯示器中。除了利用此技術製作之 2 吋觸控面板實際驗證電路功能以外，本文並進一步以模擬方式討論此技術應用於大尺寸觸控感測面板之可行性與可能面臨到的問題，結果顯示即使是 42 吋的大型面板，此技術仍可使用。

在光感測應用上，我們分別討論了背光與正光感測應用。傳統非晶矽薄膜電晶體對於背光照射時，受下閘極遮蔽而無光電流反應，且正光照射時只有在元件關區域產生 nA 等級的小電流信號，我們認為它並不適合作為感測元件。此文中我們引進另一種結構，稱為間隙型非晶矽薄膜電晶體。此電路為非對稱結構，在下閘極與汲/源極之一端有一可透光之區域，此區域可作為感光區，使得此種元件在照光時有較明顯的光電流反應。同時此元件可在開區域中具有光效應，較大的感測電流可增加感測電路之訊雜比。文中詳細討論此種元件的光敏感度，找出最適當的操作方式來設計背光與正光感測電路。接著分析在實際應用中可能會造成誤差的因子，包含：元件均勻性、溫度效應、與照光可靠度分析，尤其非晶矽材料對於長時間照光有嚴重的光電流衰退現象，稱為 Staebler-Wronski (SW)效應，若無法校正此效應之影響，則非晶矽材料將很難使用於光感測應用中。文中我們分別針對間隙型非晶矽薄膜電晶體在照光下的電流劣化行為，並提出校正方法與可整合於平面顯示器中的光感測電路。

利用所提出的觸控與光感測畫素電路技術，可使顯示面板多功能化，省去外部元件，以更輕薄化及低成本的方式，來實現具高畫質及互動功能的智慧型顯示器。

Study on the Pixel Circuits of Active Matrix Touch Panel and Light Sensor

Student: Lu-Sheng Chou **Advisor: Dr. Ya-Hsiang Tai**

Department of Photonics & Institute of Electro-optical Engineering,
College of Electrical and Computer Engineering
National Chiao Tung University

Abstract

This dissertation studies the issues about how to develop touch panel or light sensor integrated in flat panel displays using thin film transistors. The possible problems in the practical applications of the sensors and the sensing circuits are discussed and their respect solutions are proposed.

For the touch sensing, the principle of RC time delay on the scan bus, which makes the display design difficult, is applied to invent the new touch sensing circuit. A pair of consecutive scan buses is used to drive the proposed touch sensing circuit. When human touch causes the capacitance increase, the turn-on pulses of the scan bus signals overlap. In this overlapping time, the proposed circuit outputs an ON-level current as a sensing signal when it is touched. Compared to other touch sensing technologies, the touch signal of the proposed circuit is obvious and easy to be read out. Therefore, the cost of the readout IC can be reduced. Meanwhile, the large signal provides the immunity against the device variation. On the other hand, if the pixel is not activated or touched, the output current is at the OFF-level, which can save the power consumption. In this study, the different circuit configurations using RC delay

are discussed. The circuits are further implemented by amorphous silicon (a-Si) and a-IGZO TFTs to prove that the proposed circuit is universal to different kinds of TFTs. Furthermore, the circuit can be adapted in both structures of out-cell and in-cell. For the various conditions of using the circuit, we propose a general design procedure, which can be helpful to apply the circuit in flat panel displays more quickly and effectively. In addition to the demonstration of a 2 inch touch panel to check the validity of the circuit function, we further discuss the feasibility and possible issues in applying the proposed method to large panels by simulation. The results show that the circuit is applicable even for the 42-inch panel.

In the aspect of the light sensing, we respectively discuss the sensing for the backlight and the front light. The conventional a-Si TFT has little photo response to backlight illumination because the blockage of the metal gate, and it only has photo response in the nA order in the OFF region under front illumination. We think it is not suitable to be a photo sensor. In this study, we introduce an a-Si TFT with asymmetric structure, called gap-type a-Si TFT, which has a gap as a sensing region between bottom gate and one of the source and drain electrodes. The gap-type TFTs have obvious photo sensitivity in ON region not only under backlight illumination but under front illumination. The large sensing current can improve the signal-to-noise ratio. The photo sensitivity of the gap-type TFTs are examined to look for the best operation condition. After that, we analyze the error factors for the sensing in real cases, including device uniformity, temperature effect, and reliability under illumination. Especially, the a-Si suffers from a serious current degradation under continuing illumination, which is well known as Staebler-Wronski effect. If the influence of the effect cannot be offset, it will be difficult to use a-Si for light sensing. In this study, we analyze the current degradation behavior of the gap-type a-Si TFT under illumination. The calibration method and the light sensing circuits integrated in

flat panel display are proposed.

Using the proposed touch sensing and light sensing pixel circuits, a flat display can be embedded with multiple functions with no need of extra devices. In this way, the panel can be made in a thinner form and lower cost. A smart display with good image quality and interactive function can thus be implemented.

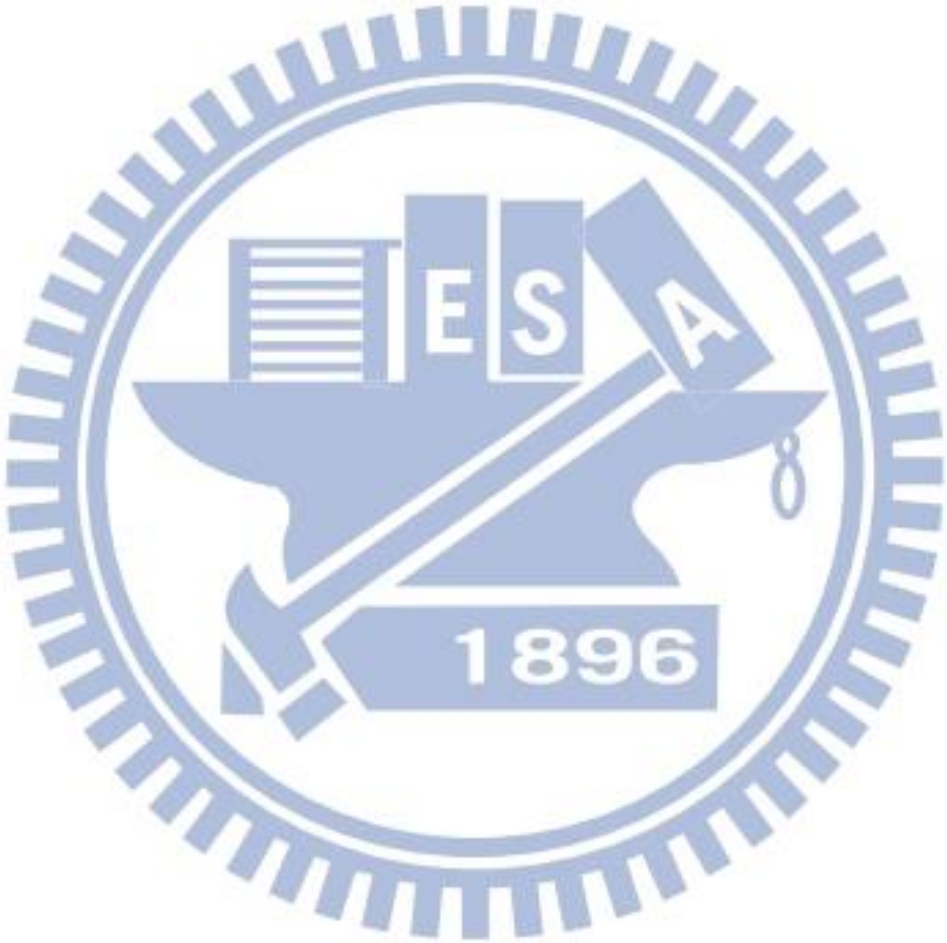

誌　謝

還記得剛考完研究所後回到外婆家，外婆問了我：「祿盛阿，你會不會一直念到博士阿？」當時心想，哪有可能!豈知北上找完教授後，回家便告訴家人我打算攻讀博士。似乎在研究所生涯的開頭，就預告了未來將有著與過往完全不同的思維與訓練。

在完成博士學位的過程中接受了許多人的幫助，最感謝的莫過於我的指導教授戴亞翔老師。感謝老師給予我許多的協助，無論是學術上的研究與心態上的調整及分享，不斷的鼓勵讓我可以慢慢累積養分藉以成長茁壯；更重要的是當我在研究所生涯後半期遭遇到各種困難時，體諒我並給予無數支援，讓我有足夠的能量克服過程中的難題，也給了未來人生不同的啟發。

此外要感謝的老師也包含了同在顯示所的田仲豪老師、冉曉雯老師與劉柏村老師。感謝田老師與冉老師除了學業知識的教授外，在申請博班逕讀時願意給予推薦。此外常從劉老師這邊得到實驗上與其他事務上的協助，也謝謝劉老師願意成為我的口試委員，與其他口試委員包括柯明道教授、張鼎張教授、林志隆教授、陳科宏教授與許鉦宗教授，對於我的研究內容給予許多寶貴的意見。對於同是口試委員的張鼎張教授於研究過程中慷慨的提供我們研究過程中許多資源，讓我的研究可以順利進行，在此也致上我至高的敬意。

承蒙眾多學長姐、同學與學弟妹的幫助，除了研究上有所進展外，也讓我在實驗室的生活可以多采多姿。感謝小黑、首席、國珮、紹文、騰瑞、歐趴的引導

讓我可以很快進入研究生生活。也謝謝贊文、立峯、光揚、家揚學長在行政與論文投稿上的協助。還有同實驗室同甘共苦的夥伴，趴趴、少宏，及大學就當同學一直到博班的耿維，感謝你一路上的幫忙與支持，感謝皓麟、俊文、士哲、彥甫學長給予資源上的協助與學術經驗上的指導。同屆中劉老師實驗室的 Dolly、光廷、俊傑、敬儒與李老師實驗室的品佐、又瑋，有你們這些同學的扶持我才能一路走到現在!

除此之外，也要感謝實驗室學弟幫忙完成許多研究上的成果。謝謝寬達與政哲幫忙完整的研究觸控技術開發與驗證；冠銘、柏成、嘉鴻協助設計 OLED 補償電路；政達、詠暄幫忙 X-ray 感測電路分析討論並協助建立相關量測機台；謝謝君毅在我最後準備論文期間協助處理許多事，讓我可以專心並順利完成論文口試。當然還需感謝其他實驗室學弟妹的幫忙，如品睿、揚順在實驗上也提供我及實驗室所需之幫助。當然受到的幫助遠遠超過在這上面所寫的人，雖無法一一提及答謝，然所受之恩惠銘感於心。

當然不能忘了我的家人還有我的女友詩敏，感謝你們全心全力的支持我，讓我可以無後顧之憂的完成我的學業，追逐人生的夢想，你們對我的恩惠榮耀了我，也讓家人的關係變得更加緊密，謝謝你們!最後，我想將這論文獻給我的外婆，雖然你來不及看到我的畢業，但你將永存我的心中，希望往後我的表現可以令你感到驕傲!

祿盛　2013 夏 於風城新竹

Contents

Figure Captions

Chapter 1

Chapter 2

Chapter 3

Chapter 4

Table Captions

Chapter 2

Chapter 3

Chapter 1

Introduction

1.1 General Background

The development of the twisted nematic (TN) [1] and supertwisted nematic (STN) [2] cell configurations, along with the necessary manufacturing technologies [3~6], resulted in the birth of the LCD industry in the late 1970s and early 1980s. The subsequent development of thin-film transistor (TFT) technology provided a further boost to the industry in the late 1980s [7~8]. The boom was significantly supported by the advancement of material technologies such as the highly reliable manufacturing of liquid crystal base materials, and the development of polymers for the alignment layer, color filter materials, and sheet-type polarizers formed from the poly(vinyl alcohol)-iodine complex [9].

Following the notebook application, in the late 1990s, the TFT LCD is gradually replaced the dominance of the cathode-ray tube (CRT) monitor in TV market [9~10]. At the beginning of the development, the TFT LCD was pursued for the improving in image quality and providing more image information in unit area. The resolution of TFT LCD is required as high as possible. Soon it had not been the only goal since the resolution is corresponding to the need for human vision. Therefore, the manufacturers aimed to scale the TFT LCD up, which can provide more image information on a TFT LCD. After overcoming some problems, such as off-axis image quality, moving picture quality, and reasonable manufacturing yields, the large-area TFT LCD can be fabricated with lower price and gradually erodes the lead of the plasma display panels even in very-large-area display application. However, fostering

the large-area LCD panel should face some questions. The first, the manufacturer needs to build new factory of next generation for large-size glass substrate, which critically raises the investment including the factory building, clean room, and other process facilities. Second, the large LCD panels also raise the technique difficulties in the peripheral equipment or process issues. Besides, building the factory for large-size LCD panels can lower the cost on unit area of panels and increase the competition for market share, but the low product price could be the reason of the deficit if the demand of display panels is insufficient [10]. Furthermore, as the viewpoint of the panel resolution, the display size should be confined by the human vision and other factors such like user space and the environment conditions.

In order to reduce the risk in slack and increase the demand for panels, the TFT LCD is going to the way that integrates sensing technologies and provides more functions for applications. Owing to the participation of sensing technologies, the position of display has been more important and almost necessary for people life, which becomes a main interface to receive the information and response the control signals of user. In addition, the lifetime of the conventional products is often determined by the malfunction of the conventional button for frequent usage. The integration of the sensing technology can effectively solve the problems and grant them the possibility of amazing applications. At present, the touch sensing and the light sensing technologies are prevalent to be applied in TFT LCD especially in mobile devices.

In 2007, Apple Corporation announced the first smart phone which supports the multi-touch function and starts an evolution of mobile phones. After that, touch screen panels (TSPs) have been widely used in other electronic products such like tablet PC, LCD monitor, portable player, etc [11~12]. Fig. 1-1 illustrates the annual growing of TSPs. To meet the rapid and abundant requirement, as shown in Fig. 1-2, an industry

has formed to provide the needed component, driver, or module of TSPs. For the aspect of the structure, TSPs can be mainly categorized into out-cell, on-cell, and in-cell types, as shown in Fig. 1-3. To compare the TSP of different structures, the additional component adhered on the display panel for sensing touch events reduces the contract ratio and brightness [13]. For the aspects of light weight, good display quality, and reducing production cost for touch screen, the in-cell TSPs have much potential to substitute for the out-cell TSPs since the touch sensing circuit of the in-cell TSPs can be integrated into display panel [13~14]. However, the out-cell TSP still dominates in current touch-sensing application due to the lower technique difficulty and higher stability.

The light sensing has been used in TFT LCD for many years. Many applications were studied and revealed including image scanner, fingerprint scanner, and active pixel sensors [15~16]. Recently, light sensing in display is used as an interactive input for 3-dimension touch sensing, which further extends the applied domain of display. In 2006, another light sensing application on console game device for body motion detection was proposed by Nintendo Corporation, Japan. The sensor embedded in the remote controller can detect the infrared to locate the coordinates and then simulate the hand feature and motion. Starting from the proposal, the body motion detection technology is generally applied to the gaming market. Fig. 1-4 illustrates another motion detection using IR detection proposed by Microsoft. However, as can be seen in Fig. 1-4, the detection method needs the additional component. If we can use the TFT as the light sensing device, the light sensor can be integrated into TFT panel so that the product can be simplified and reduces the fabrication cost.

1.2 Review and Motivation

The combination of touch sensing and light sensing technology makes TFT LCD have flexibility and possibility for more interactions between people and products. Even though many researches of them including some commercial products have been revealed individually, there is no effective method to combine the two technologies into an active matrix panel yet. Based on the in-cell TSPs concept, TFT LCD is a potential candidate to integrate the two sensing technology. Besides, in order to extend the application domain, the target should be aimed at the large size interactive display not only at the mobile electronics, which would raise the integration difficulty especially for TSPs.

In this thesis, we would examine the role of TFTs in the two sensing technologies and solve the possible issues when the panel integrates the sensing circuits. For example, if used as a light sensing device, the amorphous silicon (a-Si) TFT suffers serious current degradation under continuous illumination, i.e. Staebler-Wronski (SW) effect. Another case is that the device variation affects the sensing result of the active touch sensing circuit. The device characteristics of the TFTs would be analyzed in the respect of the applications in touch and light sensing. After that, the corresponding circuits would be properly designed and integrated into TFT LCD.

1.3 Thesis Organization

There are five chapters in this dissertation, in which can be summarized in Fig. 1-5. The general background of TFT LCD industry is introduced in chapter 1, which also introduces the applications of touch and light sensing in TFT LCD. In chapter 2, we propose the active touch sensing circuit and design a 42-inch touch panel using our proposal. After that, the light sensing is categorized into backlight sensing and front-light sensing and discussed in chapter 3 and chapter 4, respectively. In the two

chapters, the SW effect under backlight and front light illuminations are studied to find the calibration methods for practical application. Finally, the summarization of all experimental results in this dissertation and the suggestions for the future work are presented in chapter 5. The structure is in the other way listed below for indexing:

Chapter 1 Introduction to Interactive Sensing Technology

1.1 General Background

1.2 Review and Motivation

1.3 Thesis Organization

Chapter 2 Touch Sensing

2.1 Introduction

2.2 Scan Pulse Distortion and Overlapping

2.3 Sensing Circuit Evolution

2.4 Circuit Discussion and Demonstration

2.5 Large Panel Simulation

2.6 Summary

Chapter 3 Backlight Sensing

3.1 Introduction

3.2 Device Property

3.3 Error Analysis

3.4 Backlight Sensing in Flat Panel Display

3.5 Summary

Chapter 4 Front-light Sensing

4.1 Introduction

4.2 Device Property

4.3 Error Analysis

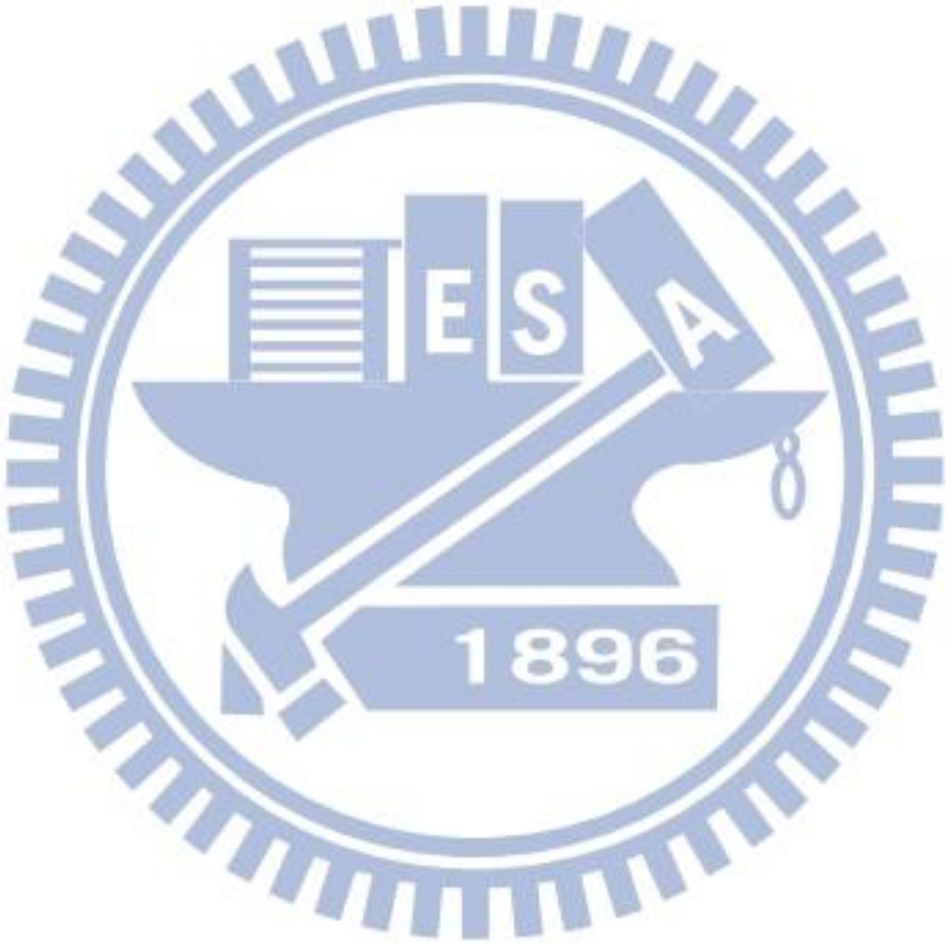

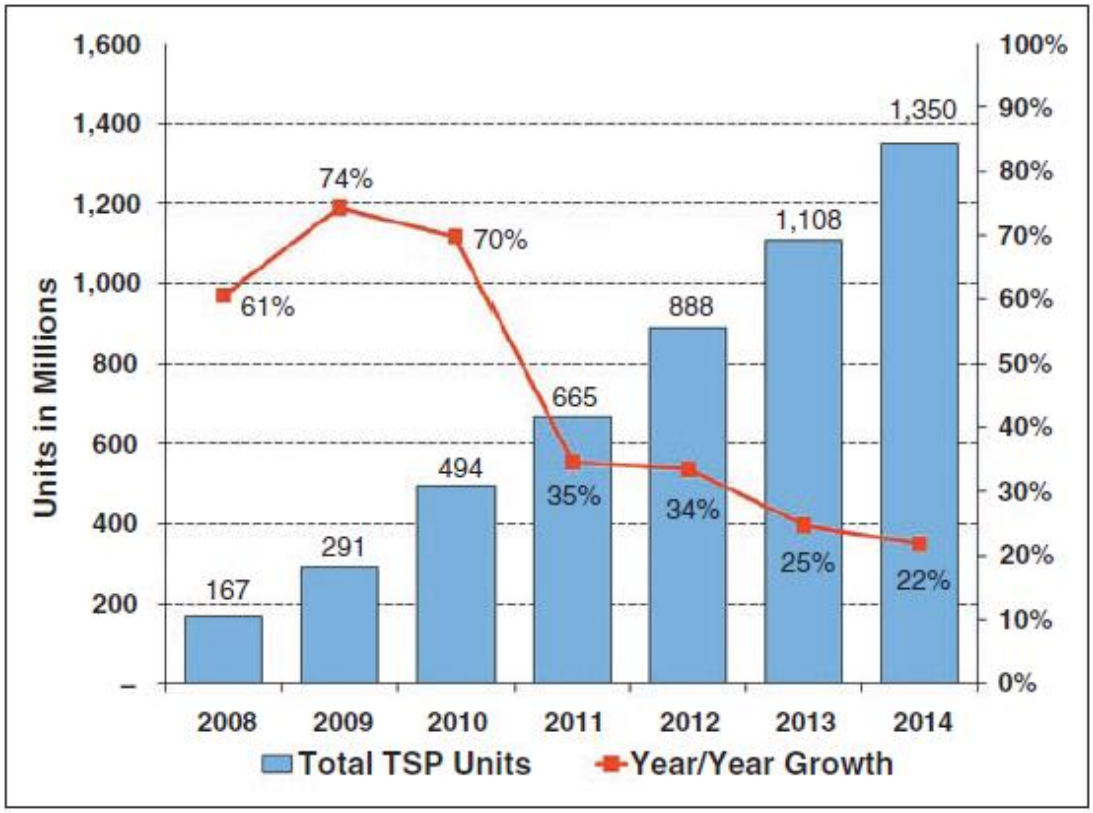

Fig. 1-1 Touch-screen-panel worldwide units forecasted to show year-over-year growth from 2008 to 2014

(*Source: Displaybank* Touch-Screen Panel Market and Issue Analysis, *March 2011*.)

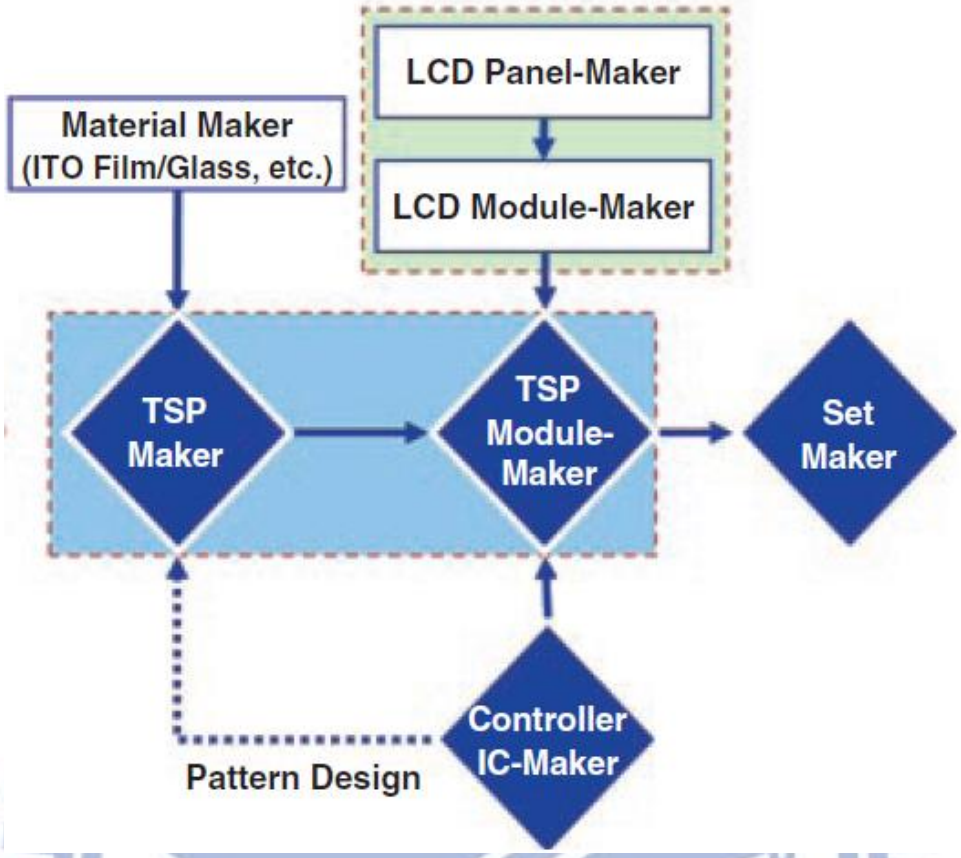

Fig. 1-2 The diagram of the TSP industry

(*Source: Displaybank, op.cit*)

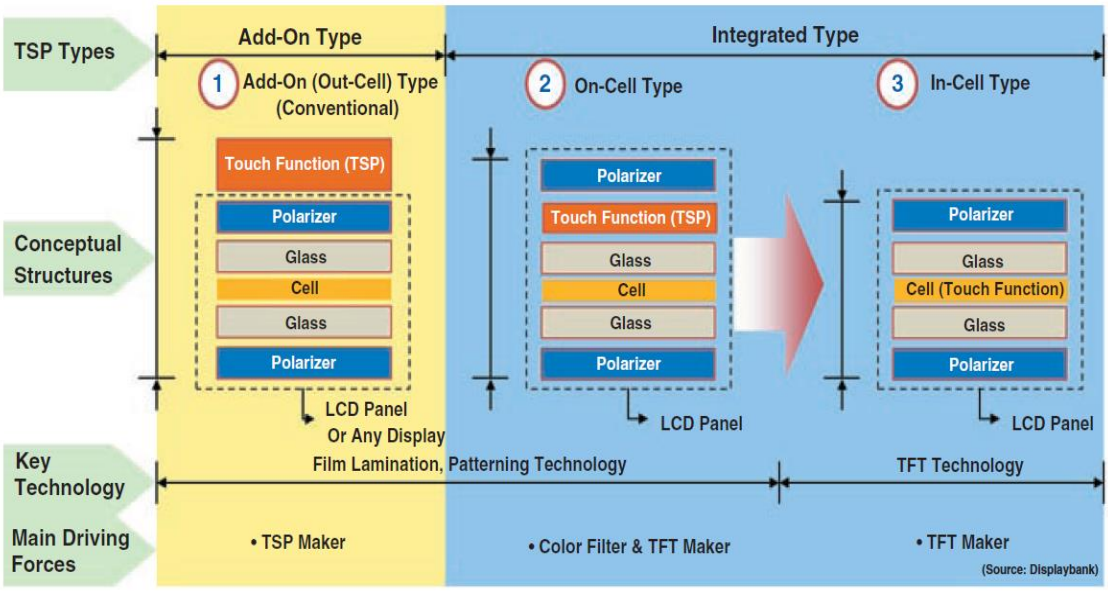

Fig. 1-3 The structure categorization of TSP, which also indicates the difference between the out-cell (embedded) and in-cell (integrated) type TSP
(*Source: Displaybank, op.cit*)

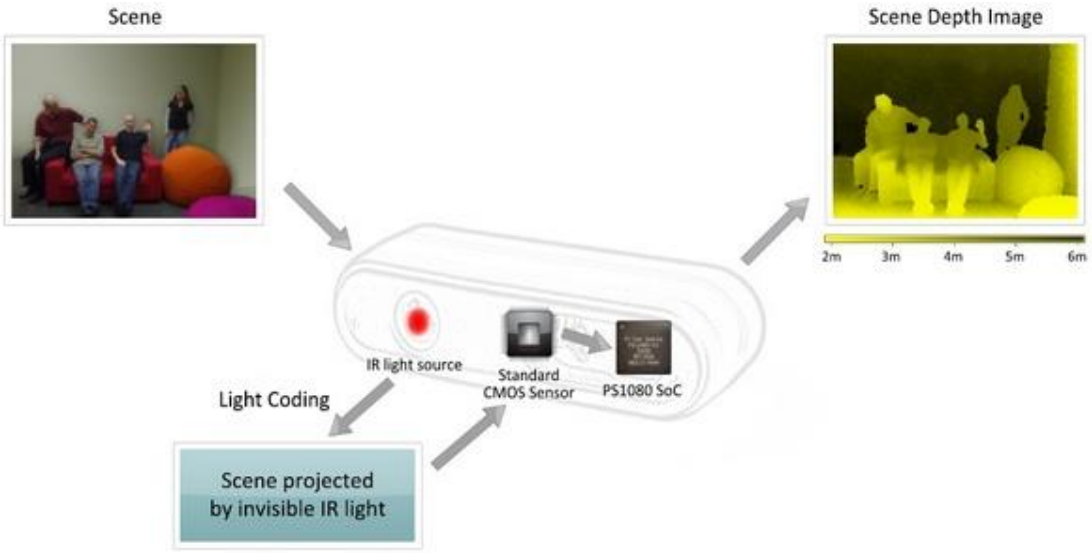

Fig. 1-4 The sensing work on Microsoft Kinect

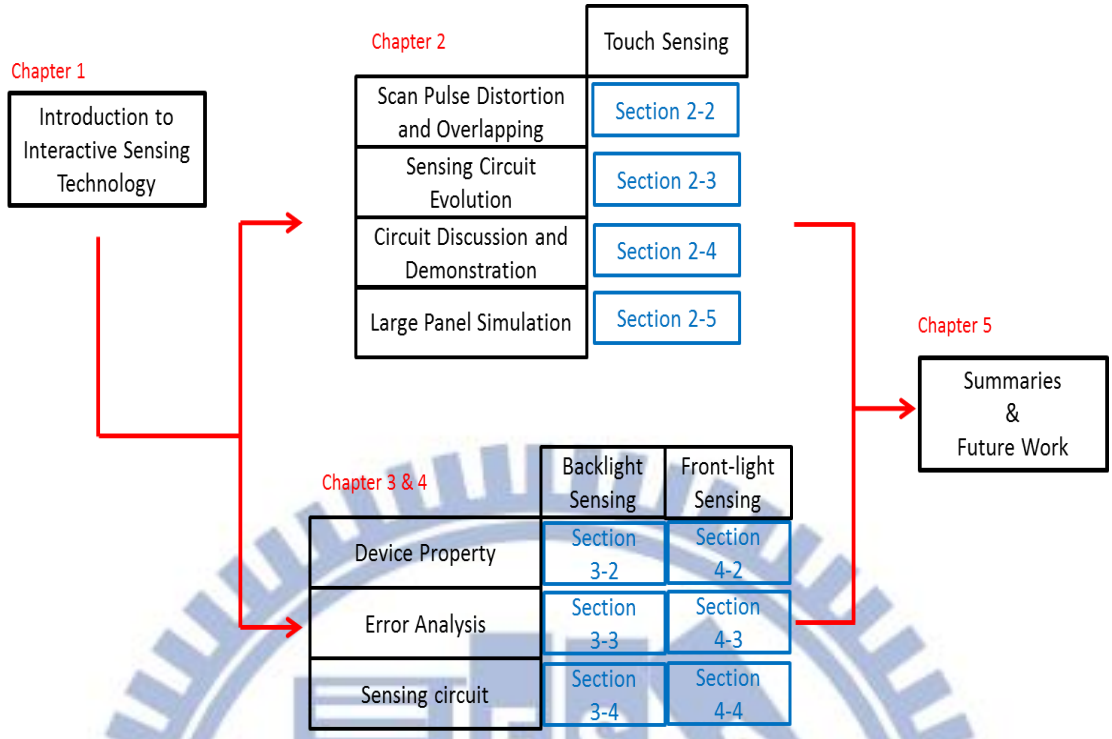

Fig. 1- 5The figure of this dissertation structure

Chapter 2

Touch Sensing

2.1 Introduction

In addition to the structure difference, as shown in Fig. 2-1 [17], TSPs have various sensing methods mainly including resistive [14,18~20], capacitive [13,21~26], and optical sensing [27~29]. The same type TSP in both of in-cell and on-cell structure faces some identical problems. Photo detection touch sensors have been revealed to be sensitive to the ambient light, which easily causes sensing noise, since they determine the touch signal using the light reflection or absorption. For resistive touch sensors, although they have the advantage of low cost, the poor reliability lowers their potential for the application in high-valued productions. Comparing to the two types touch sensors, the capacitive touch sensors are dominant in most high-valued products benefiting from the merits of high reliability, high sensitivity, and easiness for multi-touch sensing. However, they suffer some problems for large size touch panels. The touch signal of the capacitive sensor is determined by the output current difference between touch and untouched event [25~26]. The signal gets distorted by the parasitic resistance and capacitance on the signal bus in a large size panel, which makes the readout ability of the external circuit become more critical for large area application.

Moreover, in addition to above identical problems, the in-cell TSPs using thin film transistors have extra issues as following description. Firstly, in order to increase the open ratio, source follower is usually adapted to buffer the voltage signal to the read out bus. Nevertheless, as a unity-gain buffer, the source follower cannot amplify

a small voltage signal. Second, because of the threshold voltage difference between the input and output of a source follower, a sensing error can be arisen from the threshold voltage variation of thin film transistor (TFT) devices. Furthermore, whether pixels are touched or not, the source followers consume power to put out the sensed voltages, which power should be further reduced.

In this work, we want to discuss a novel active touch sensing circuit, which can be implemented in on-cell and in-cell structure. Meanwhile, it can effectively overcome the above mentioned issues for large-area in-cell TSPs.

2.2 Scan Pulse Distortion and Overlapping

In display, the original scan signal is given as a pulse, which is shown in Fig. 2-2. When the N_{th} scan pulse turns off, the $(N+1)_{th}$ scan pulse becomes turn-on immediately. As we know, there are some parasitic resistances and capacitances on the scan line. When a scan pulse propagates on the scan line, it gets distorted by the parasitic resistances and capacitances, so that the pulse at scan far end has delay with a RC time constant, and its shape is shown in Fig. 2-3. In Fig. 2-3, we can see that as the N_{th} scan pulse not completely turning off, the $(N+1)_{th}$ scan pulse starts to turn on. It causes there a temporary pulse overlapping which keeps TFT turned on when the new data comes on to the shared data bus. It causes the error of the pixel voltage and it is not what we want to see in display. On the contrary, in the proposed touch sensing circuit, we intentionally use the TFT ON current which is induced by pulse overlapping to detect whether pixel is touched or not.

2.3 Sensing Circuit Evolution

2.3.1 2T1R1C Pixel Circuit

Fig. 2-4 shows the sensing circuit which composed of two single-gate TFTs connected in series, one resistance R, and one sensing capacitance Csen. We feed two consecutive scan pulses N-1 and N at node B and A, respectively. When sensing pad is untouched, the pulse at node C is almost the same as that at node B, and the two TFTs are not in ON state at the same time. In such a case, there is no current occurs when pixel is untouched. On the other hand, when sensing pad is touched by human's hand, the pulse at node C is seriously distorted by the resistance R and sensing capacitance Csen. The distorted pulse at node C overlaps with the pulse at node A temporarily. The pulse overlapping when sensing pad is touched causes both TFTs turn ON concurrently. Therefore, when pixel is touched, there is a significant ON current, which can be a judgment for whether pixel is touched or not.

Fig. 2-5 shows the schematic of the sensing circuit with the input signals and its measurement result. In laboratory-level experiment, the RC low-pass filter is connected by discrete components including a capacitor of 50 pF and a resistor of 10 Mohm, and a readout resistor of 1 Mohm is used to transfer the current to voltage signal for the oscilloscope measurement. For the touched case, V_A is high and V_C is not low enough to turn off the TFT. The spikes in the output voltage waveform (V_{out}) on the readout resistor indicate the touch events. In other words, when touch event occurs, it results in a significant transient current. On the other hand, for the untouched case, no current is observed. It implies that the proposed sensing method does not consume readout power when sensing circuit is not touched.

2.3.2 1T1R1C Using Dual-Gate IGZO TFT

A similar sensing circuit using a dual-gate IGZO TFT can be used to replace the two single-gate TFTs, as shown in Fig. 2-6. It comprises a dual-gate IGZO TFT, a resistor R, and a sensing capacitor C_{sen}. The top and the bottom gates of the TFT are

connected to the two successive scan pulses, respectively. The difference is that the scan pulse is fed to the top gate by way of an RC low-pass filter.

The process flow of the dual-gate a-IGZO TFTs is described as following. Shaped Ti/Al/Ti gate electrodes were capped with SiNx gate dielectric which was deposited by plasma enhanced chemical vapor deposition (PECVD). For the S/D metal, Ti/Al/Ti was formed by successive deposition with DC sputtering at room temperature. By patterning and dry etching these layers, the S/D electrode was formed. After that, the active layer of 30-nm-thick a-IGZO film was deposited by DC magnetron sputtering system using a target of In:Ga:Zn = 1:1:1 and defined after etching. Finally, devices were capped by the passivation at 280℃, and then ITO were patterned for top gate. The device cross-section and the symbol of a dual-gate TFT are shown in Fig. 2-7.

From previous references, the electrical characteristics of dual-gate IGZO TFT are greatly improved with respect to the conventional single-gate IGZO TFT, which is shown in Fig. 2-8 [30~31]. In addition, we also investigated the I–V characteristics of the dual-gate IGZO TFT with different bias voltages applied to each gate. Fig.2-9 shows the transfer curves of drain current (Id) versus bottom-gate voltage (V_{BG}) for the dual-gate IGZO TFT at different top-gate voltages (V_{TG}). These transfer curves exhibit parallel shifts with respect to different V_{TG} values. This phenomenon is attributed to attraction and expelling of free carriers in the active layer by the top-gate. As illustrated in Fig. 2-10, the TFT is kept OFF by biasing V_{TG} at -10V even when the V_{BG} is as high as +10V, and vice versa. It implies that, the threshold voltage of the dual gate IGZO TFT using the bottom-gate in its normal operation can be controlled by the top-gate and vice versa.

The following explains the operation of pulse overlapping method in more detail. For most of the time, both the top and bottom gates of the dual-gate TFT are set

at -10V, and the TFT is turned off. Just before the V_{BG} pulse coming to the bottom gate, the pulse of V_{TG} is sent to the top gate through the RC circuit. If no touch event occurs at this time, the RC time delay is small. Thus, the slightly distorted V_{TG} pulse can fall in time to -10V to turn off the TFT before the V_{BG} comes in. On the other hand, if a touch event happens, it results in large RC time delay. The larger RC delay leads to more serious pulse distortion and prolongs the voltage falling time of V_{TG}. This delay time keeps the TFT from turning off by the time that the bottom-gate switches to +10V. In such a case, a significant transient ON current flows through the TFT to be the sensing signal. Consequently, we can use the method to detect touch events. Fig.2-11 shows the laboratory-level test result.

2.3.3 1T1R1C pixel circuit

Another 1T1R1C pixel circuit using conventional single-gate TFT and its laboratory-level test are shown in Fig. 2-12 and Fig. 2-13, respectively. Comparing to the previously proposed circuit, it further omits a vertical bus of V_{DD} from the pixel, which make the new circuit more suitable for the in-cell touch sensing. The simple circuit can decrease the consumption of aperture ratio and increase the transmission.

In operation, when the panel is untouched, the scan pulse $V_{scan,N-1}$ is firstly fed to node B and raise the voltage of node B, V_B , to 10V. At this time, the TFT does not output current because there is no voltage difference between drain and source. Then, although the scan pulse $V_{scan,N}$ comes in and raises the voltage of node A, V_A, to make a voltage difference between drain and source, the V_B has fallen in time to -10V to turn off the TFT. On the other hand, if touch event increases the sensing capacitance, which consequently increases RC time-constant, the scan pulse $V_{scan,N-1}$ gets a distortion when it reaches the gate of TFT. Therefore, it needs more time to lower the voltage from 10V to -10V. When the scan pulse $V_{scan,N}$ rapidly raises from -10V to10V,

a transient ON current is produced by the pulse overlapping.

For a good design, the transient ON current should occur only when the selected sensing pixel circuit is touched. To avoid false current, we introduce a time interval, T_{enable}, between two consecutive gate pulses, which ensure V_B can get back to -10V before V_A starts rising. T_{enable} avoids the intrinsic distortion owing to the parasitic RC influence on row bus in the large area active matrix. It is noteworthy that the distortion on V_C without touch is resulted from the parasitic capacitance and resistance of the transistor. The parasitic capacitance and resistance emphasize the importance of T_{enable}.

As can be seen in the circuit schemes, the proposed circuit is mainly operated by the scan pulses. The operation of the scan pulses is identical to that in display driving even the use of T_{enable}. In general display scan driving, T_{enable} is used to ensure that the Clc cannot be influenced by the data voltage of the next pixel. Therefore, the display and touch sensing scan pulses should be able to be provided by the same scan driver. In practical signal process, each data line could be connected to a charge integrator and biased by the integrator [25].

2.4 Circuit Discussion and Demonstration

2.4.1 Circuit Advantages

One of the values of the proposal is universal to the backplane structure, including on-cell and in-cell. Although the design results are different, the effective circuit and the design procedures are the same. For example, the obvious difference for the two structures is the sensing capacitor fabrication. In the on-cell structure, the touch sensing array can be fabricated individually and then attached to the display panel. In this case, the sensing capacitor can be formed by the cover glass sandwiched

in between finger and the electrode fabricated in the touch sensing array and protected by the cover glass. On the other hand, in the in-cell structure, the capacitor in this RC circuit can be the liquid crystal capacitance (Clc), which is formed by the electrodes made on the TFT substrate and the common electrode on the color filter substrate. The Clc can be increased by the external forcing to compress the gap of the two electrodes [25~26]. However, although the capacitor fabrications are different, the capacitance can be proper calculated and simulated. Furthermore, the proposed sensing circuit is also suitable to different TFT types, such as amorphous silicon (a-Si) TFT, oxide TFT, and poly-silicon (LTPS) TFT. In addition to the previous test using IGZO TFT, Fig. 2-14 shows the test results of 2T1R1C and 1T1R1C sensing circuit using a-Si TFT. For our test devices, since the Vth controlled ability of the top gate of dual-gate a-Si TFT is not so obvious like dual-gate IGZO TFT, no test result of the sensing circuit using dual-gate a-Si TFT is included in this dissertation.

The in-cell types of touch panel which detects the change in the liquid crystal capacitance [25~26] usually have two disadvantages. One is that, the amplifying TFT outputs large current even in the case without touch and thus keep consuming power whether pixels are touched or not. The other issue is the threshold voltage shift of TFT. In a sensing array, different sensing pixels on the vertical line share the same readout circuit. Because of the threshold voltage variation of the TFTs in different sensing pixels, touch signal and untouched signal in different pixels could be harder to distinguish by the same readout circuit. Although the uniformity of a-Si TFT is excellent, the device variation of other type TFTs including LTPS or oxide TFT could affect the circuit performance. In addition, the threshold voltage of TFT would shift under electrical stress of usage.

The proposed circuit only output current when the selected pixel is touched so that the power consumption could be reduced. Furthermore, the effect of threshold

voltage variation on the proposed circuit can be avoided, as shown by the simulation result in Fig. 2-15. We use the same a-Si TFTs size and charge integrator to perform the simulation. As can be seen in Fig. 2-15(b), there still is a 0.4V difference between touched signal and untouched signal when threshold voltage shifts 5V in one pixel but -5V in another pixel. In our design, the output signal is more dependent on the overlapping time of the pulses than the threshold voltage of the TFT. This provides the big tolerance of the threshold voltage variation.

2.4.2 Demonstration Using a-Si TFT

In the demonstration, a transistor with a proper fixed gate bias, namely, R_{TFT} is used to replace the resistor. The alternative pixel circuit is shown in Fig. 2-16. Besides, the voltage bias for R_{TFT} in every sensing pixel is fixed, so it can be provided by V_{com}. By doing this, it is practical in fabrication to save more aperture area than implementing the resistor with a long metal wire. Fig. 2-17 shows a demonstration of the proposed circuit using a-Si TFT in a 2-inch 9x9 array.

2.5 Large Panel Simulation

In this section, we design a 42 inch a-Si active touch panel using the proposed circuit and discuss the problems arisen from the large size.

2.5.1 Design Consideration, Procedure, and Results

There are many factors to design the large-area panel of the proposed sensing method, such as bus line width, size of TFTs, and sensing capacitance. For example, to make the sensing area becomes larger, the scan line width can be made thinner but it will cause a large parasitic resistance on the scan line and thus a serious RC time constant delay. The delayed scan pulse at scan far end might result in a false touch signal. When this case happened, the same readout setting cannot be applied at both

scan near and far ends. On the contrary, if the scan line width is designed to be wide, it squeezes the area of sensing region. In such a case, the small sensing area corresponding to the small sensing capacitance may not make large difference in the RC time constant between the cases of touched and untouched. Another example is the size of R_{TFT} and the driving TFT. Increase in the driving TFT size can improve the ability to charge the data bus and the read out circuit, while the gate capacitance of TFT increases accordingly. Therefore, the difference of total capacitance at sensing node when pixel is touched or untouched is less significant, and the intrinsic RC time constant delay of scan pulse increases.

Due to these intertwined design factors, a design procedure is proposed to support our task, as shown in Fig. 2-18. It contains the following steps:

Step1: Specify panel size, aspect ratio, and resolution

Step2: Design line width of scan and data line

Step3: Calculate the area of sensing region, which value is the area of one pixel pitch subtracting the area of bus line and TFTs of one pixel. For a fast estimation, the area of TFTs is ignored because it is much smaller than the area of bus line. The value of sensing capacitance can be calculated accordingly.

Step4: Design sizes of both driving TFT and R_{TFT}.

Step5: Calculate the parasitic capacitances and resistances on the buses.

Step 6: Verify the design with SPICE simulation.

The design procedure is repeated until the design passes the criteria concerning the significant voltage difference between touch and untouched. In this paper, the target of our design is to produce a voltage difference larger than 0.2V, which is good enough for a common voltage comparator in the peripheral readout circuit to judge the touch event. Table 1 lists our final design results.

2.5.2 Four-Corner Simulation

Since the large touch panel suffers from serious parasitic capacitance and resistance on the scan and data buses, the intrinsic RC delay of these buses can possibly make the sensing pixel fail. Therefore, the simulations were conducted for the four pixels of the four corners of the designed 42 inch touch panel. The simulation results shown in Fig. 2-19 include the scan pulses and the output signals of the four pixels when they are touched and untouched. The output signal of the pixel at the scan far end is larger than that at the near end owing to the intrinsic bus delay. The output signal from the pixel at data near end is larger than that from the data far end, because the current signal from the data far end has to pass through the parasitic resistances and capacitances of the data bus, while the current from the pixel at the data near end comes out directly. For the worst cases, the smallest touched signal appears at scan near end and data far end, and the largest untouched signal appears at scan far end and data near end. The worst-case difference is shown by the two dash lines of the output signal in Fig. 2-19. This difference between the touched and untouched signals is still larger than our design target of 0.2V.

2.5.3 Current-Induced Voltage Drop on Scan Bus

There is yet another concern of the proposed circuit that when many pixels on the same scan line are touched simultaneously, every touched pixel drains current from the scan bus. This is not an issue for the 2T1R1C pixel circuit and the 1T1R1C using the dual-gate TFT since the sensing current comes from the individual voltage bias buses in column. For 1T1R1C using single-gate TFT, the total sensing current drained from the same scan bus in row flowing through resistances of scan bus results in the voltage decrease of the scan pulse. In this case, we need to confirm the circuit can still function when the heavy load of multi-touch happens.

The pixel circuits of 3T1C and 2T1C shown in Fig. 2-20 and Fig. 2-21, respectively, were simulated for the two cases without and with the voltage drop on the scan bus. For the both circuits in a row of 10 and with all the pixels touched simultaneously, the simulation results of the scan pulse high voltage are shown in Fig. 2-22(a) and 2-22(b), accordingly. It can be observed that there is more decrease of scan pulse high voltage in 2T1C circuit than in 3T1C circuit. However, the decrease is as small as 0.22V.

We simulate the worse situation that when the scan pulse high voltage decreases from 10V to 7V, which corresponds to hundreds of pixels on the same scan line are touched simultaneously. The result is shown in Fig. 2-23. It can be seen that the minimum touched signal is still larger than the maximum untouched signal for 0.2V, which still meets the design target. The concern of voltage drop owing to multi-touch on the scan bus for the large area panel can be relieved.

2.6 Summaries

A simple but novel concept of pulse overlapping detection for the active matrix touch panel is proposed. The proposed circuit has many advantages. Firstly, the output signal of the transient on current of TFTs is significant and thus can be easily readout by low cost ICs. Secondly, current signal only occurs when a pixel is touched. The power consumption in operation is greatly reduced. Moreover, device variation can be tolerated, which is the major advantage over the other active touch panels of the source follower type. A 42 inch touch panel of the proposed method is successfully designed by the proposed design procedure. The proposed circuit can provide an excellent way of implementing large area active matrix touch panels.

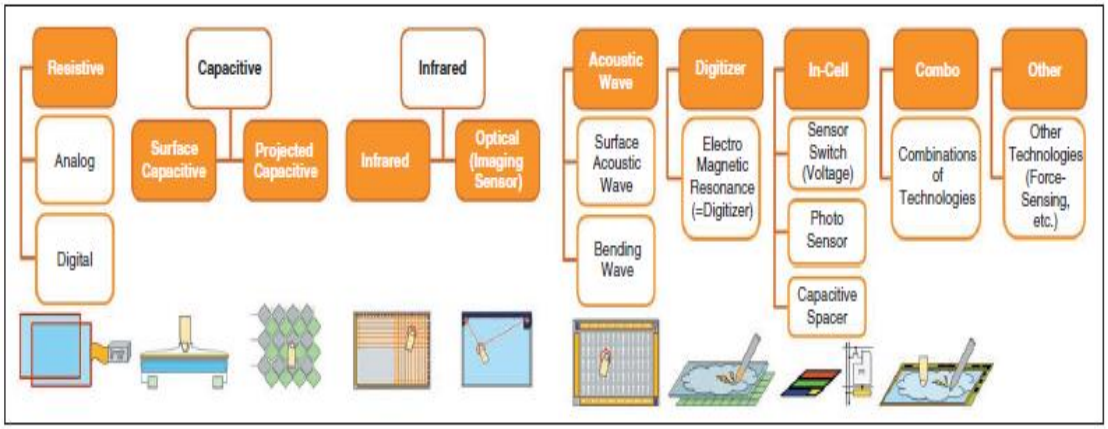

Fig. 2-1 DisplaySearch divides touch into ten categories with 14 sub-technologies

(Source: DisplaySearch 2009 Touch Panel Market Analysis)

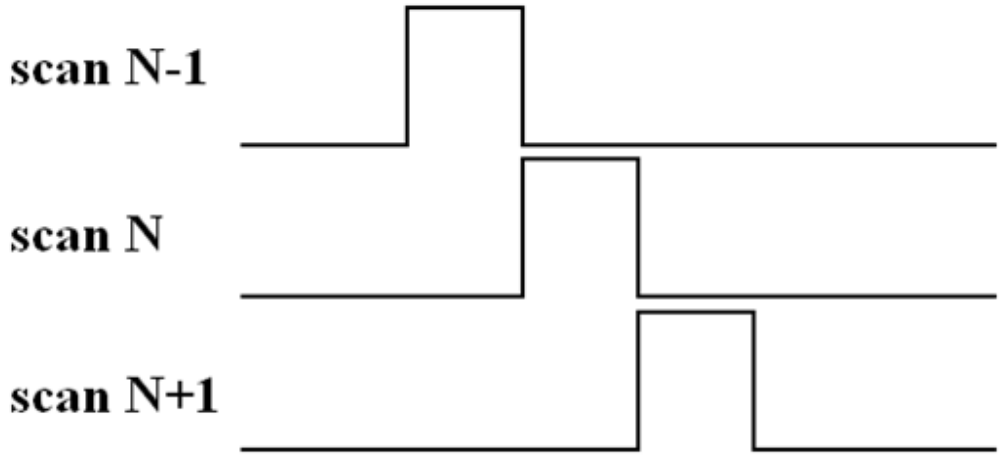

Fig. 2-2 The original scan signal of display at scan near end

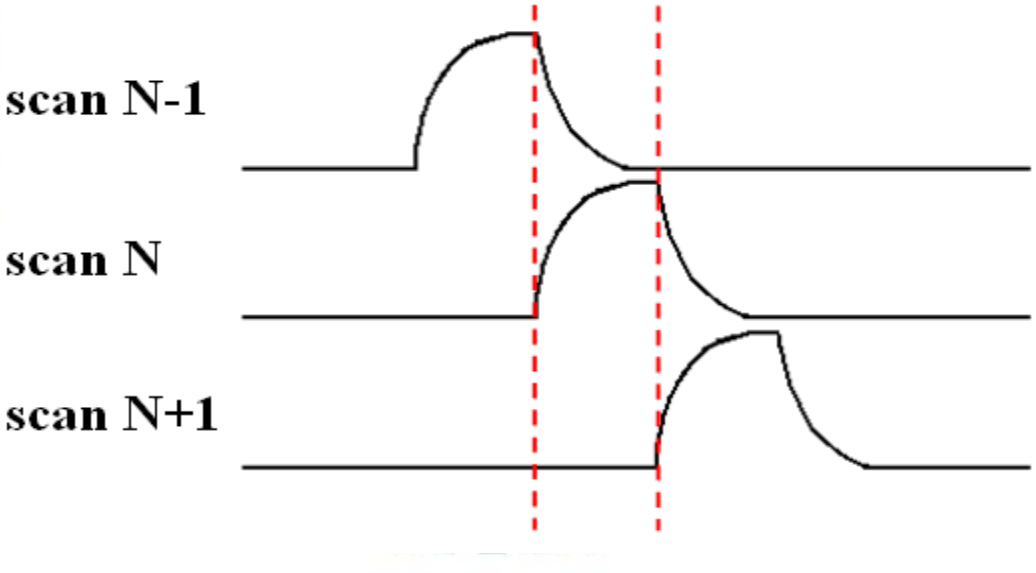

Fig. 2-3 The original scan signal of display at scan far end

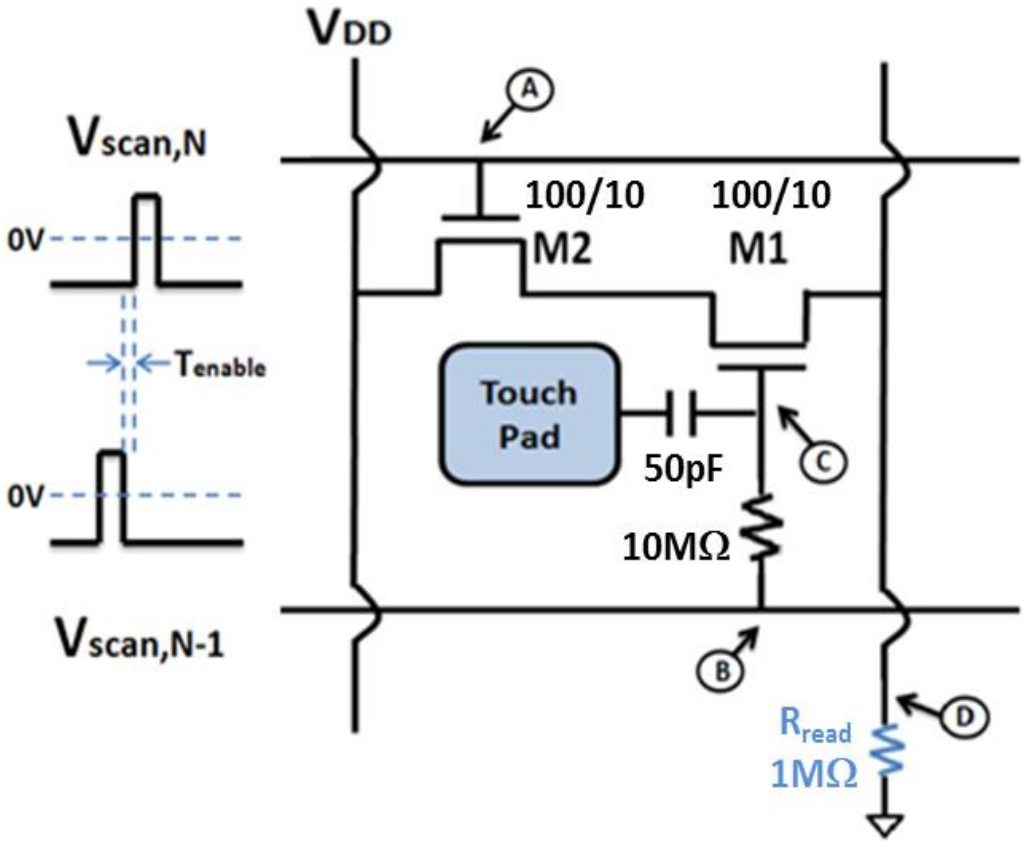

Fig. 2-4 The 2T1R1C sensing circuit using two single-gate IGZO TFT

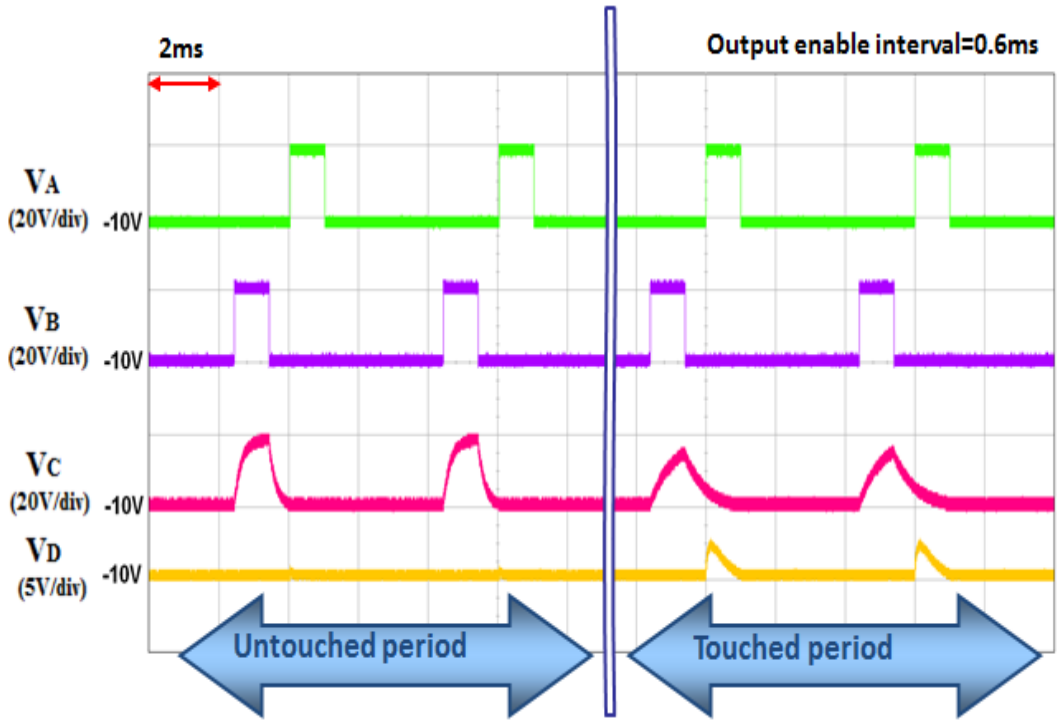

Fig. 2-5 The sensing result of the 2T1R1C pixel circuit

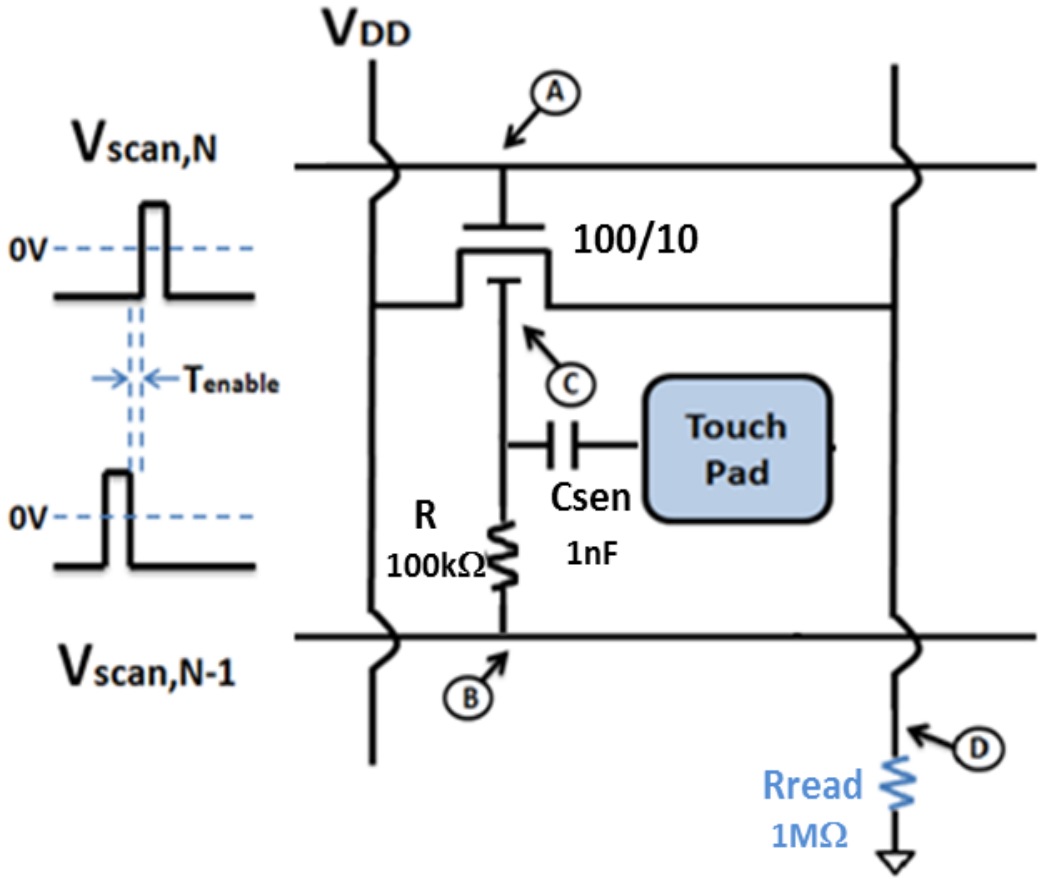

Fig. 2-6 The first touch sensing pixel circuit using dual-gate IGZO TFT

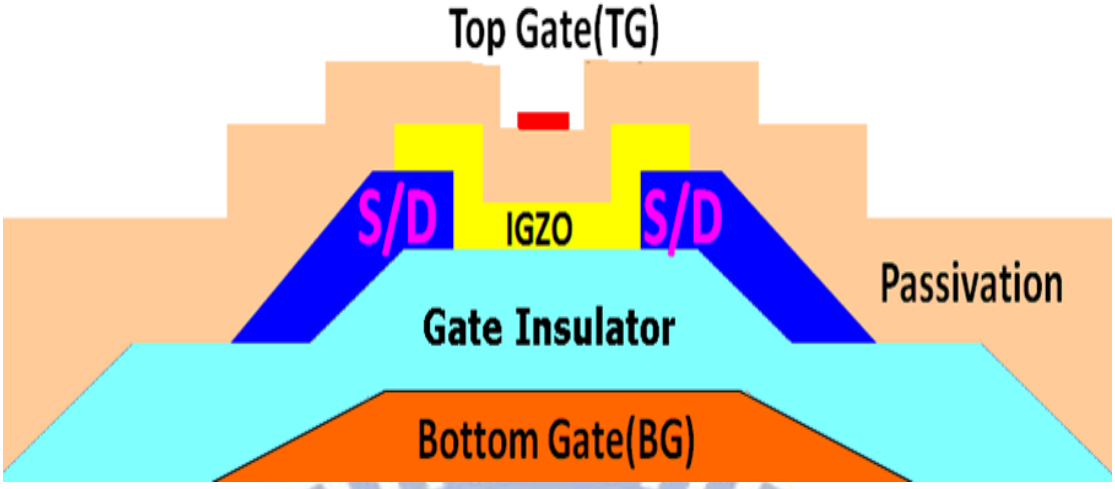

(a)

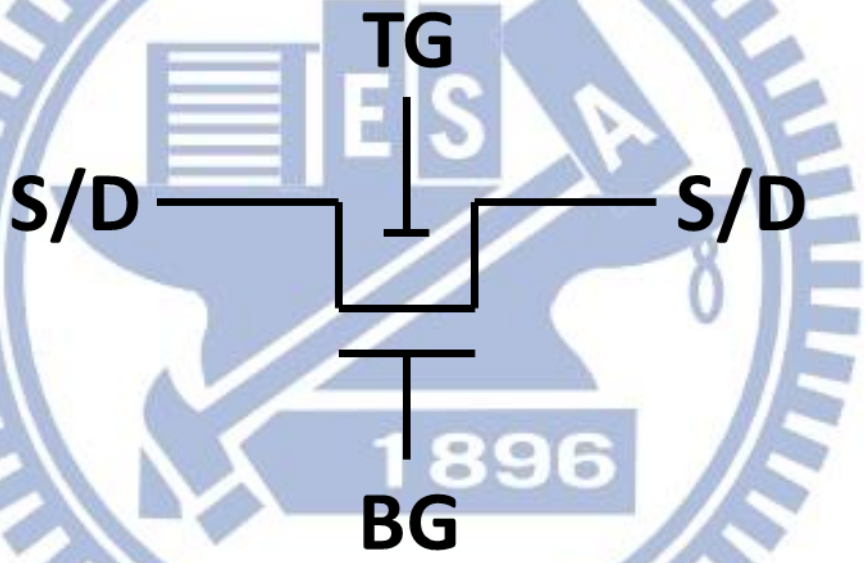

(b)

Fig. 2-7 (a) The cross-section (b) the symbol of the dual-gate IGZO TFT

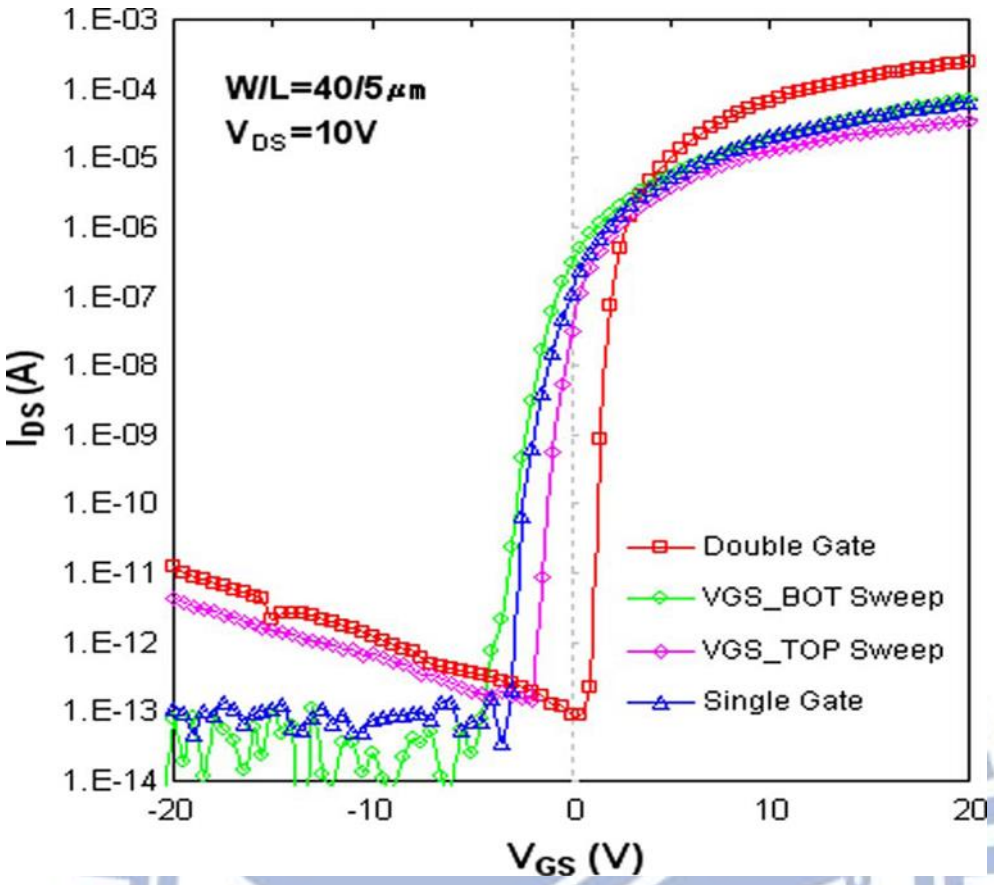

Fig. 2-8 The transfer characteristics of the dual gate TFT.

[IEEE Electron Devices Letter, Vol. 31, no. 3, pp. 219-221, 2010]

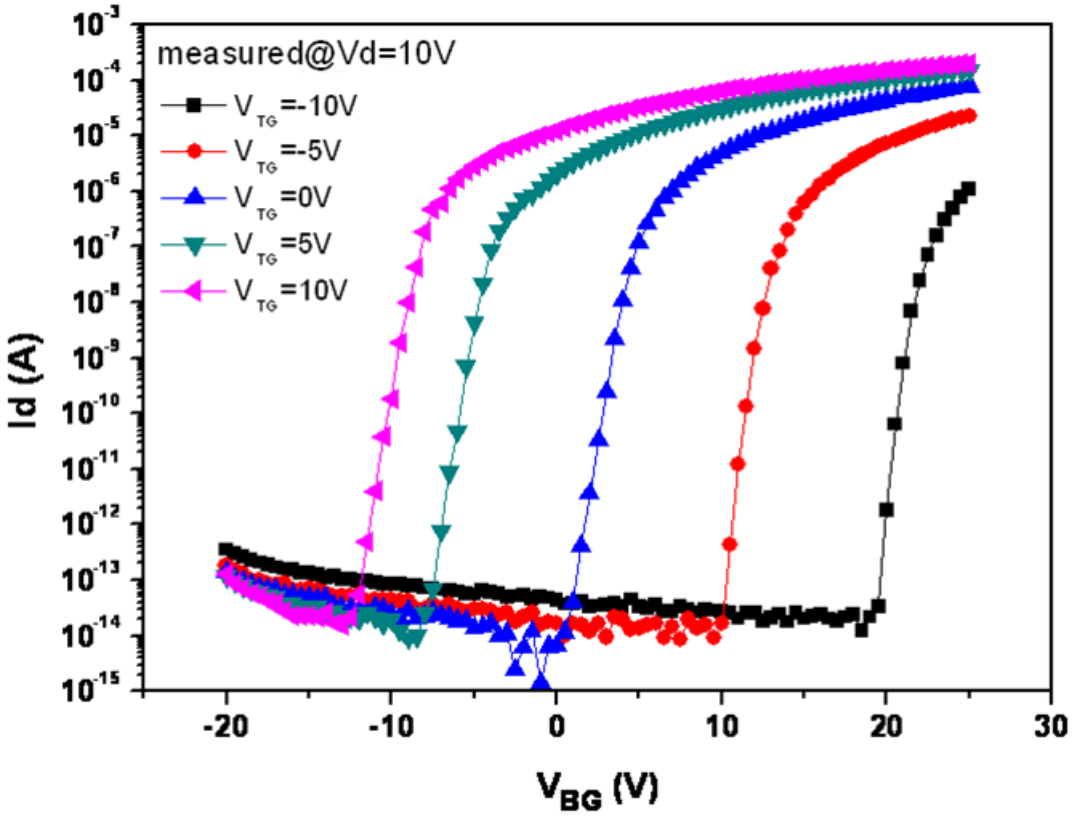

Fig. 2-9 Id–V_{BG} transfer characteristics of the dual gate TFT under five different measurement conditions

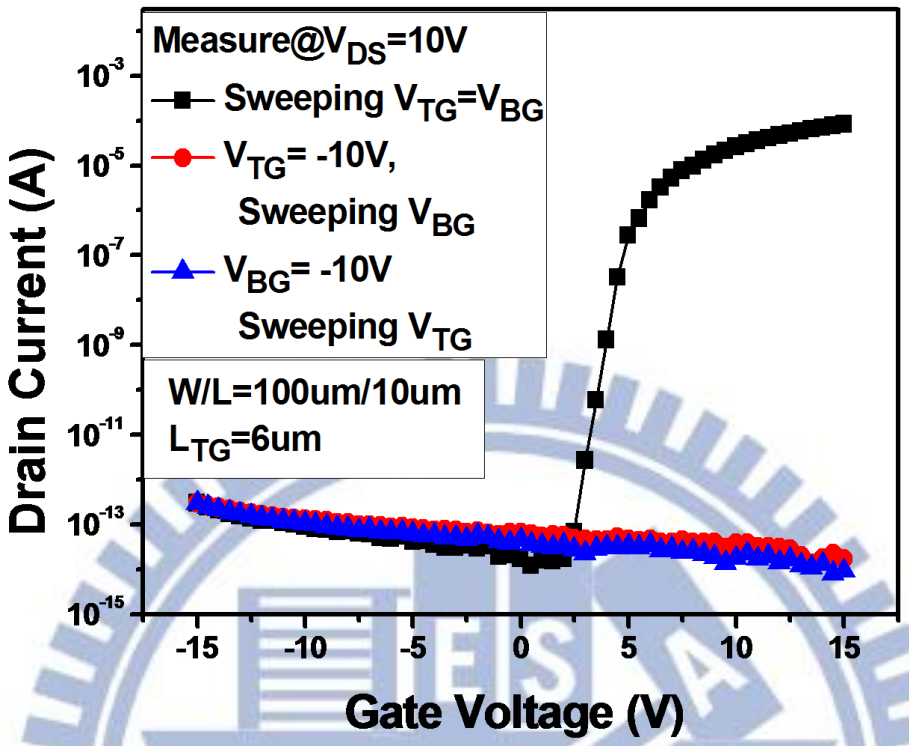

Fig. 2-10 The transfer characteristics of the dual gate IGZO TFT (a) sweeping V_{TG} = V_{BG} (b) V_{TG} = -10V, sweeping V_{BG} and (c) V_{BG} = -10V, sweeping V_{TG}.

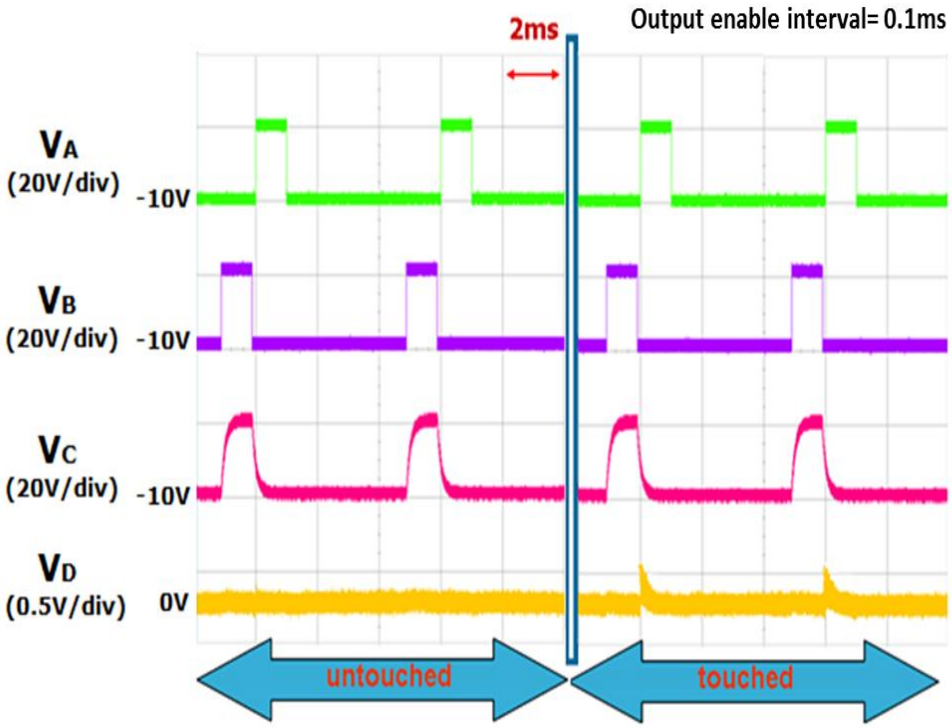

Fig. 2-11 The sensing result of the first touch sensing pixel circuit using a dual-gate IGZO TFT

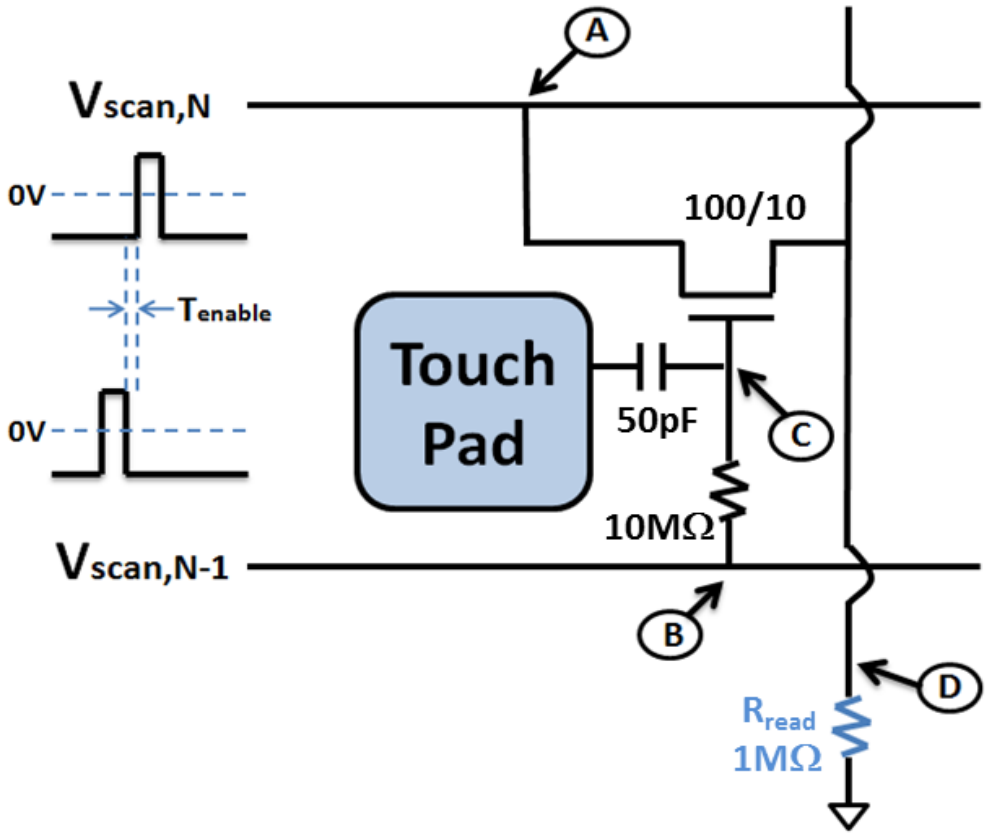

Fig. 2-12 The 1T1R1C sensing pixel circuit using a single-gate IGZO TFT

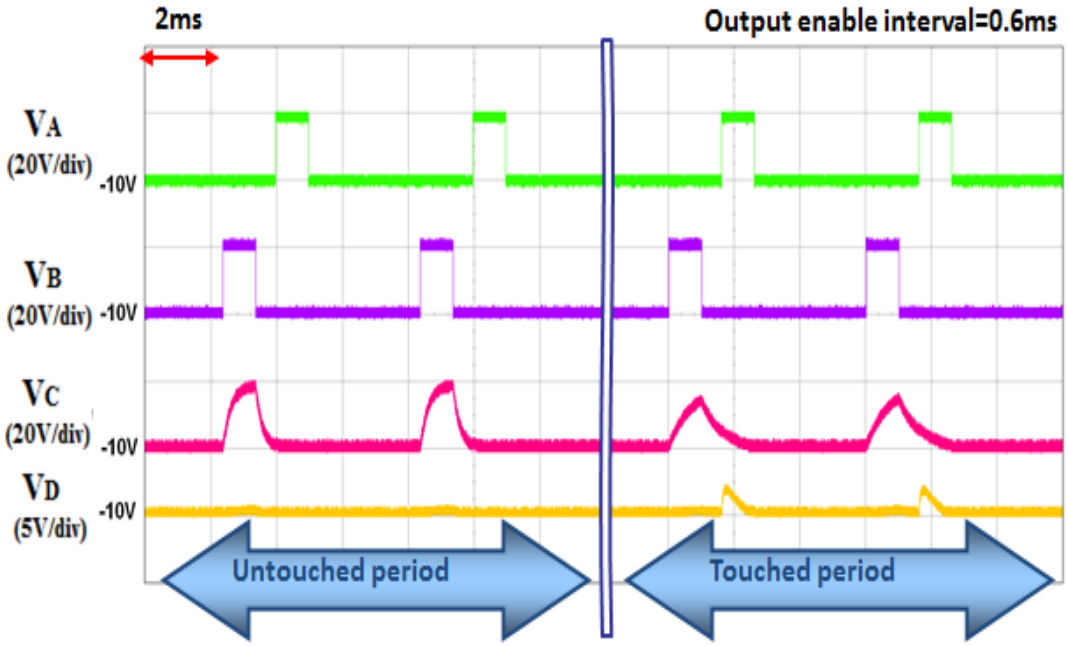

Fig. 2-13 The sensing result of the 1T1R1C pixel circuit

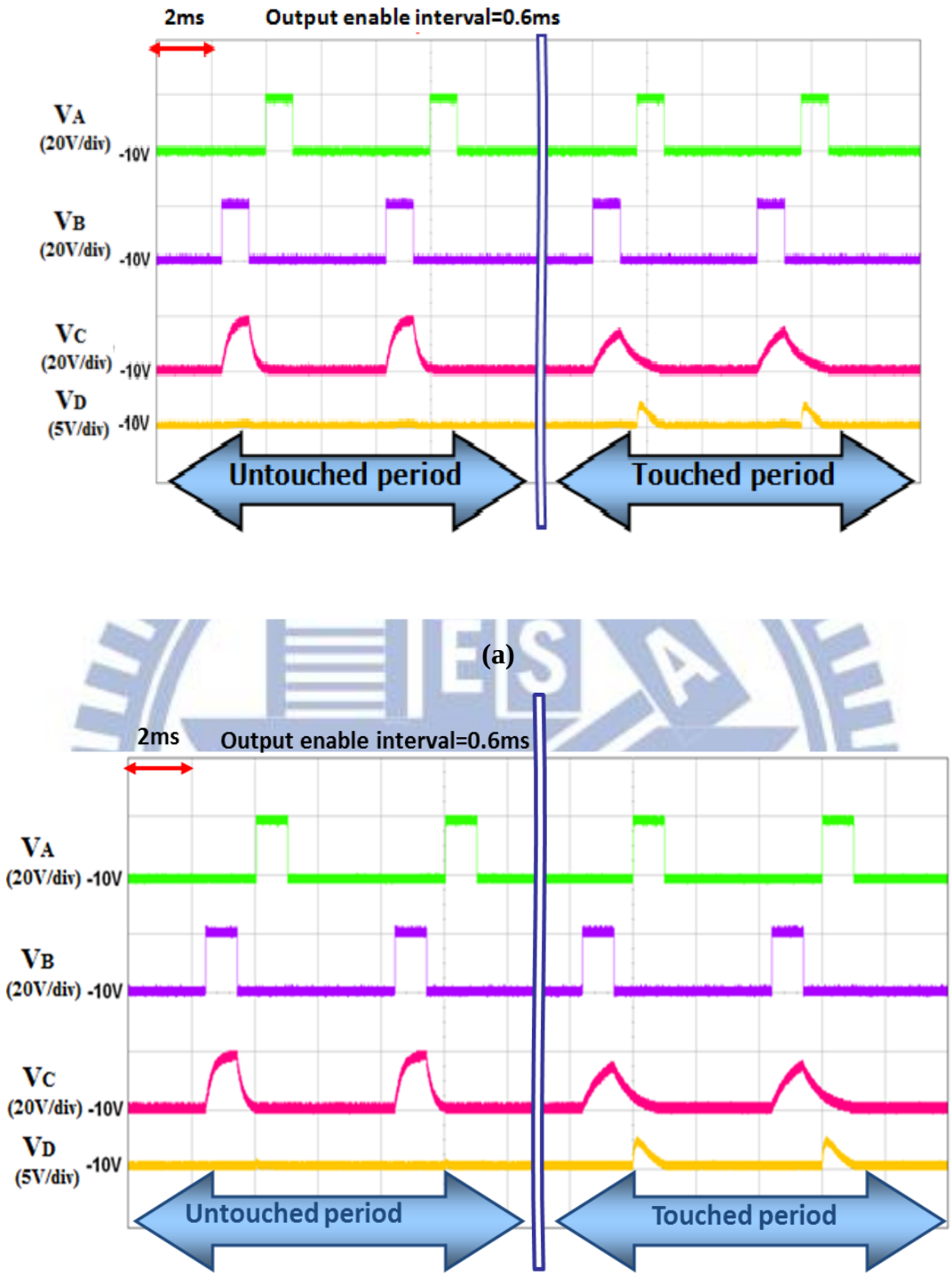

Fig. 2-14 The sensing results of (a) the 2T1R1C (b) the 1T1R1C pixel circuit using single-gate a-Si TFT

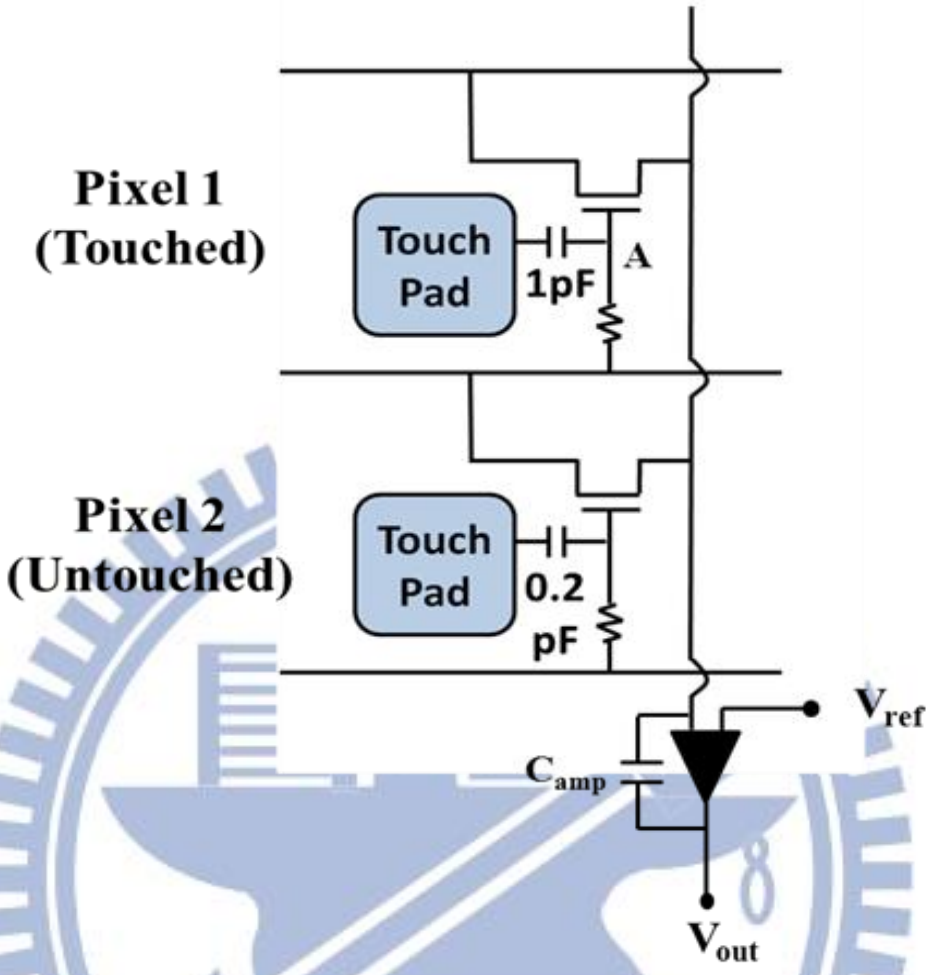
Pixel 1
(Touched)
Touch
Pad
1pF
A
Pixel 2
(Untouched)
Touch
Pad
0.2
pF
V_{ref}
C_{amp}
V_{out}

Figure 2-15(a)

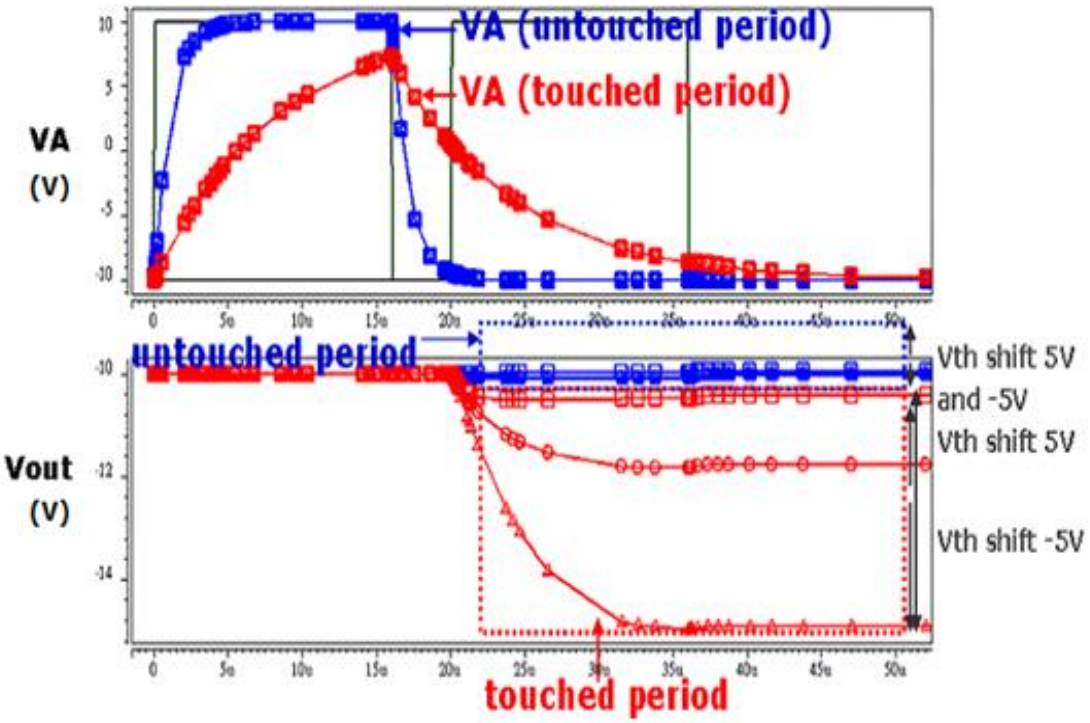

Figure 2-15(b)

Fig. 2-15 The verification of the threshold voltage shift of the TFT. (a) Pixel 1 and pixel 2 illustrate touch and untouched cases, respectively. (b) The simulation result indicates that the proposed circuit is able to distinguish the sensing difference even when the threshold voltage shift of the TFT is 5V.

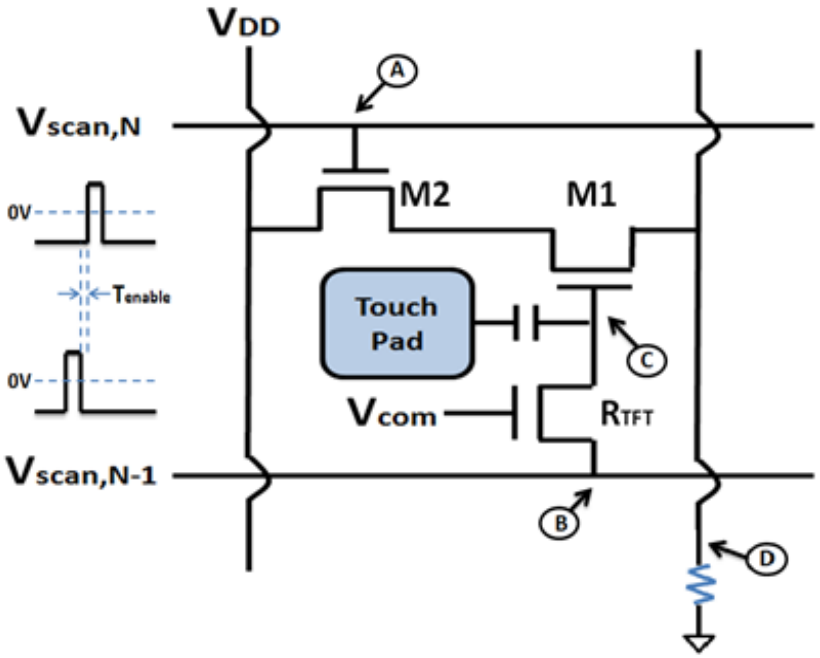

(a)

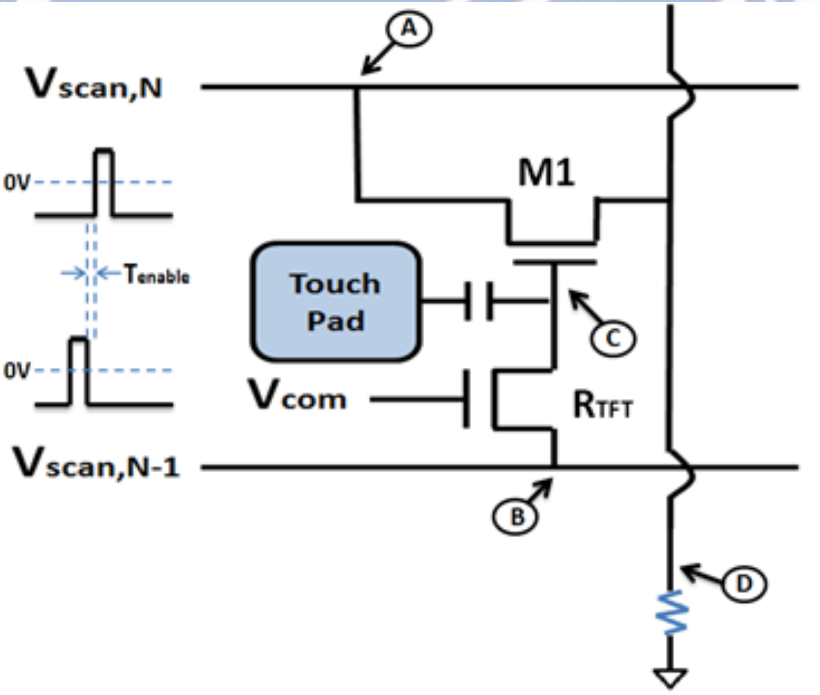

(b)

Fig. 2-16 The (a) 3T1C (b) 2T1C touch sensing circuit in which the transistor with a fixed gate bias replaces the resistor component in the RC low-pass filter.

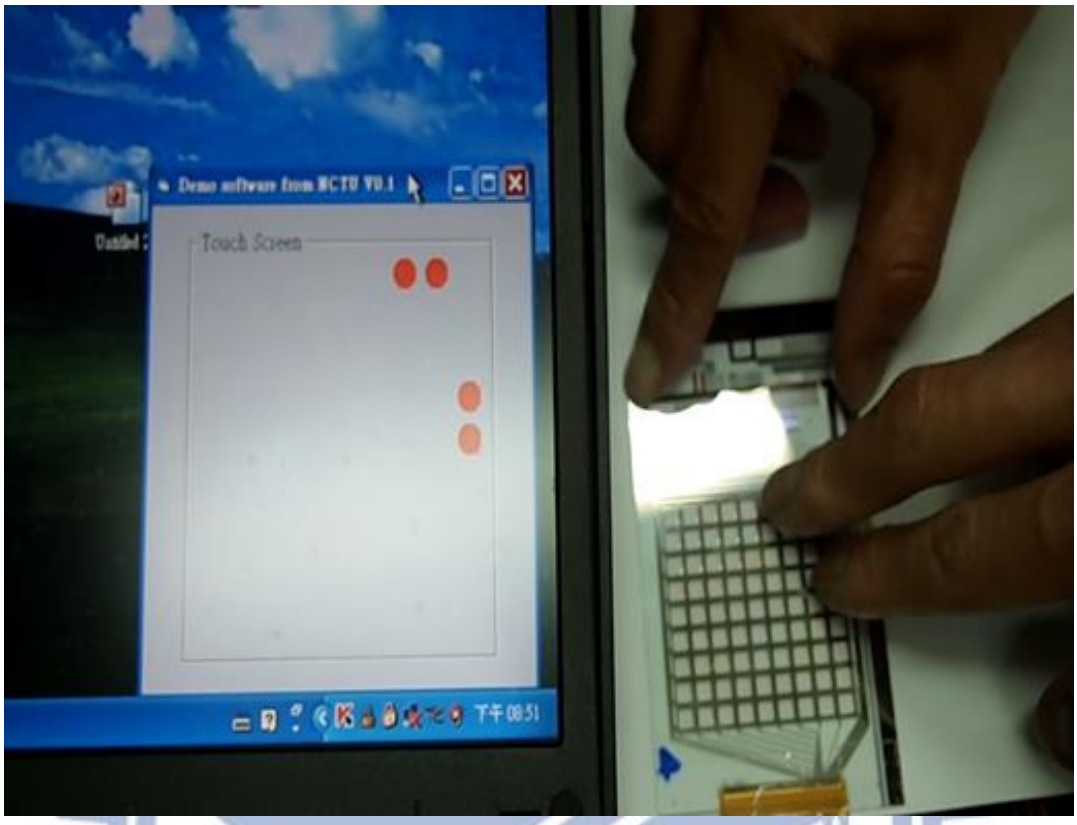

Fig. 2-17 A demonstration of the 2 inch touch panel

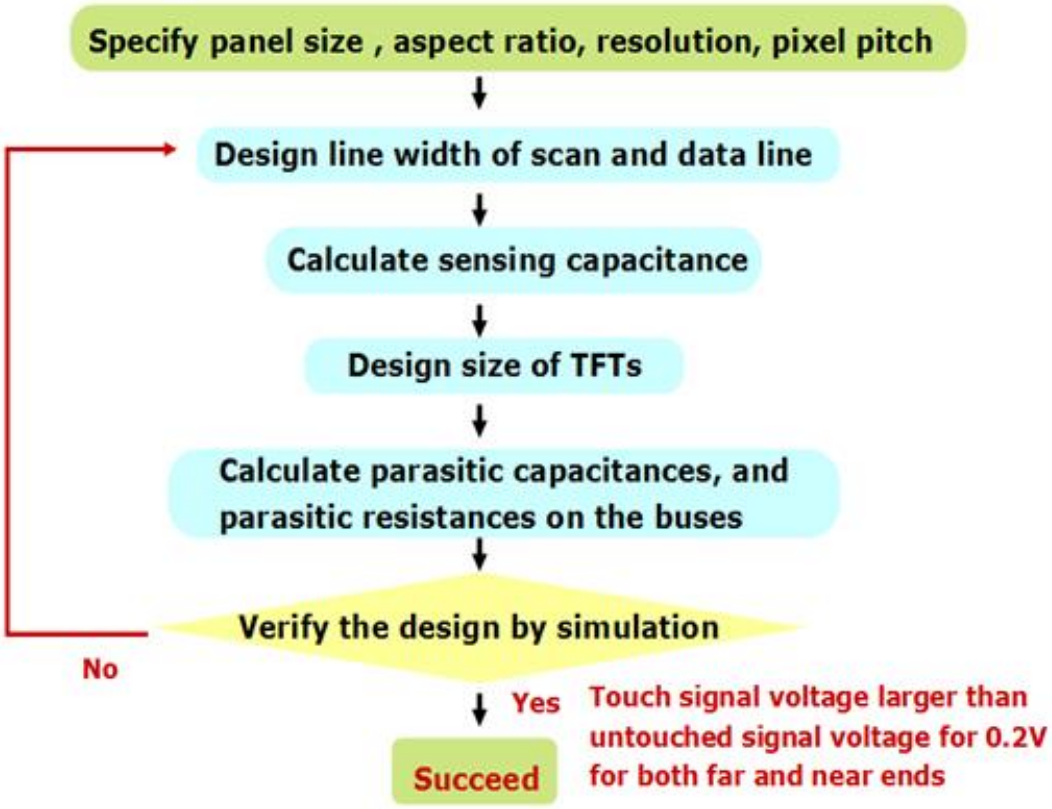

Fig. 2-18 Flow chart of design procedure

Item	Specification
Panel size	42 inch
Aspect ratio	16:9
Frame rate	60 Hz
Pixel pitch	1.9×1.9 mm×mm
Pixel shape	Square
Resolution	480 × 270

Table 2.1 The specification of the designed 42 inch touch panel

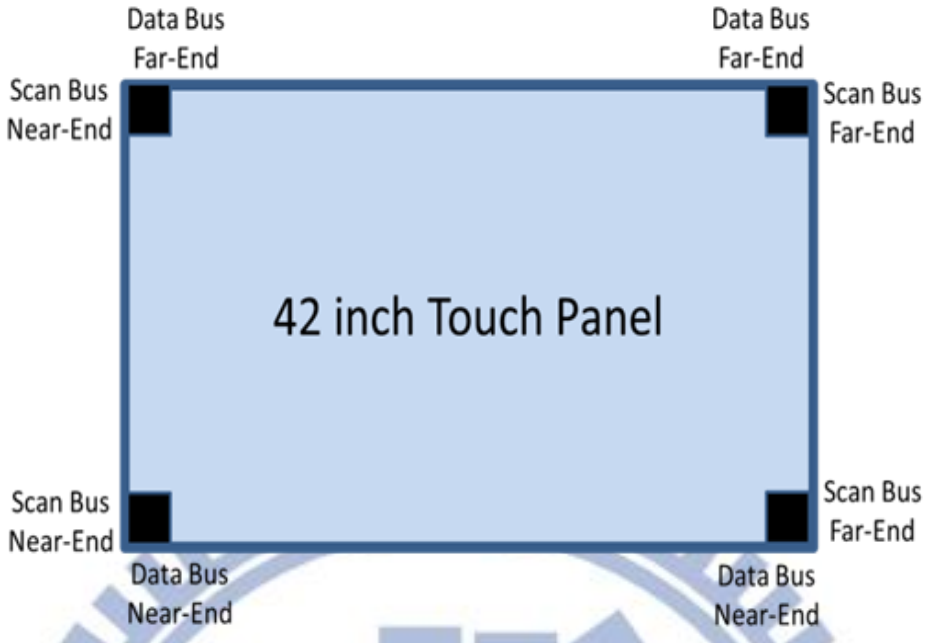

(a)

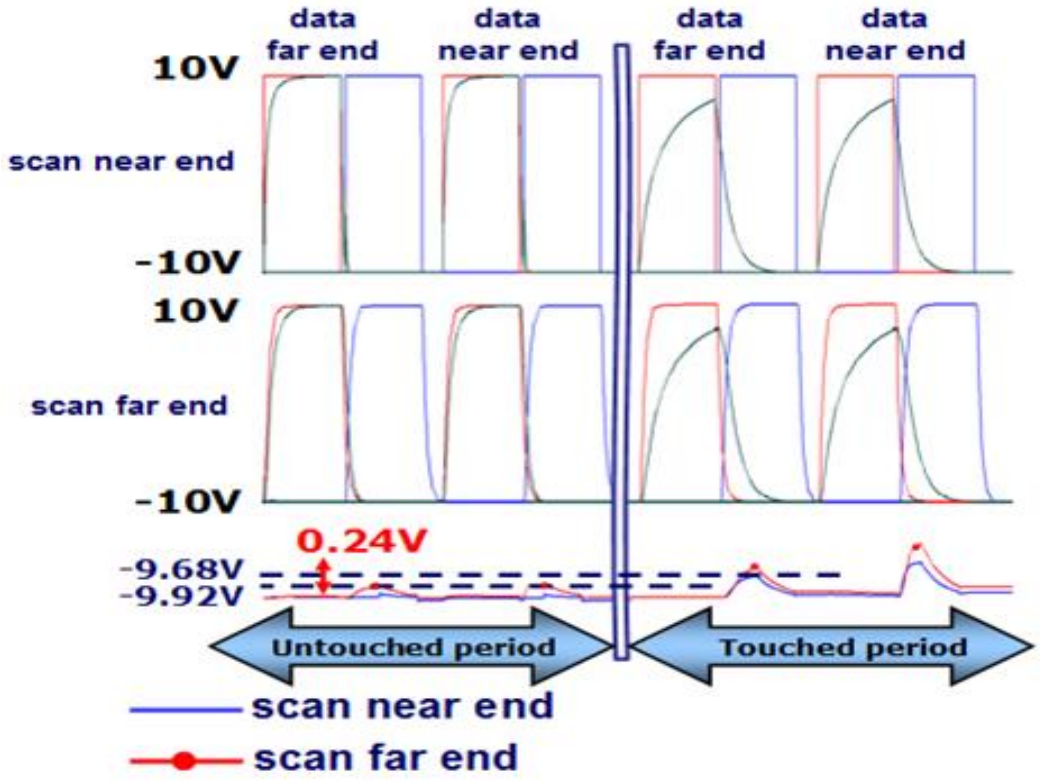

(b)

Fig. 2-19 (a) the locations of four corners in the panel (b) Four corners simulation result of the designed 42 inch touch panel using the proposed 2T1C circuit

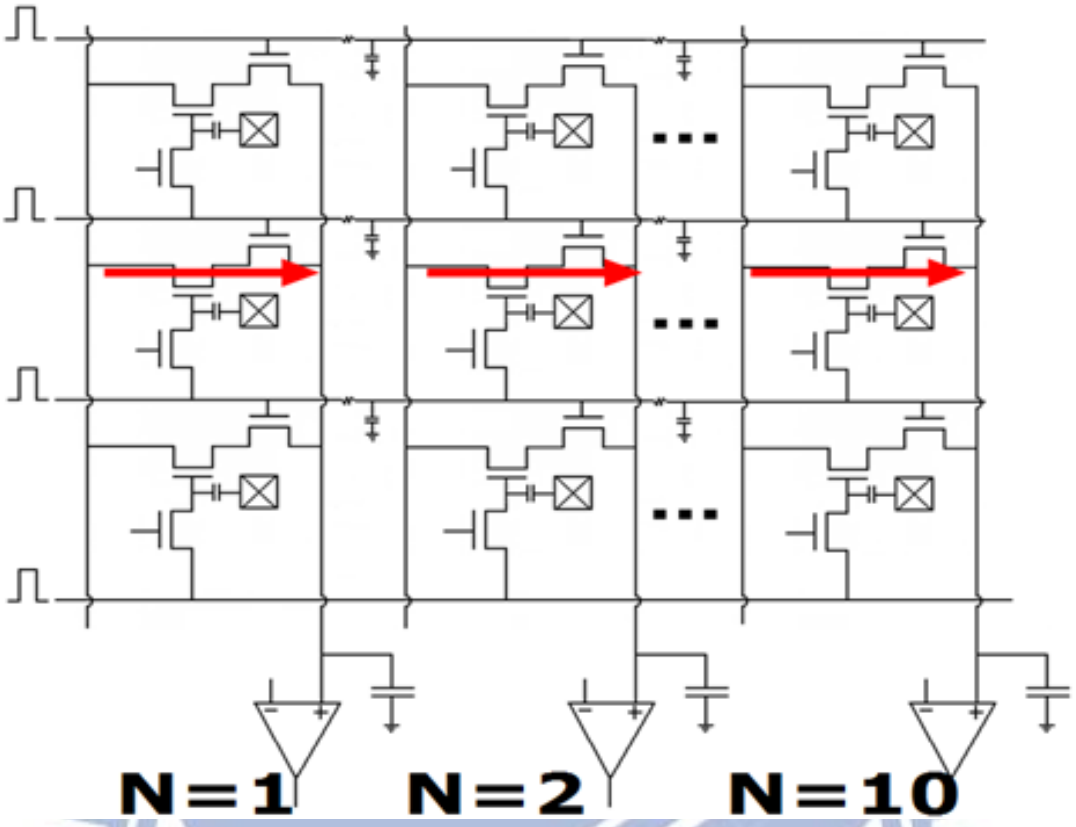

Fig. 2-20 3T1C circuit without voltage drop on the scan bus for the simulation of multi-touch situation

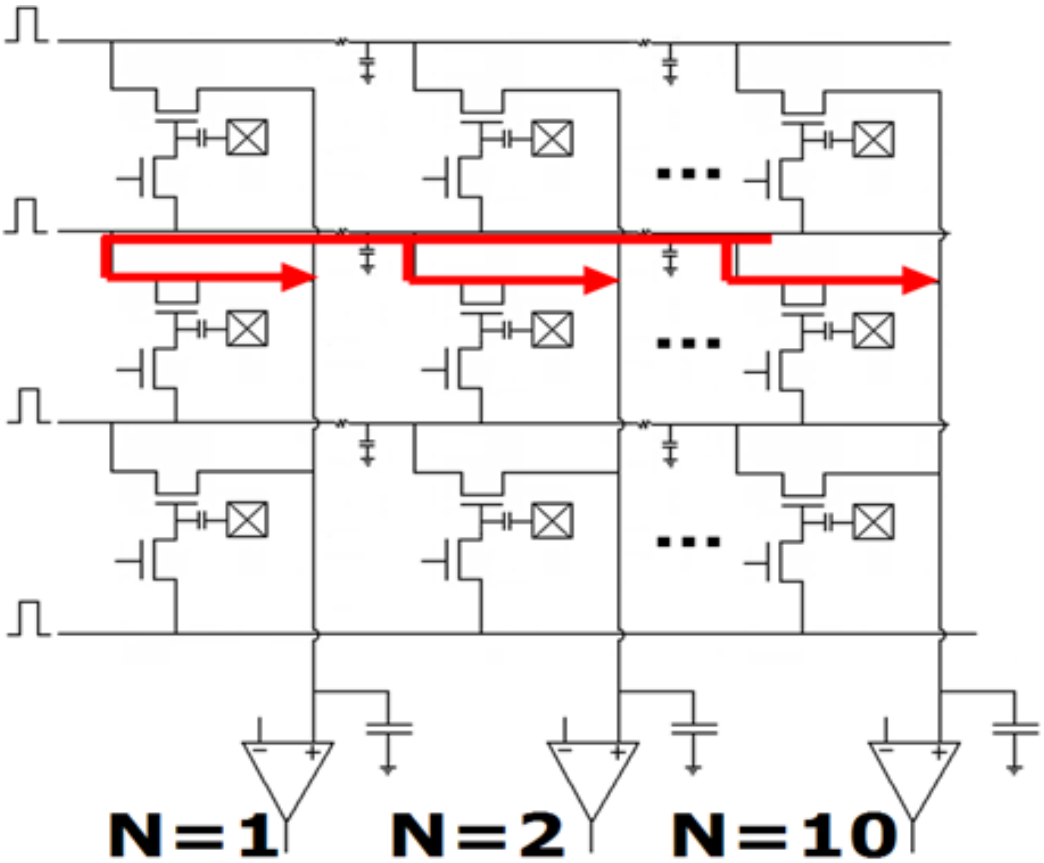

Fig. 2-21 2T1C circuit with voltage drop on the scan bus for the simulation of multi-touch situation

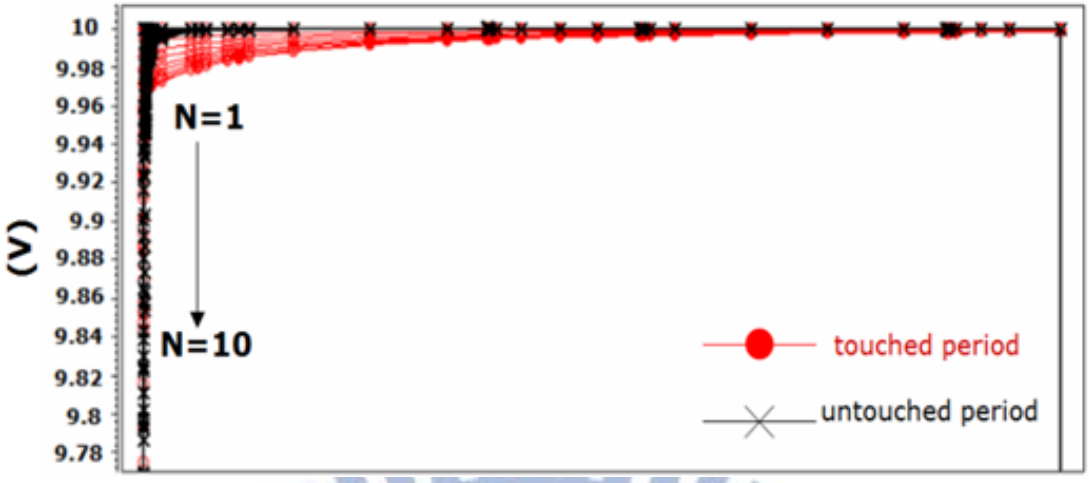

(a)

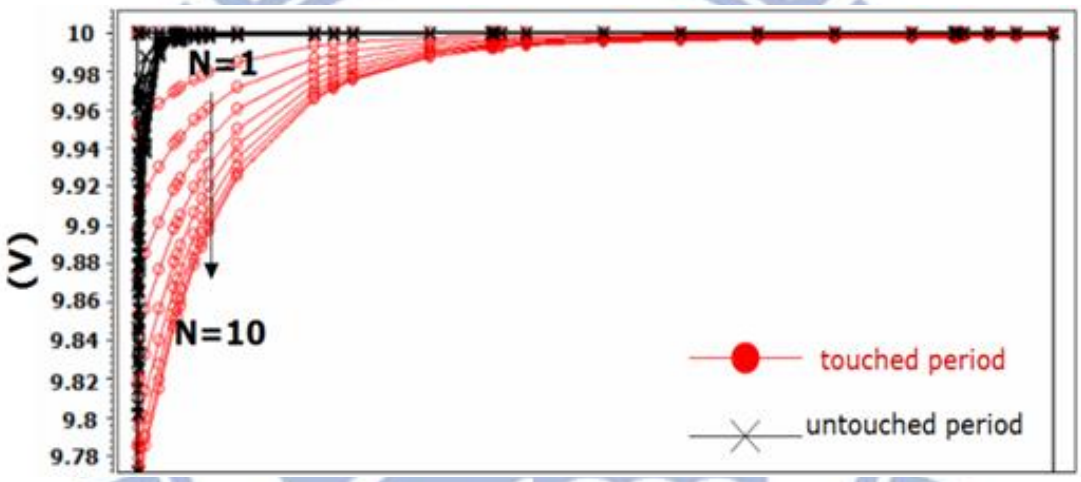

(b)

Fig. 2-22 (a) Simulation result of pulse high of multi-touch situation with 3T1C circuit (b) Simulation result of pulse high of multi-touch situation with 2T1C circuit

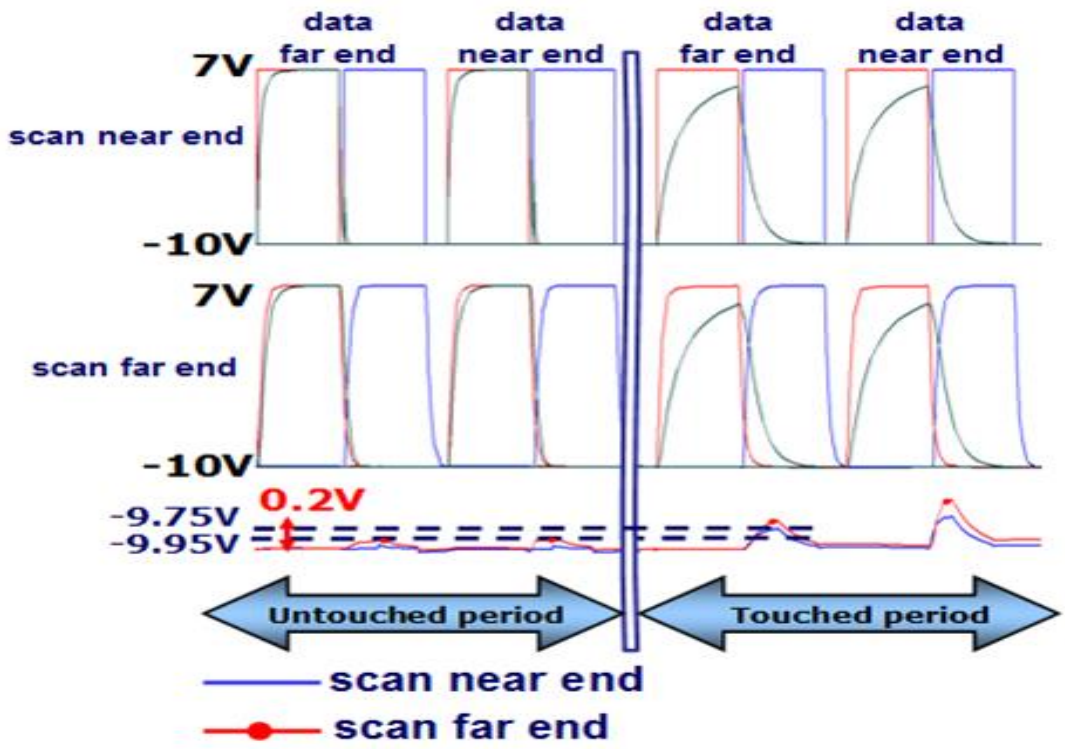

Fig. 2-23 Four corners simulation result of 2T1C circuit when pulse high decrease

Chapter 3

Backlight Sensing in Flat Panel Display

3.1 Introduction

For LCD-based products, 90% power consumption is attributed to backlight [32]; accordingly, backlight power saving is considered one of the most effective ways to reduce LCD energy dissipation. In recent years, the light-emitting diode (LED) backlighting is sought to replace the fluorescent backlighting because of the advantages including ultra wide color gamut, increased contrast through local dimming, improvement in motion picture response time by scanning, lower power consumption, and elimination of mercury [33~37]. However, the LED backlight modules could be non-uniform in large panel or degrade after a long time operation [38], which directly influences the image quality and limits the competitiveness of LED backlight in large-size flat display panels.

In this chapter, we propose the backlight sensor for the accurate backlight intensity. The degraded LED backlight can be corrected by the feedback of the backlight sensor [39], so the lifetime of display can be prolonged. Moreover, the using of backlight sensors can enhance the performance of backlight-control technologies. For example, the local dimming technology means that it can adjust the backlight intensity according to the frame which would be showed. Fig. 3-1 is the schematic of backlight local dimming. The backlight sensors can be used to detect the light intensity and determine the intensity whether or not to achieve the value that it should be.

3.2 Device Property

Before proposing the sensing circuit, we should fully study the photo response of sensing devices. Fig. 3-2(a) and Fig. 3-2(b) show the cross-sections and the transfer characteristics of the illuminated conventional a-Si TFT, respectively. We find that the conventional TFT does not have any photo reaction. This phenomenon is easy to figure out from the inserted diagram in Fig. 3-2(b). The bottom gate metal blocks all the possible backlight which would illuminate on active layer. Therefore, the conventional TFT does not be considered to be our backlight sensing device.

To reduce the effect of gate metal shielding, a non-conventional structure is proposed as the sensing device. Comparing to the conventional a-Si TFT, the non-conventional structure TFT has a gap which exists between bottom gate and one of top metal electrodes (source or drain). We define the gap size as i and call this structure TFT as "gap-type TFT" [40]. Since it has the same fabrication process as the conventional a-Si:H TFT, the light sensor can be integrated in panel without changing the mask number and extra cost. The basic process flow is described as following. After the deposition and patterning of gate metal on the glass substrates, three layers, i.e., silicon nitride (SiNx, 3500 Å), a-Si:H, and n+ a-Si:H films, were successively deposited in a plasma enhanced chemical vapor deposition (PECVD) system. After source/drain electrodes were made, the n+ a-Si:H region with length (L) of 5 μm between the source/drain electrodes was etched off by a reactive ion etch. Then, a passivation layer was used to cap the channel region.

The transfer characteristics of gap-type TFTs (i=30um) are showed in Fig. 3-3. Since the gap-type TFT is asymmetric, it can be alternatively operated. Fig.3-3(a) is the gate-near-drain mode, and Fig. 3-3(b) is the gate-near-source mode. For further discussion, we define the ratio of the TFT drain current under illumination (I_{D_illum})

to that in the dark (I_{D_dark}) as $R_{L/D} = I_{D\_illum} / I_{D\_dark}$ [41]. We can find that the $R_{L/D}$ of the gate-near-source one is larger not only in OFF region (Vgs = -10V) but also in ON region (Vgs = 10V). In aspect of application, the gate-near-source one has better photosensitivity to be the sensing device. From Fig. 3-3(b), the $R_{L/D}$ can achieve to 4 orders both in OFF region and ON region.

Since the operating region of sensing device should be properly in sensing circuit, we examine the device performance in different operation regions. Fig. 3-4 shows the OFF current and ON current versus the backlight intensity. They cannot be compared directly because of the different current levels. To analyze the photosensitivity in detail, we normalized the curves of Fig. 3-4 (a) (b) and show the results in Fig. 3-5(a). Next, we differentiate the normalized current to the illumination intensity. The relative photosensitivity versus illumination intensity is showed in Fig. 3-5(b). There is an intersection point at about 10000 lux. It means that the sensing device operated in ON region has better photosensitivity under 10000 lux illumination. On the contrary, the device operated in OFF region has better photosensitivity above 10000 lux. On the basis of the following reasons, we decided to operate the sensing device in ON region to sensing backlight. In TFT-LCD, backlight must pass through the polarizer and then achieve the TFT array layer. The actual backlight intensity illuminate on the TFT array would not over 10000 lux. Another reason for choosing ON region is that the ON current is higher about 2 orders than OFF current, which can reduce the effect of noise and be read easily.

The non-conventional TFT can detect the backlight because the gap exists. Fig. 3-6 shows the transfer characteristics of the gate-near-source TFT with different gap sizes (i = 5um、12um、30um). When the gap increases, the photosensitivity will be higher in ON region. Theoretically, we should use the gap as large as possible for

great photosensitivity of the backlight sensing, but it will reduce the pixel aperture ratio. Besides, for the TFTs of the various gap lengths, the different dark current levels lead us to hardly analyze and apply to sensing circuit. To reduce the variables, we use the gap size i = 30um to be the experimental devices.

For further understanding of the relation between the gap and the photo effect, we design different structures of gate-near-source TFT, as shown in Fig. 3-7(a). It can be seen that there are two gates in the new devices, and the length between original bottom gate and the drain is still 30 um. The function of the extra gate is to shield the backlight illumination. The extra gate does not be given any bias, in other words, it is floating. The new devices are benefit to control the photo response without dark current change. We define "Open-ratio" to name the new structures. For example, the original structure which gap can be illuminated entirely then we call it open-100%. If the area of gap is shielded 67% from backlight illumination by floating gate, then we call it open-33%. Fig. 3-7(b) shows that I_{D_illum} is proportional to the open-ratio. It means that the photo effect is proportional to the illuminated area of the gap.

3.3 Error Analysis

After realizing the device properties, some factors caused error on sensing TFTs are considered in this section.

3.3.1 Device Uniformity

3.3.1.1 ON Current Variation

The measured ON currents of eight devices with respect to the illumination intensity are shown in Fig. 3-8(a). Four of them are on sample-A glass substrate and the other four are from another glass substrate sample-B. We average the eight measured currents, and take it as the reference. Then, the originally measured current

is looked up the illumination intensity according to the reference. This corresponding backlight intensity is called $Lux_{measured}$. Since it is different from the device really shined, the light intensity (Lux_{real}), the error can be defined as "$\frac{Lux_{measured} - Lux_{real}}{Lux_{real}}$". Fig. 3-8(b) shows the error from the on current variation of the eight devices. It has a maximum error 7.5% at 5400 lux illumination.

3.3.1.2Threshold Voltage Shift

For the effect on Vth shift, we simulate it by changing Vgs level. Fig. 3-9(a) shows the ID at Vgs=9V, 10V, and 11V, which represents the influence of Vth shift ±1V in the case of Vgs=10V. We find that there has little change owing to Vth shift. It can be understood from the insert diagram in Fig. 3-9(a). The diagram shows the *ID_illum* is almost independent of the gate voltage in ON region. Similarly, we take the Vgs=10V as a reference, and then calculate error of the cases of the Vgs=9V and Vgs=11V corresponding to the backlight intensity. From the result of Fig. 3-9(b), the maximum error is only 3.28%, which shows that the threshold voltage shift will not cause too much influence to light sensing.

3.3.2 Temperature

In application, the sensor is embedded in TFT array, and the panel's internal temperature will change during usage. Thus, we need to consider the temperature effect of device. Assume 40℃ is the panel's normal operating temperature, and it is subject to ±5℃ variation. Fig. 3-10(a) shows the measured current of device-1 at 35℃、40℃ and 45℃. Calculating the error of four devices, we find the maximum error can be up to 16.4%, which cannot be neglected and needs to be reduced.

Fig. 3-11(a) shows the curves of the photo drain current versus temperature. With the temperature increasing, the drain current also raises gradually [42]. We fit

these curves linearly and define the slopes as a temperature coefficient (TC). Under different illumination intensities, we can get the different TCs. It means that the device does not have the identical response to temperature under different illumination intensities. Fig. 3-11(b) further shows the relation between TC and illumination intensity for four devices. We find there is an obvious variation of temperature response from device to device. This phenomenon will make it more difficult to develop a calibration method. Therefore, for reducing the error caused by temperature variation, we propose to control the temperature of the panel instead of calibrating it. When the temperature variation is controlled within ±3.5℃, and the error can be reduced to 10%.

3.3.3 Device Reliability

3.3.3.1 Staebler-Wronski (SW) effect

Several possible sensing error factors like device uniformity, temperature, and instability of a-Si must be considered. However, from the study of photo current response of a-Si:H TFTs, Staebler-Wronski (SW) effect is a dominant influence to light sensing [43~45]. The predominant explanation of the effect is that the illumination leads to the creation of additional meta-stable states in the band gap of the amorphous silicon, by breaking the weak bounds of the hydrogen atoms to the silicon, which decreases the lifetime of excess carriers and thus reduces the photoconductivity.

To study the SW effect, we use 19160 lux backlight to illuminate the device, and the stress time is from 0 sec to 4800 sec. Fig. 3-12 shows the result of optical stress. It can be observed that the current degrades obviously with stress time increasing. In addition, the exposure time of the measurements (15 sec.) is much less than light stress time (600 ~4800 sec). Hence, we neglect the degradation resulted

from measurements. Compared with other error factors, SW effect is very serious. If it is not calibrated, the device cannot be applied at all. In this work, a method will be proposed to solve this issue. Before explaining the calibration method, we mentioned the I_{D_illum} is proportional to the illuminated area of gap. After optical stress, the device with larger open-ratio will suffer from worse stress because the gap area is larger. The different stress levels will result in the nonlinear dependence of photo current on the operation as shown in Fig. 3-13.

3.3.3.2 Calibration method of Staebler-Wronski effect

Before introducing the calibration method, we define the ID/Open-ratio as the new index. The ID/Open-ratio versus open-ratio before stress is shown in Fig 3-14 (a). It can be found that the ID/Open-ratio is independent of open-ratio before stress. Since the device's degradation level associates with illuminated intensity, stress time as well as illuminated area, it implies that the larger open-ratio structure will degrade more. Fig. 3-14 (b) shows ID/Open-ratio behavior of the stressed devices. The one with 100% open ratio degrades most. The smaller open-ratio structure subjects to smaller influence from SW effect. The first idea coming to mind is to find the open-0% structure which means it will not be stressed by backlight. Since there is no open-0% structure of gap-type TFT, which will become conventional TFT and insensitive to backlight, it could be alternatively achieved by extrapolating the ID/Open-ratio behavior with different open ratios. For example, Fig. 3-15 (a) shows the result of extrapolation. A formula in the form of y=a+b*[exp^(-x/c)-1] by OriginPro software is used to extrapolate the case of 0% stress.

After the calibration, the maximum error shown in Fig. 3-15 (b) can be reduced to about 13.6%. Here the "Error" is defined as $[(Lux_{measure}-Lux_{real})/ Lux_{real}]$. For the case without the calibration, the value, $Lux_{measure}$, can be evaluated from the measured

drain current of the gap-type TFT. The initial relationship between illuminations and drain current of the gap-type TFT can be obtained by the behavior shown Fig. 3-6(c). For the proposed calibration, the drain current of open-0% structure of gap-type TFT can be obtained by extrapolation to evaluate the value $Lux_{measure}$ based on the illuminated characteristics of Fig. 3-14(a). In the Fig. 3-15(b), the "without correction" curves present the errors produced by SW effect on Open-100% gap-type TFTs, and the "with correction" curves present the errors modified by the proposed calibration method. In the proposed method, the different open-ratio gap-type TFTs will be implemented in neighboring sensing pixels to ensure these gap-type TFTs are exposed to almost equal illumination intensity and our calibration can be thus executed. This result indicates that the calibration method is very effective to lower the influence of SW effect.

In reality, the backlight intensity is not always fixed. Therefore, it would be of practical interest to verify the feasibility of the aforementioned calibration method under changed backlight stress. In the following study a two-step backlight illumination is used. From 0 to 3600 sec, the devices are stressed by l0000 lux backlight. And in the following 3600 sec, the devices continue to be stressed by l9160 lux backlight. Because of the different stressed intensities, the curves present two different degradation rates as shown in Fig.3-16. As for the calibration method, Fig. 3-17(a) shows the characteristics stressed by the two-step light intensities and illustrates the same trend as Fig. 3-15 (a), which is stressed under the fixed backlight intensity. The same proposed method is used to calibrate the influence of SW effect. The error in different stress condition is shown in Fig. 3-17(b). It can be seen that the proposed calibration method still can calibrate the SW effect effectively under the changing backlight illuminating situation.

3.4 Backlight Sensing Circuit

3.4.1 Sensing Circuit and Operation

Based on the results mentioned above, a new light sensing circuit with only one readout bus is proposed. The schematic diagram of 4T2C circuit and its timing diagram are shown in Fig. 3-18(a). The sensing part is composed of a reset TFT, a photo TFT, two capacitors, Cc and Cs. The readout part is composed of a source follower and a switch TFT.

The operating principles can be described as two periods, as shown in Fig. 3-18(b). In the reset period, the signal of scan line 1 (-10V~10V) becomes “high”, and the reset TFT is turned on. Thereby, the voltage of node A is charged to Vcom (5V). In the discharging period, the scan line 1 signal becomes “low”, reset TFT is turned off. Meanwhile, the signal of the scan line 2 becomes “high”, the photo TFT is operated in ON region. The backlight is turned on during the discharging period. At the same time, the voltage of node A rise to a relatively high voltage to Vcom owing to the couple effect from the voltage changing of scan line 2 through Cs. Then, the photo current, which is determined by the intensity of the illumination, drained away through the photo TFT. The voltage of node A would be discharged by the photo current of photo TFT, and then voltage change at node A can be followed by source follower and readout through switch TFT line by line. The Cc is especially added to divide voltage of node A to a proper V_D for photo TFT when coupling happened. Meanwhile, it can make sure the voltage at node A be lower than the drain voltage of source follower (Vg, on in our case) for its proper working.

3.4.2 Simulation

Since there is no photo current model for SPICE simulation, we cannot simulate the photo current under different illumination directly. We have to modify the

simulation method according to illuminated characteristics of device. Fig. 3-19 shows the illumination dependence of I_D-V_D characteristics curve; the drain current increased while the illumination intensity enhanced. Then, we fit the curve in the formula, which can be expressed as "ID = $I_0(L)$ + $A_0(L)\times V_D$". The $I_0(L)$ and $A_0(L)$ are intercept and slope, which are illumination dependent. Therefore, we use the different current sources and resistors in parallel to represent the different photo currents of TFT. Table 3-1 shows the values of $I_0(L)$ and R_0 = 1/ $A_0(L)$ at Vgs=10V at different illumination intensities. For the simulation at different illumination intensities, we change the value of $I_0(L)$ and R_0 accordingly. Table 3-2 lists the simulation condition, and Fig. 3-20 shows the SPICE simulation results of light sensing circuit. The illumination intensity can be monitored by the slope of the discharging voltage.

The equivalent circuit and layout of sensor integrated in pixel are shown in Fig. 3-21. We can see the proposed light sensing circuit is compatible to panel's scan lines, and it only needs a readout line to output the signal. Taking 52" full HD panel as example, namely, pixel size of 200x600 um^2, the aperture ratio reduces from 84% (without sensor) to 78% (with sensor). The scarification in aperture is acceptable.

In order to solve the SW effect, a sensing unit should consist of different gap-type TFTs, as shown in Fig. 3-22. Another question comes to us is how dense the backlight sensors are needed to be embedded in the pixel array? Fig. 3-23 shows an example schematic of panel with local dimming function. But the actual situation must be decided according to the arrangement of the backlight modules.

3.5 Summaries

In this chapter, we use a non-conventional TFT, namely, the gap-type structure, to be the backlight sensing device. Taking advantage of its higher current level and

good photosensitivity in ON region to sense light intensity, we proposed a light sensing circuit which is designed to be integrated into pixel and compatible to panel's scan lines. The circuit simulation result by H-spice is quite as we expect. Moreover, we analyze the possible factors that can affect the sensing accuracy. The SW effect is the most serious problem. Nevertheless, it can be reduced significantly by proposed calibration method.

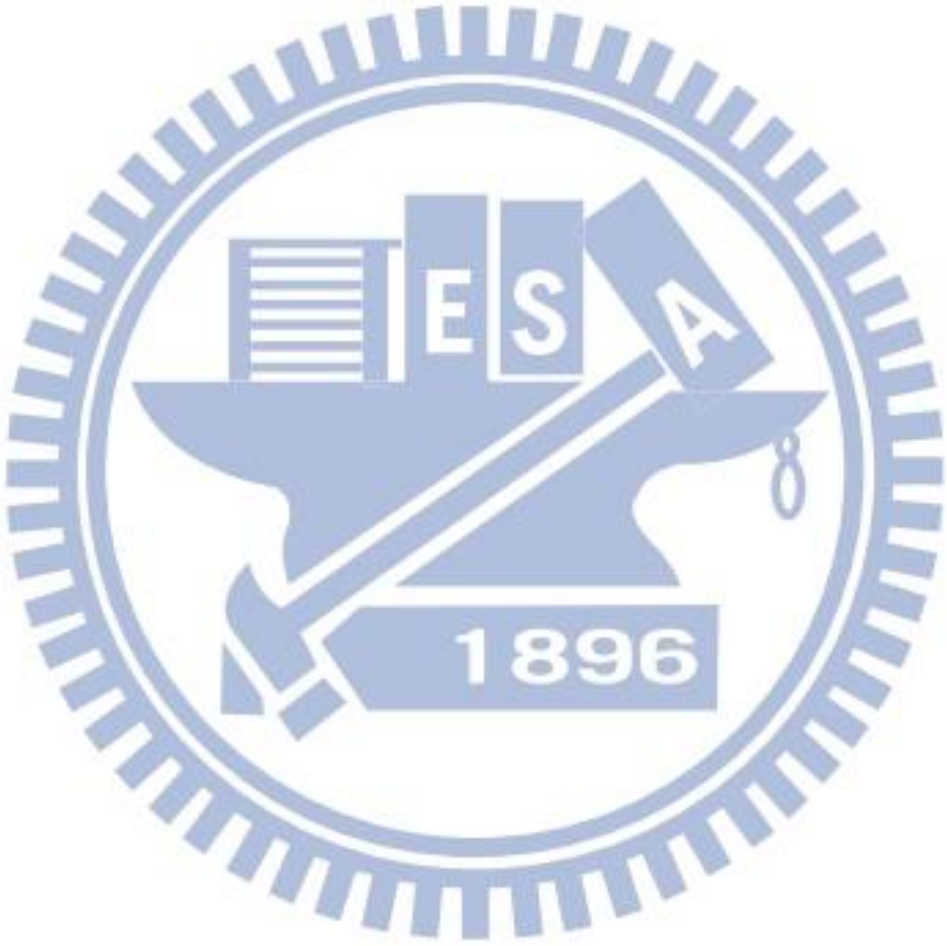

Fig. 3-1 Schematic of local dimming function by LED backlight

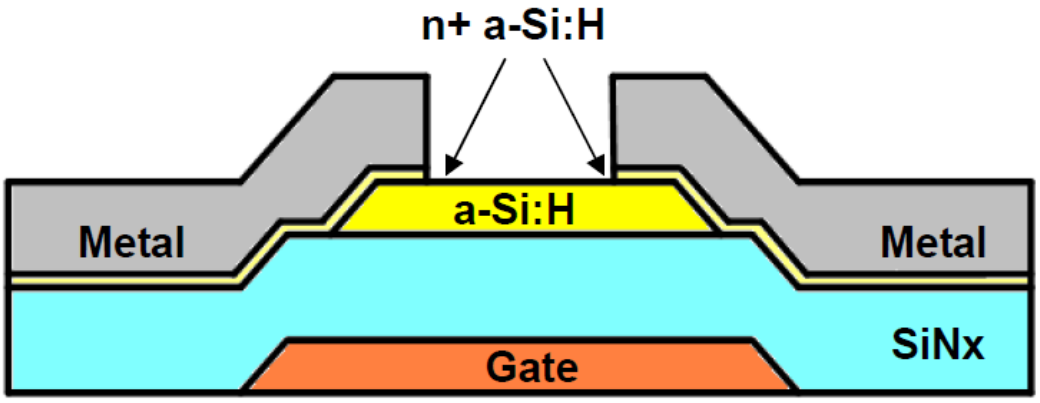

(a)

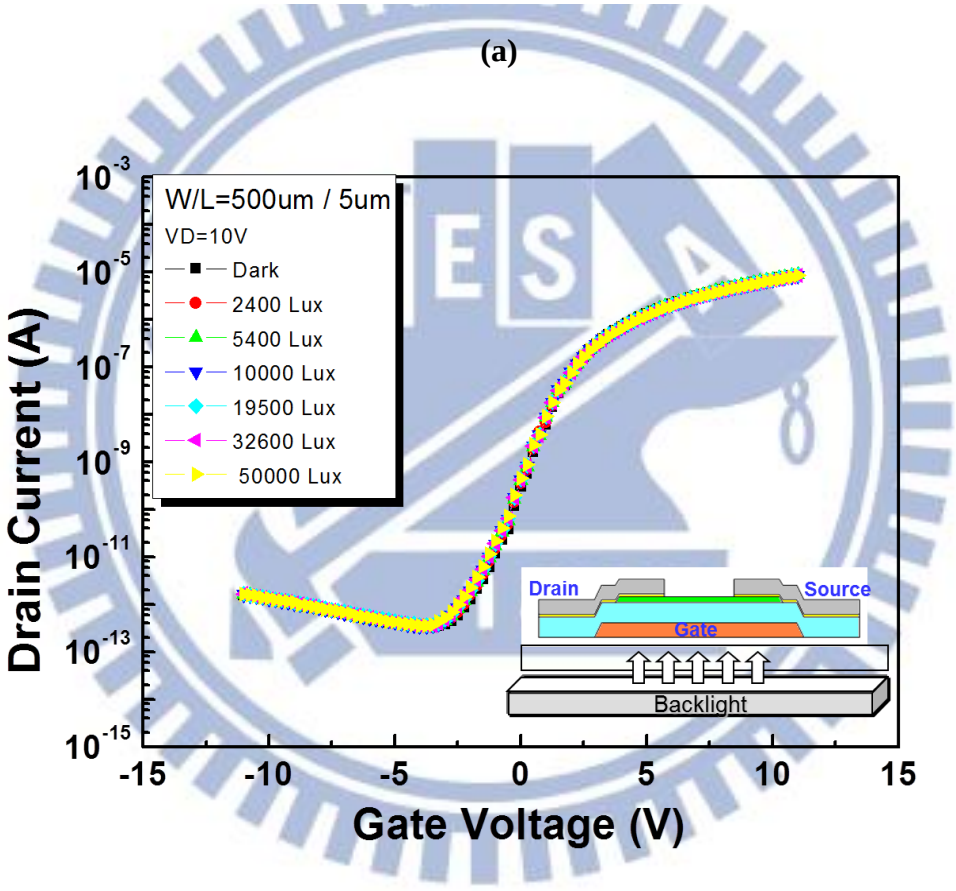

(b)

Fig. 3-2 (a) Cross-section and (b) Transfer characteristics of the conventional a-Si TFT

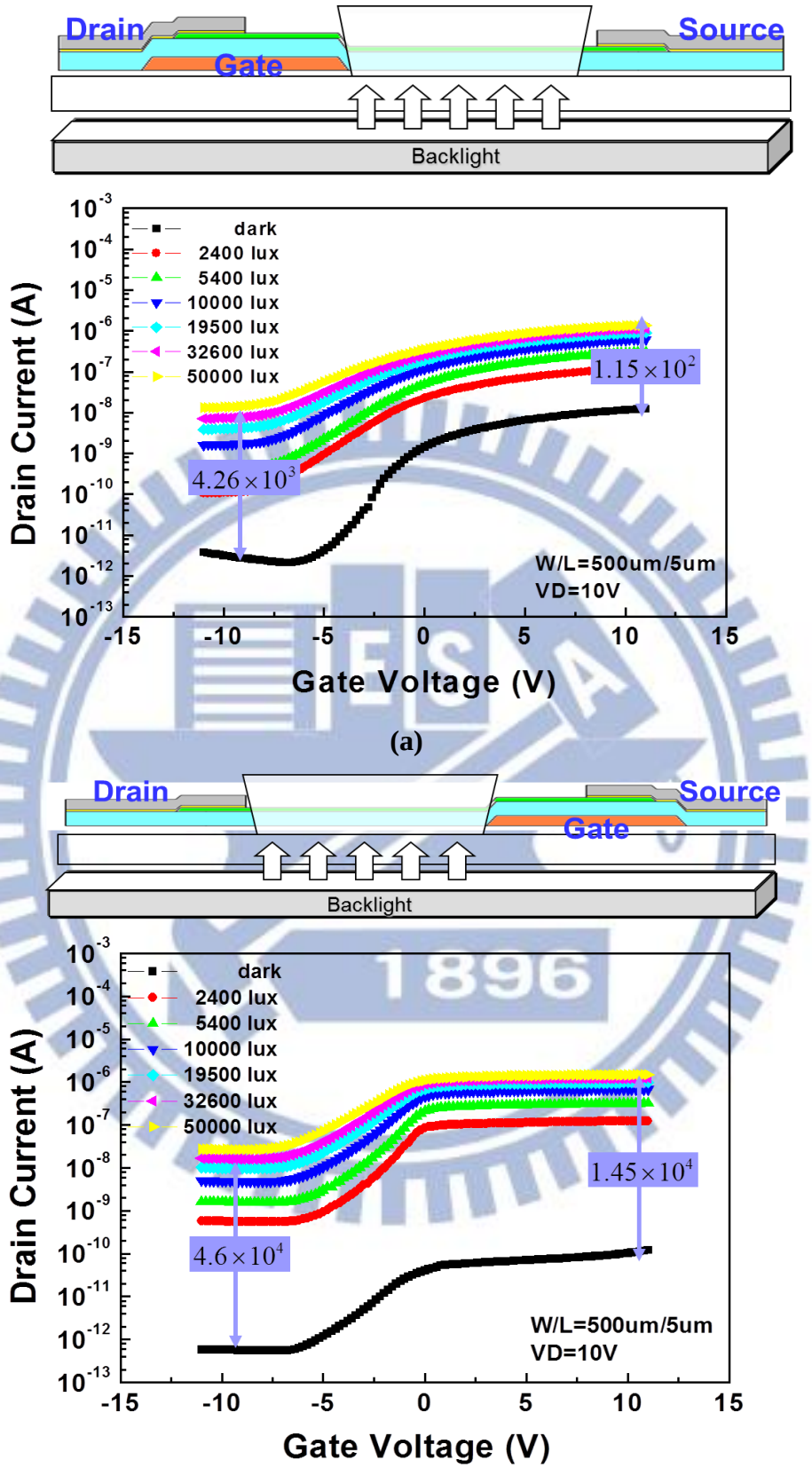

Fig. 3-3 Transfer characteristics of the gap-type a-Si TFT with (a) gate-near-drain mode and (b) gate-near-source mode

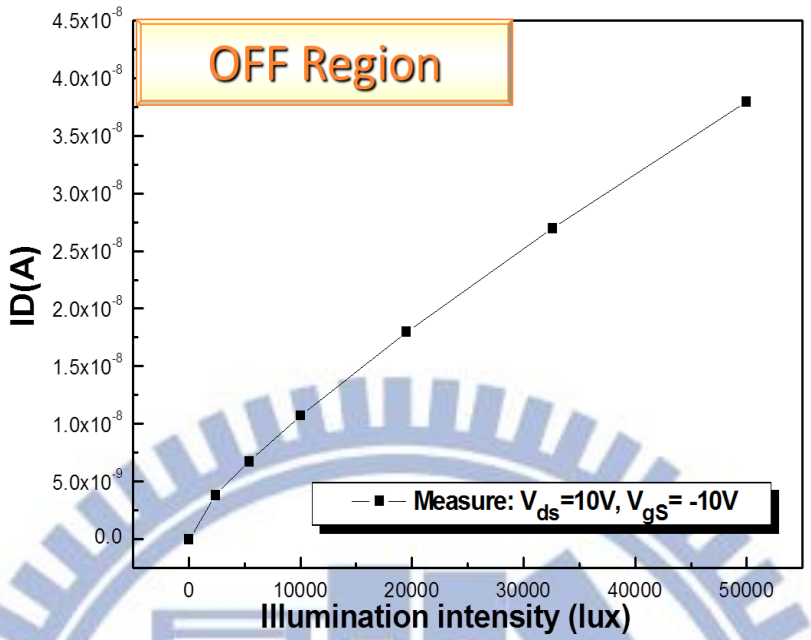

(a)

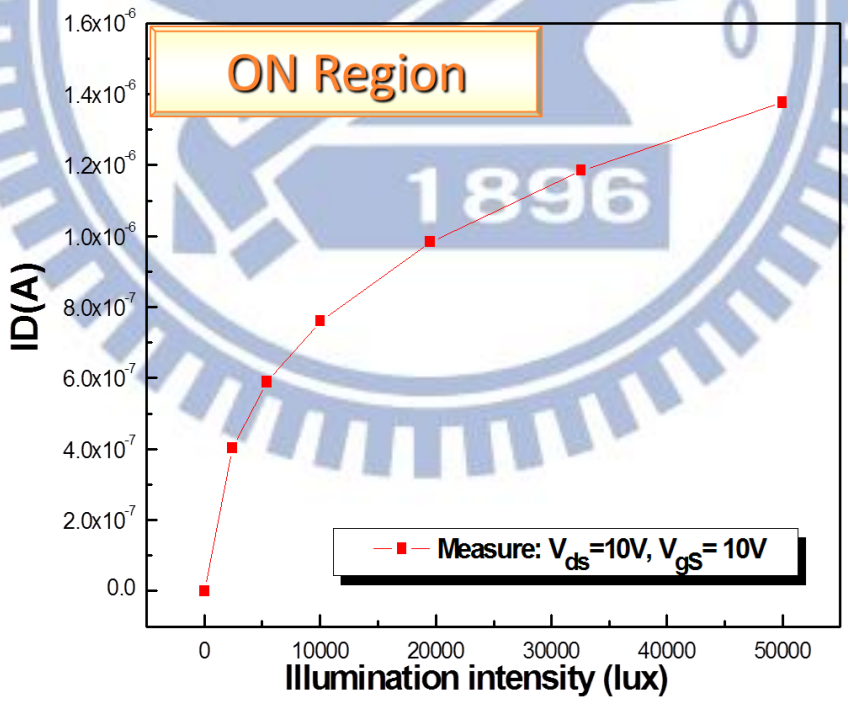

(b)

Fig.3-4 Drain current versus backlight illumination intensity (a) in OFF region (b) in ON region

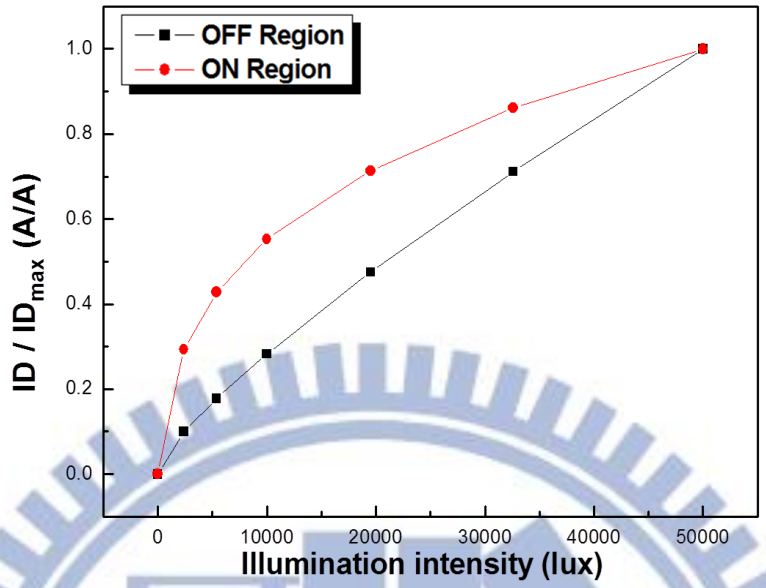

(a)

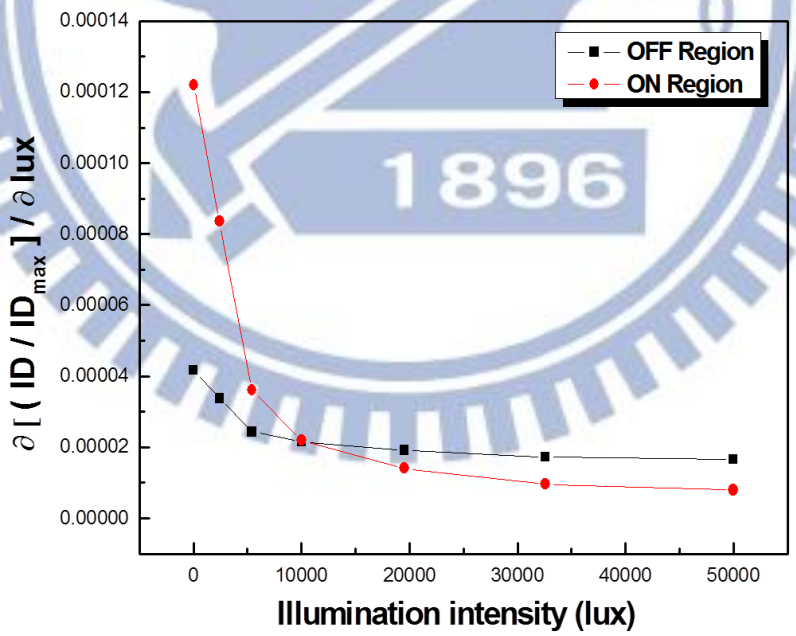

(b)

Fig.3-5 (a) The normalized drain current versus backlight illumination intensity of ON region and ON region (b) The relative photosensitivity of ON region and OFF region

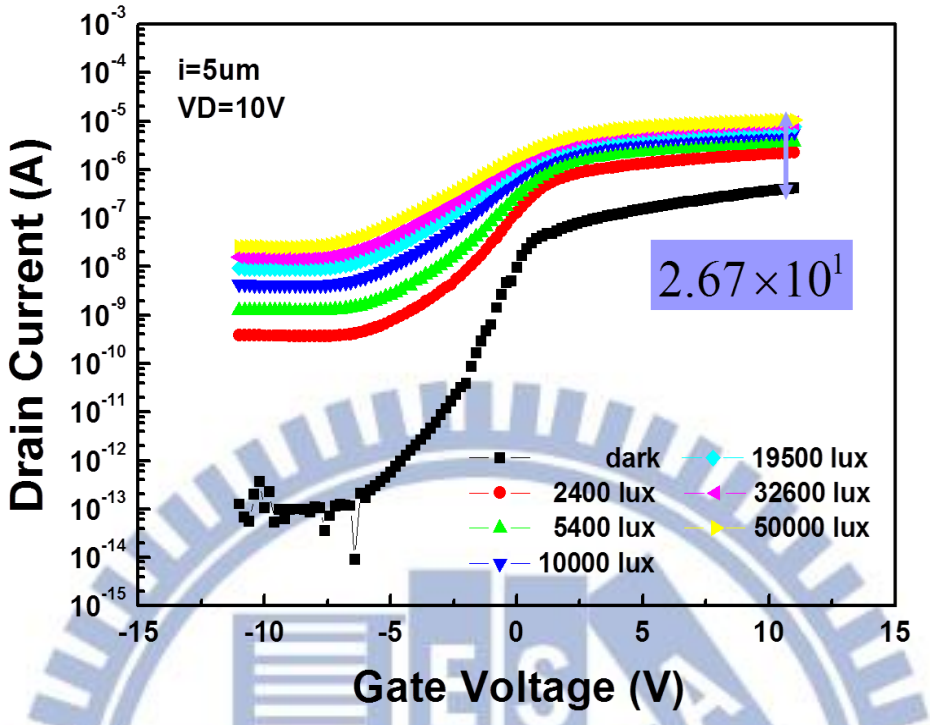

Fig. 3-6 (a)

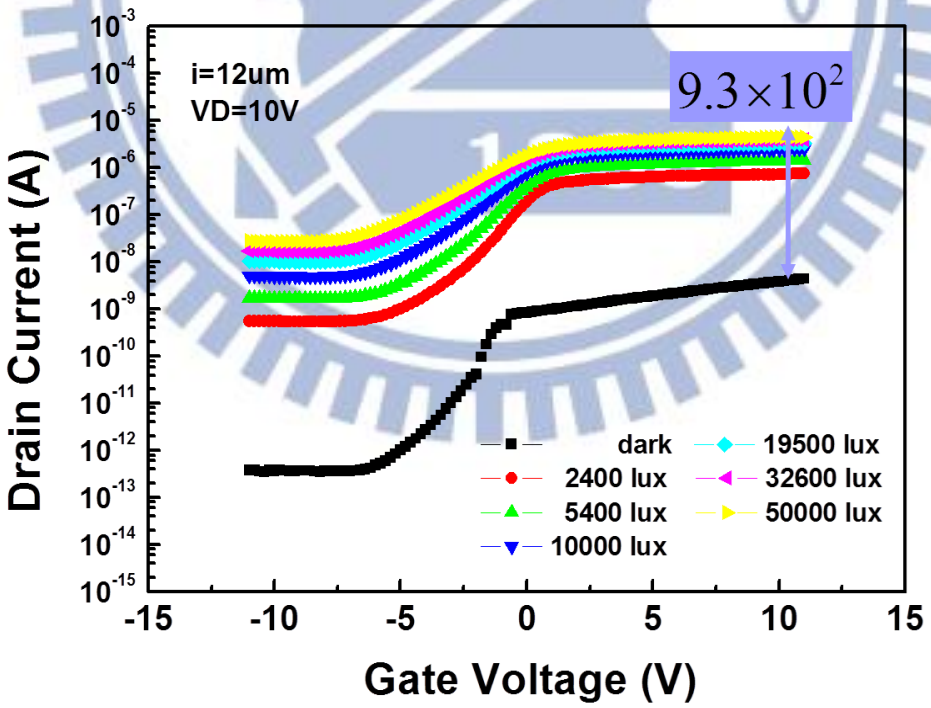

Fig. 3-6 (b)

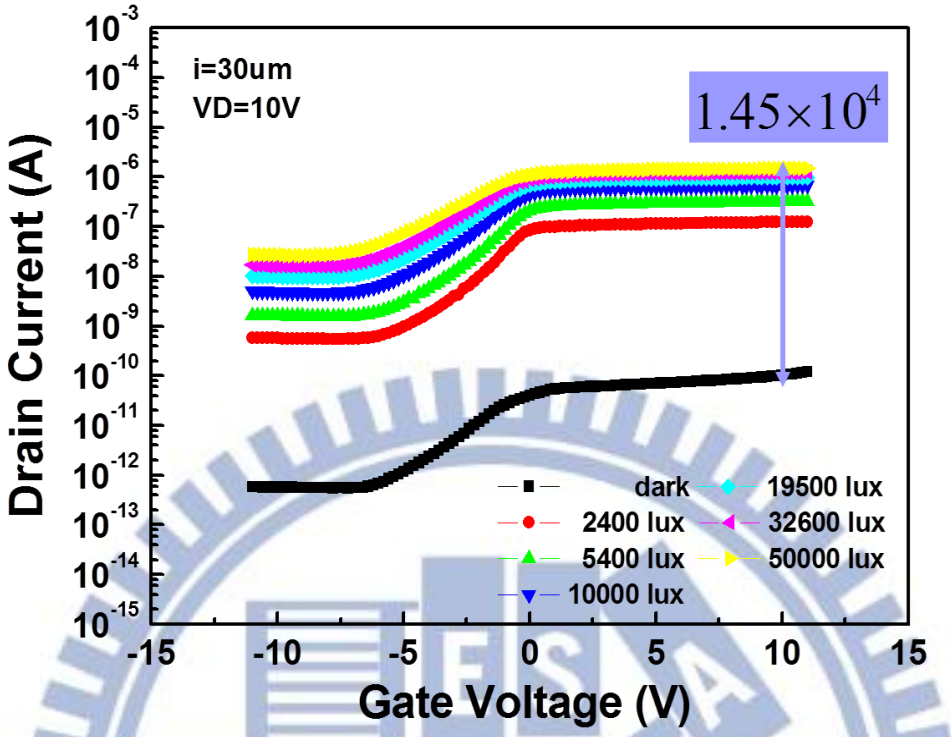

Fig. 3-6 (c)

Fig. 3-6 Transfer curves of the gap-type TFT with different gap lengths (a) i=5um (b) i=12um (c) i=30um

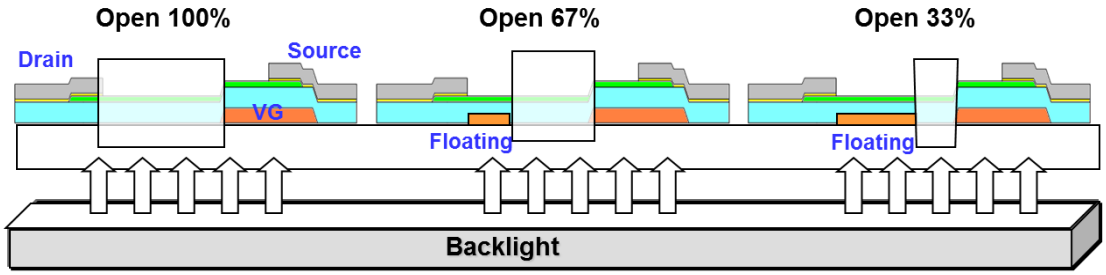

(a)

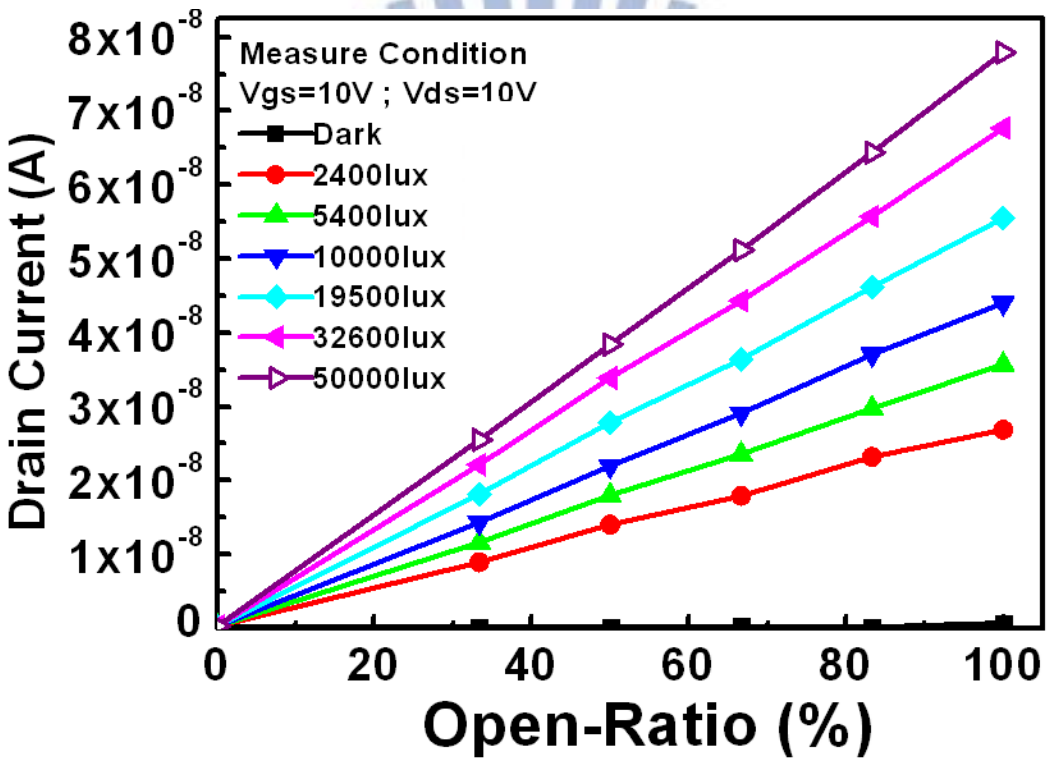

(b)

Fig.3-7 (a) Schemes of gap-type TFTs with different open-ratio (b) The relation between I_{D_illum} and open_ratio

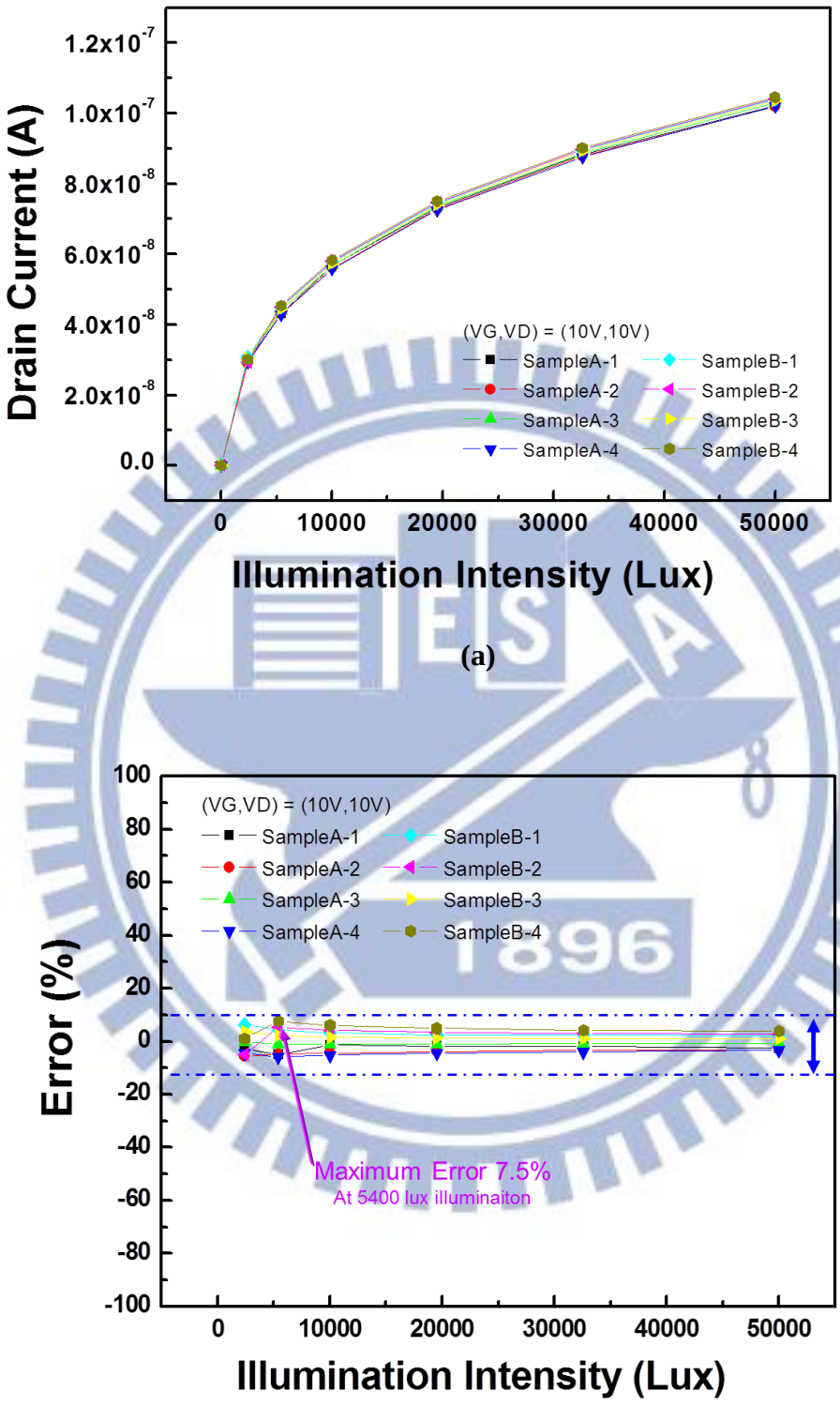

Fig. 3-8 (a) The drain current versus illumination intensity curves of 8 devices and (b) Error analysis of ON current variation between the measured light intensity and the illuminated light intensity

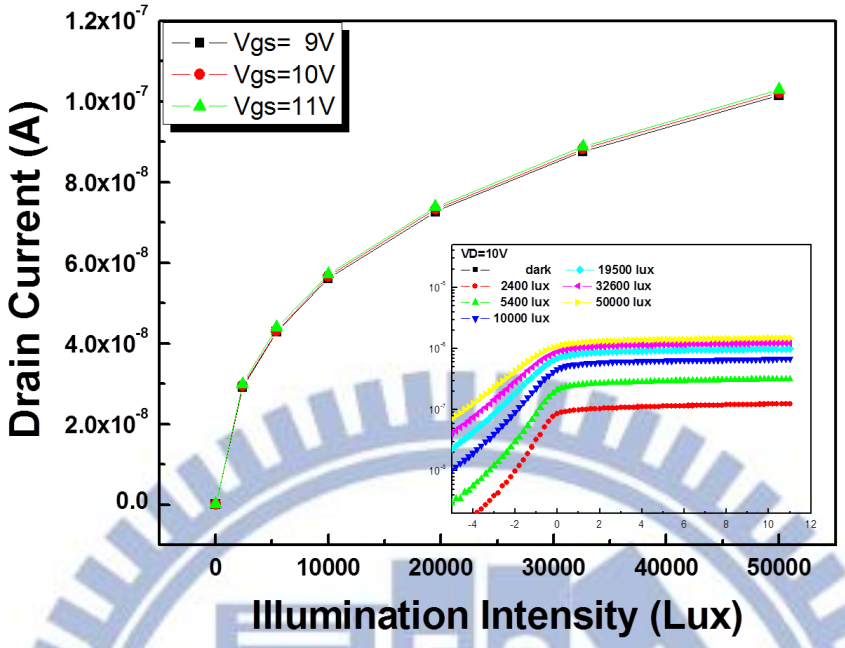

(a)

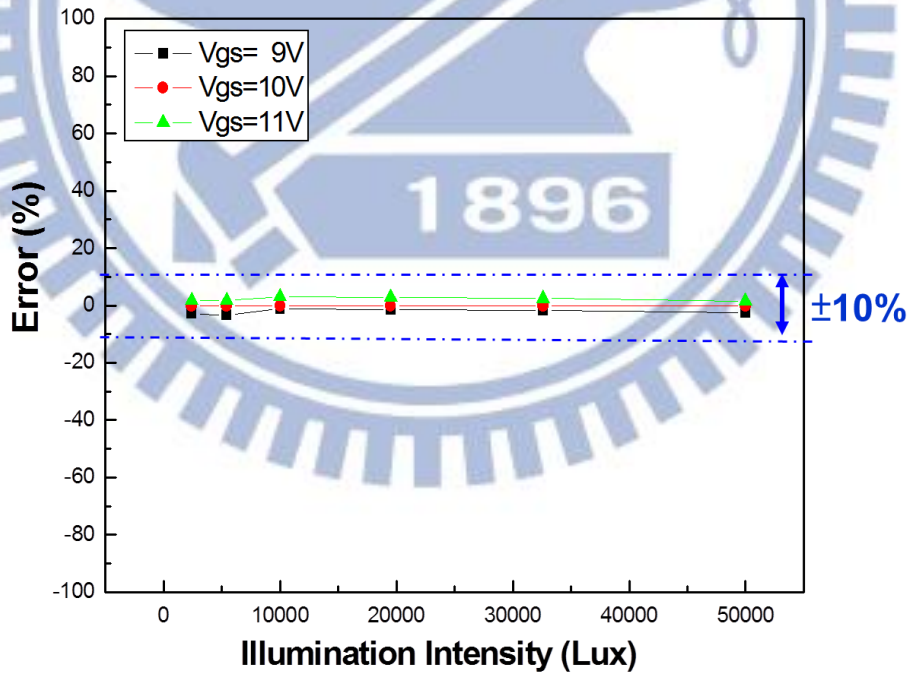

(b)

Fig. 3-9 (a) The drain current versus illumination intensity at Vgs=9, 10, 11 V and (b) Error analysis of the threshold voltage shift between the measured light intensity and the illuminated light intensity

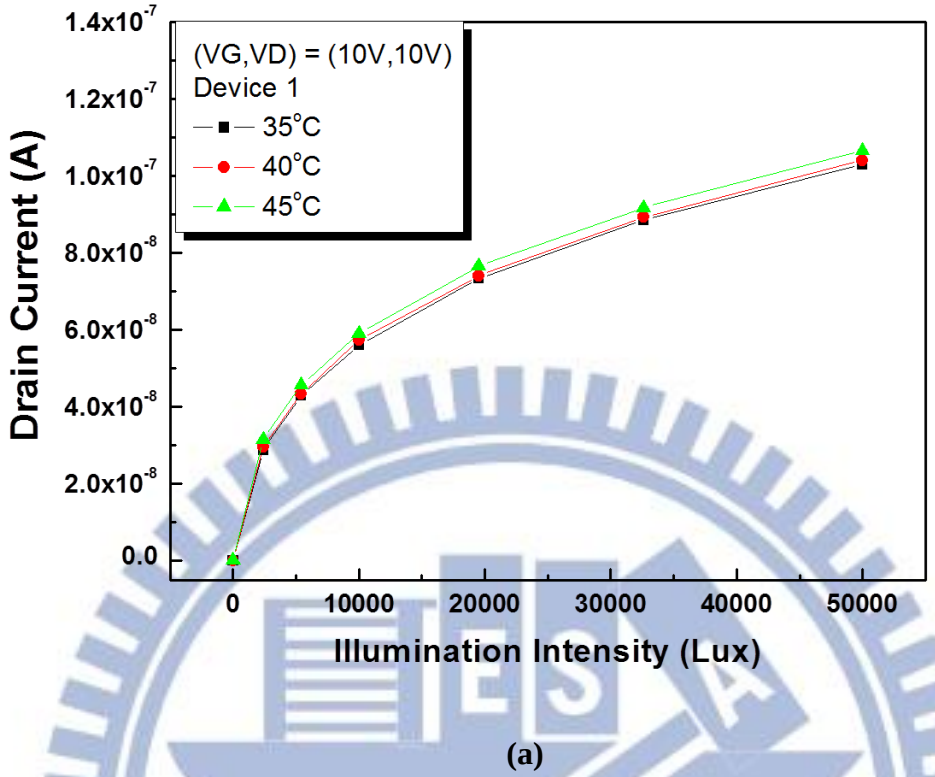

(a)

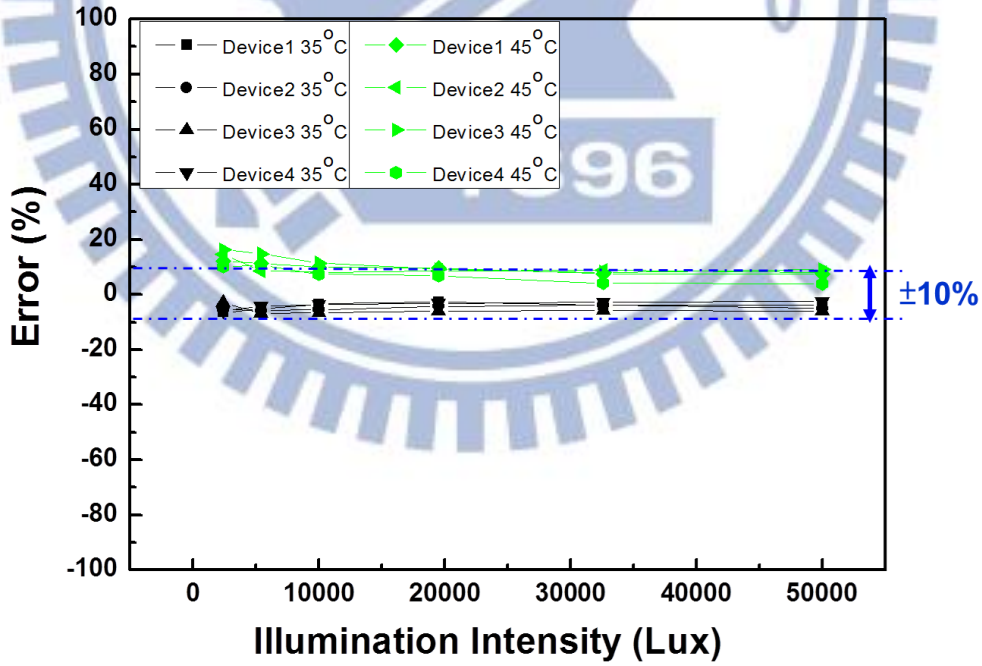

(b)

Fig. 3-10 (a) The drain current versus illumination intensity at T= 35, 40, 45 °C and (b) Error analysis of temperature variation between the measured light intensity and the illuminated light intensity

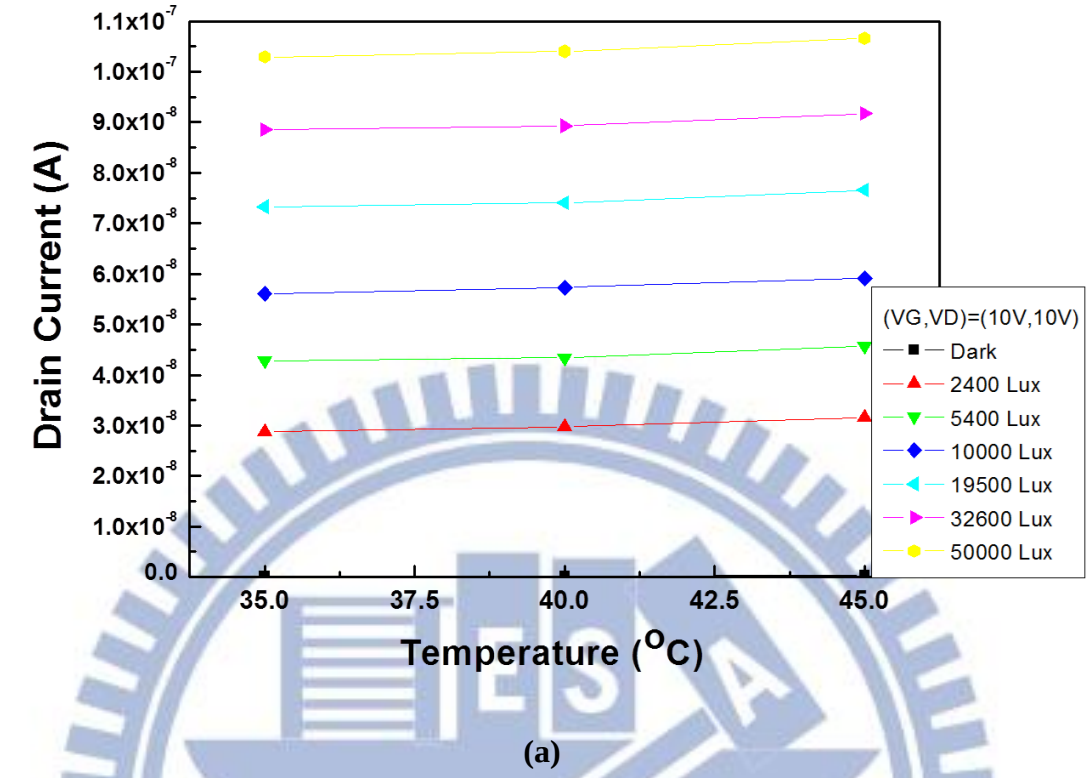

(a)

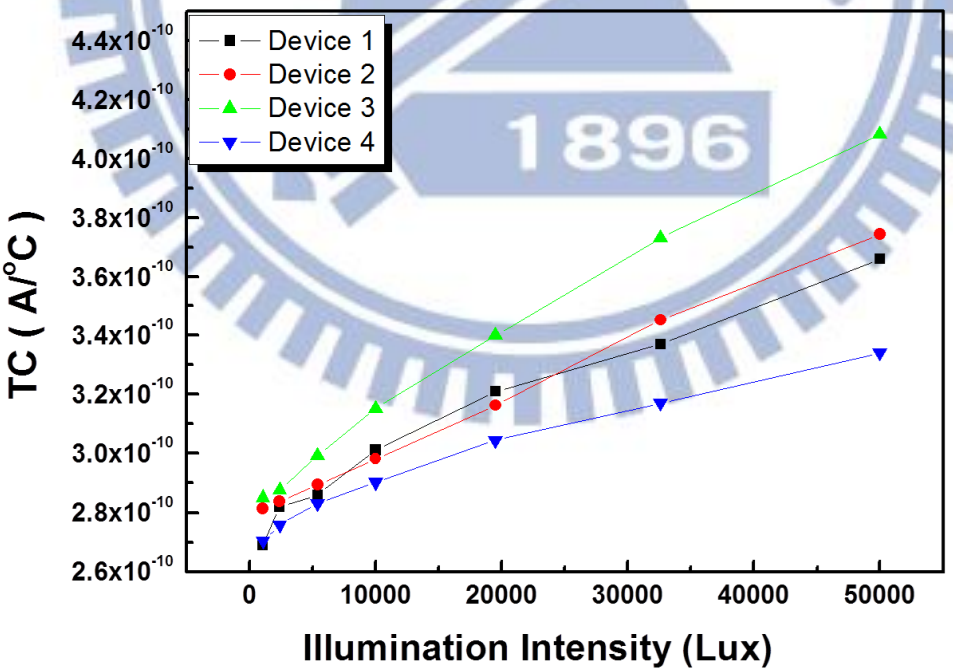

(b)

Fig. 3-11 (a) The drain current versus temperature at Vgs= 10V, Vds= 10V and (b) The TC versus temperature curves of 4 devices

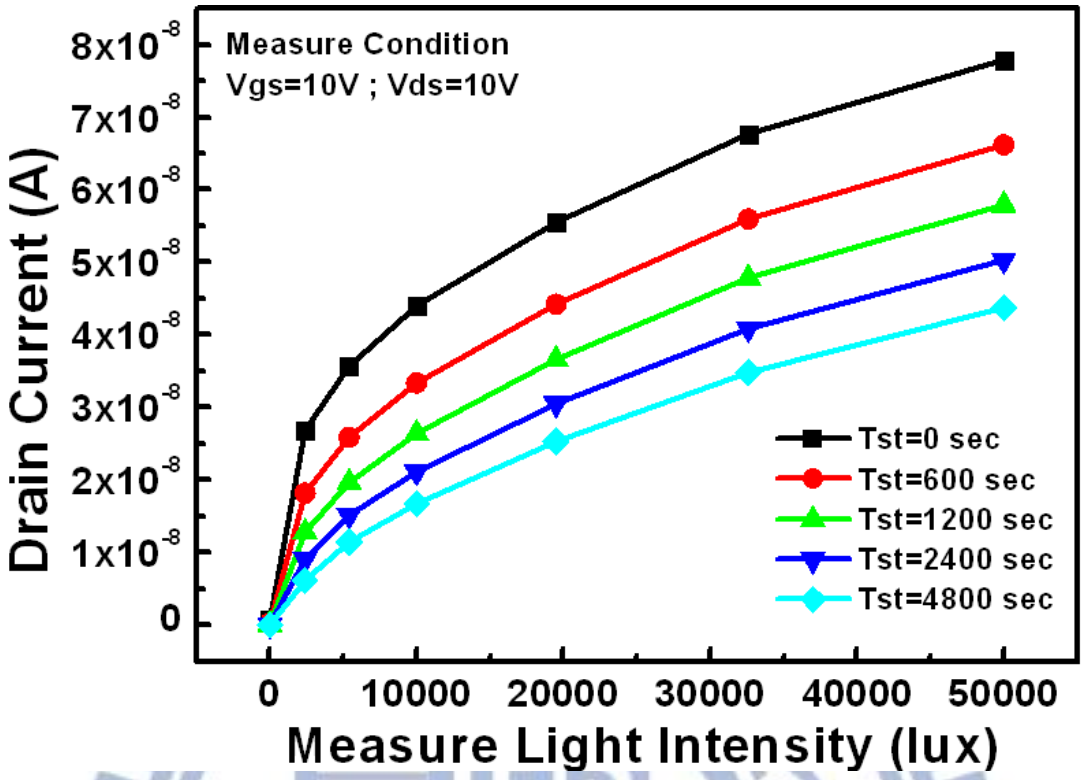

Fig. 3-12 The measured current of a-Si TFT under optical stress

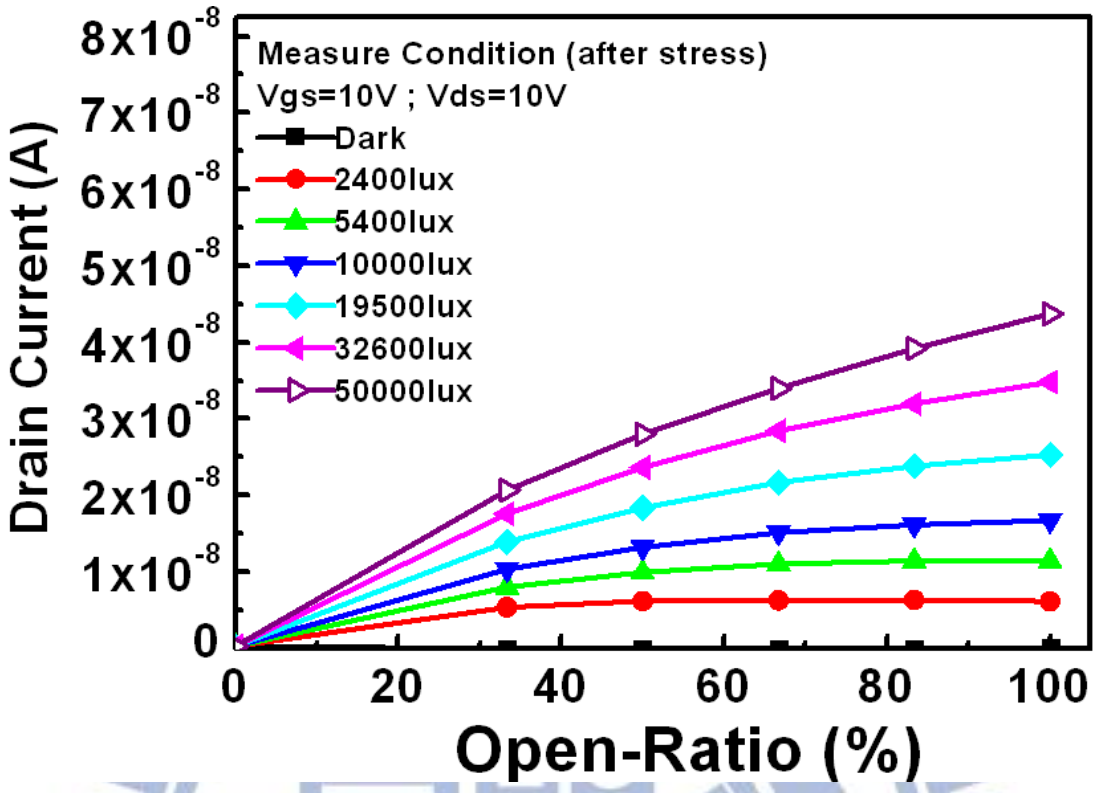

Fig. 3-13 The relation between I_{D_illum} and open_ratio after optical stress

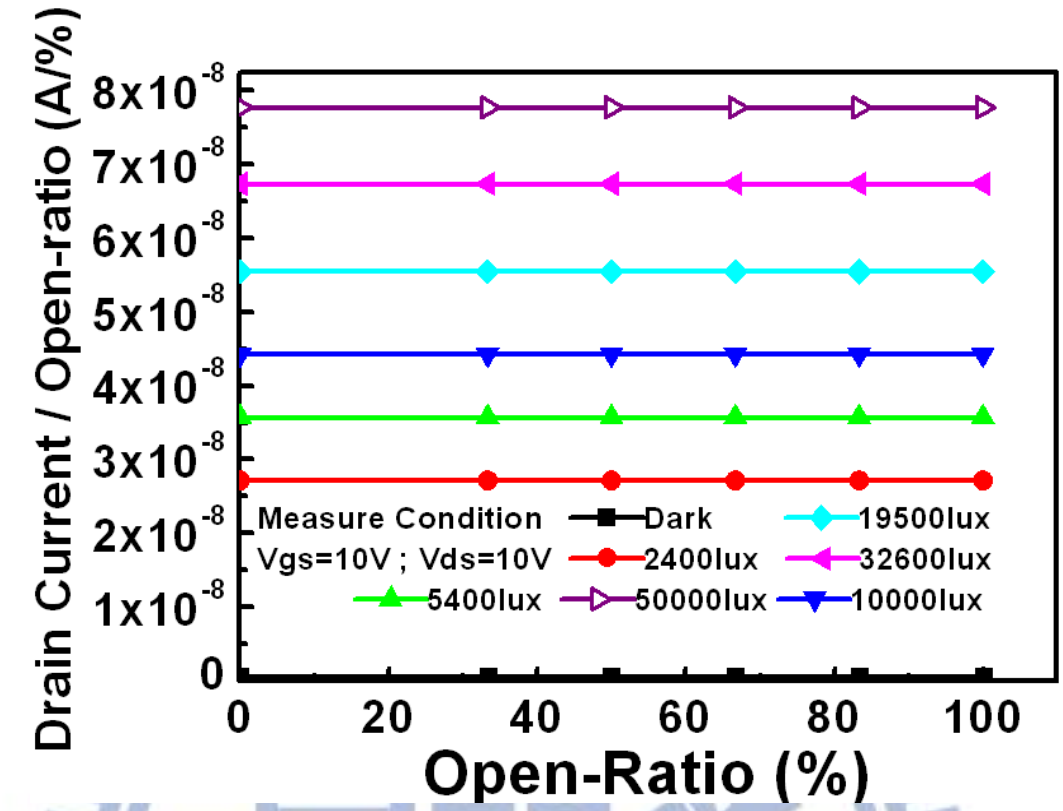

(a)

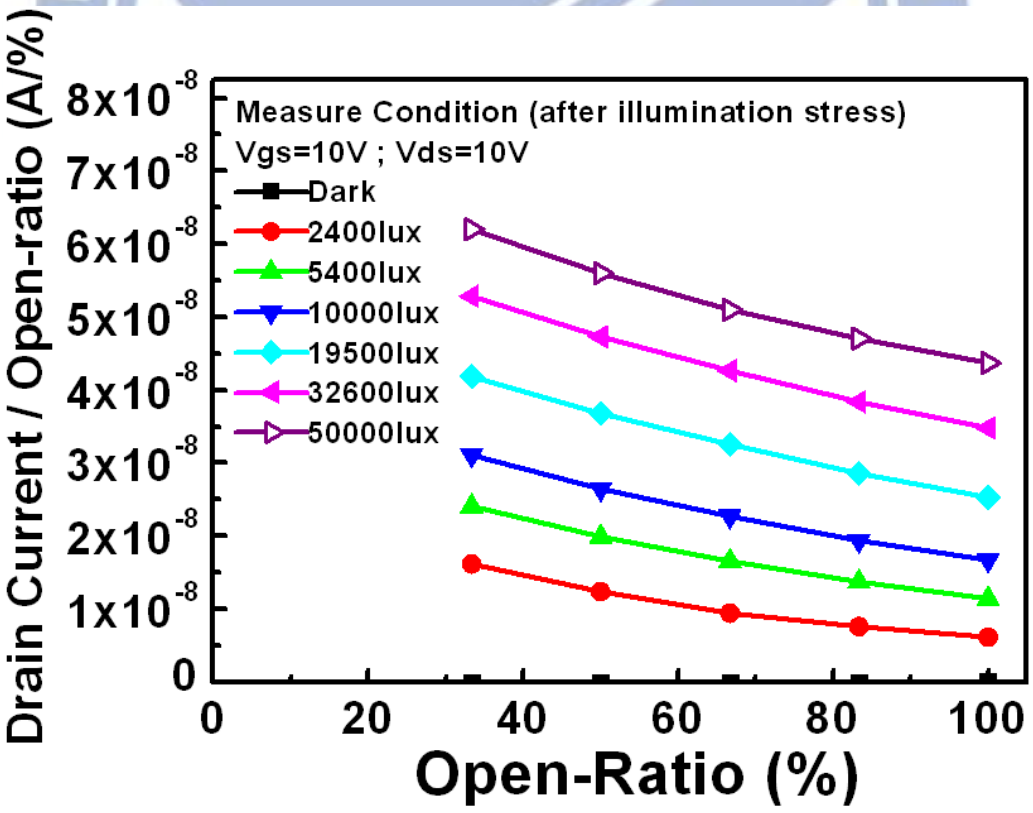

(b)

Fig. 3-14 The ID/Open-ratio versus open-ratio (a) before (b) after optical stress.

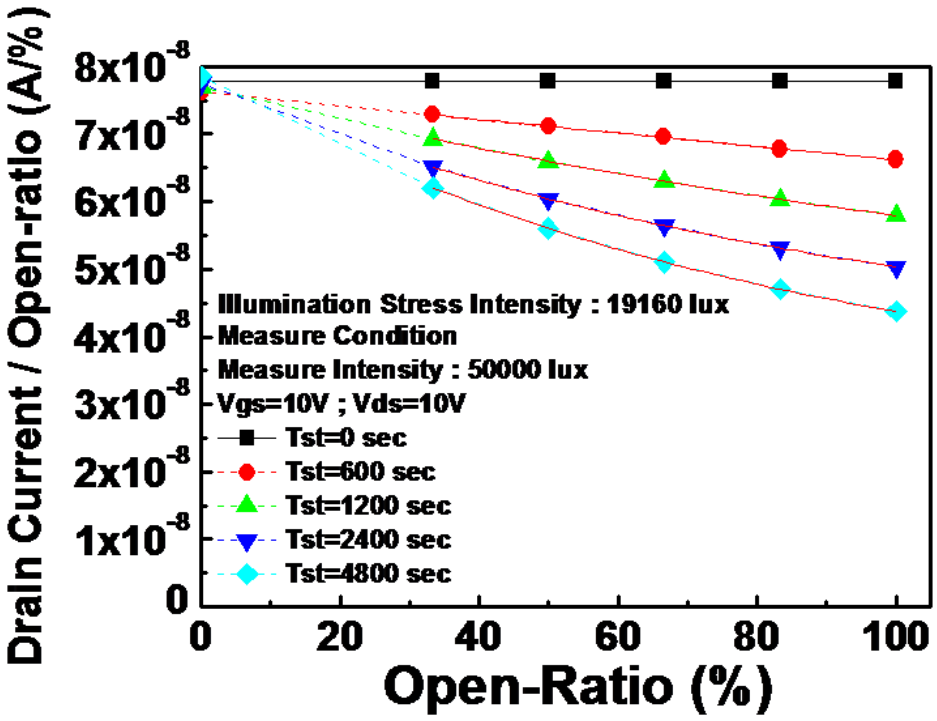

(a)

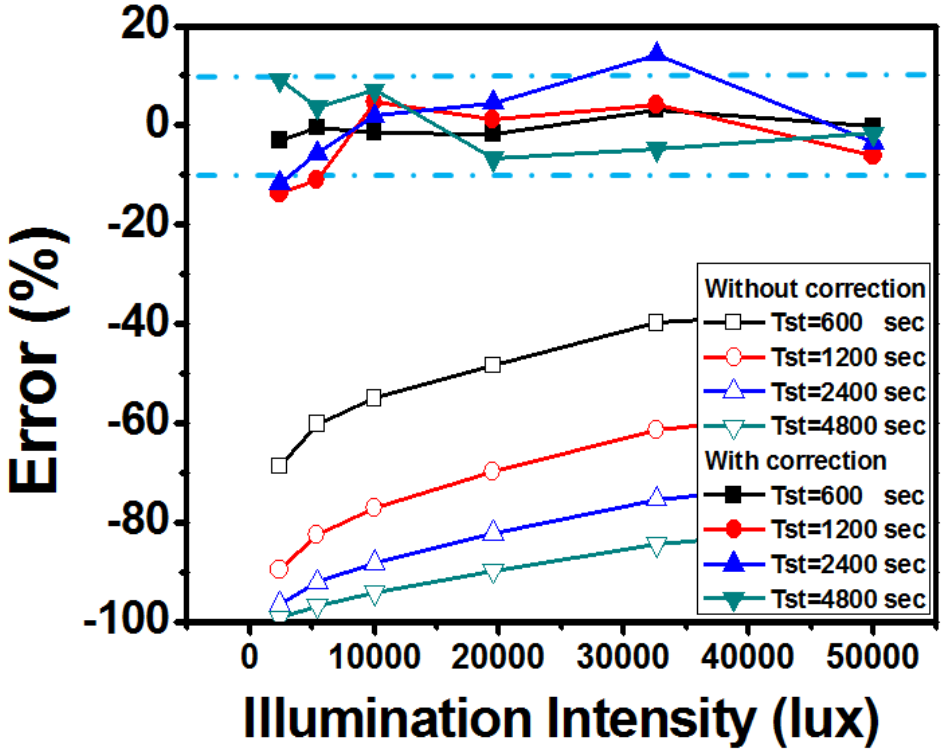

(b)

Fig. 3-15 (a) Calibration of SW effect and (b) error analysis with/without calibration

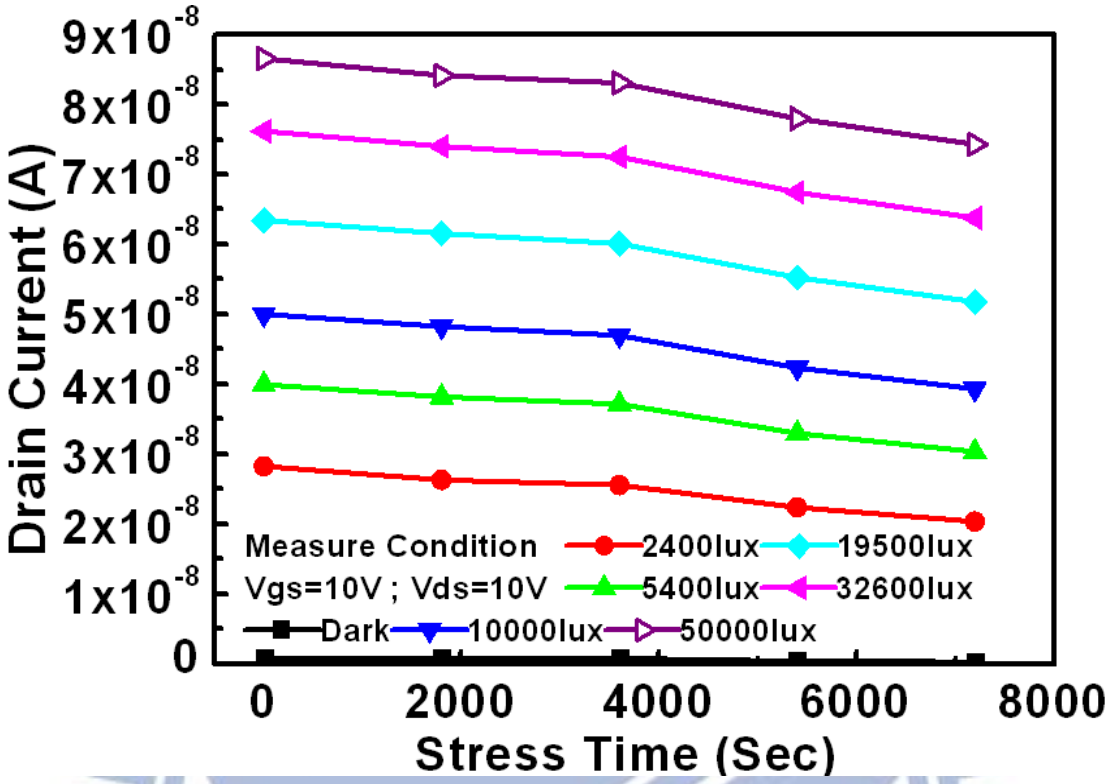

Fig. 3-16 The different stress intensities, the curves present two different degradation rates

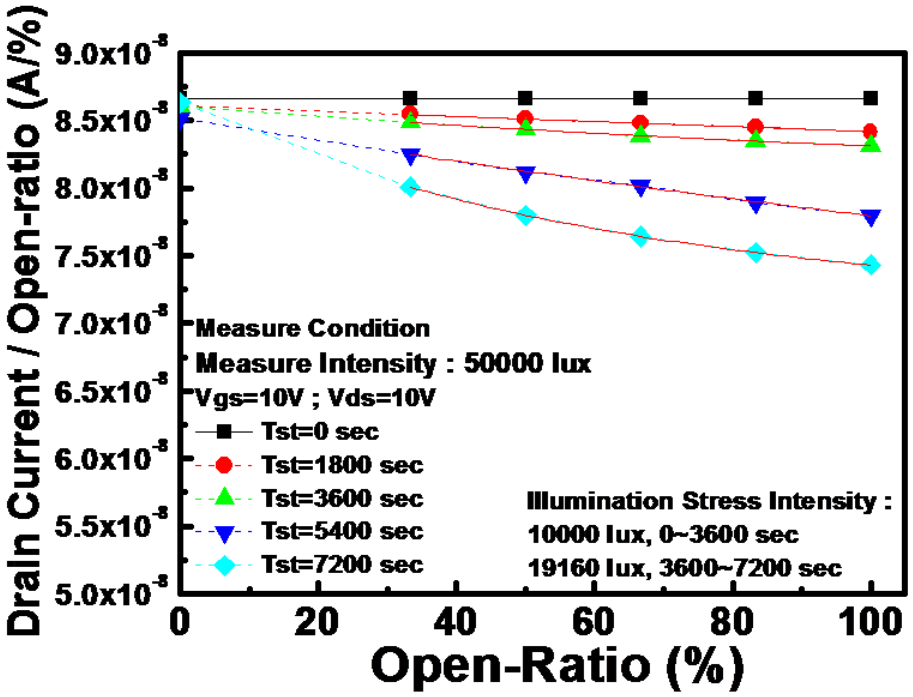

(a)

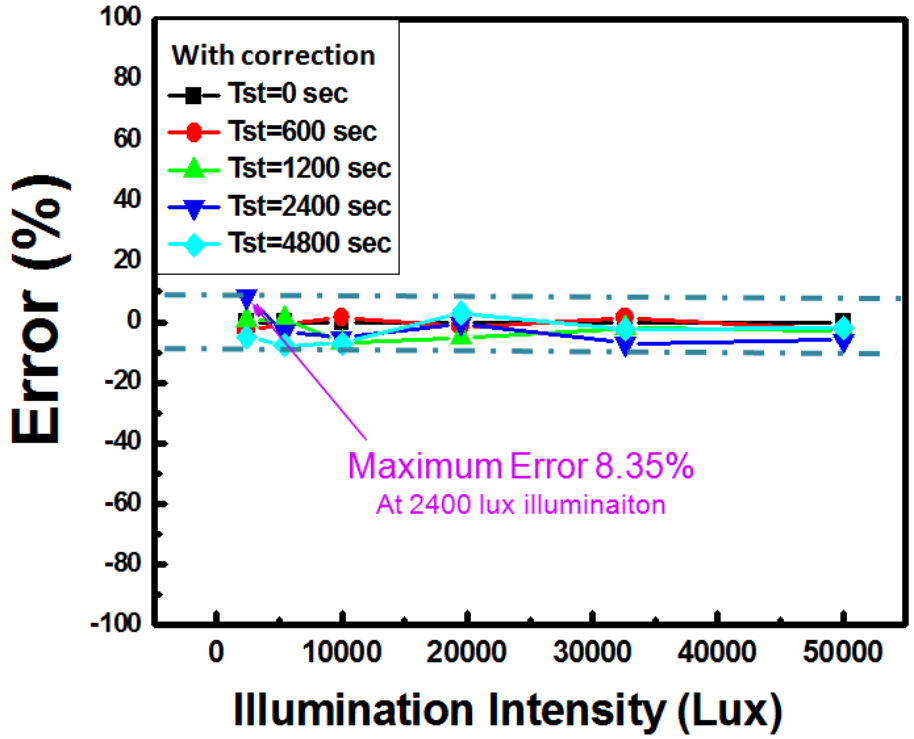

(b)

Fig. 3-17 (a) Calibration of SW effect and (b) error analysis under two-step stress intensities

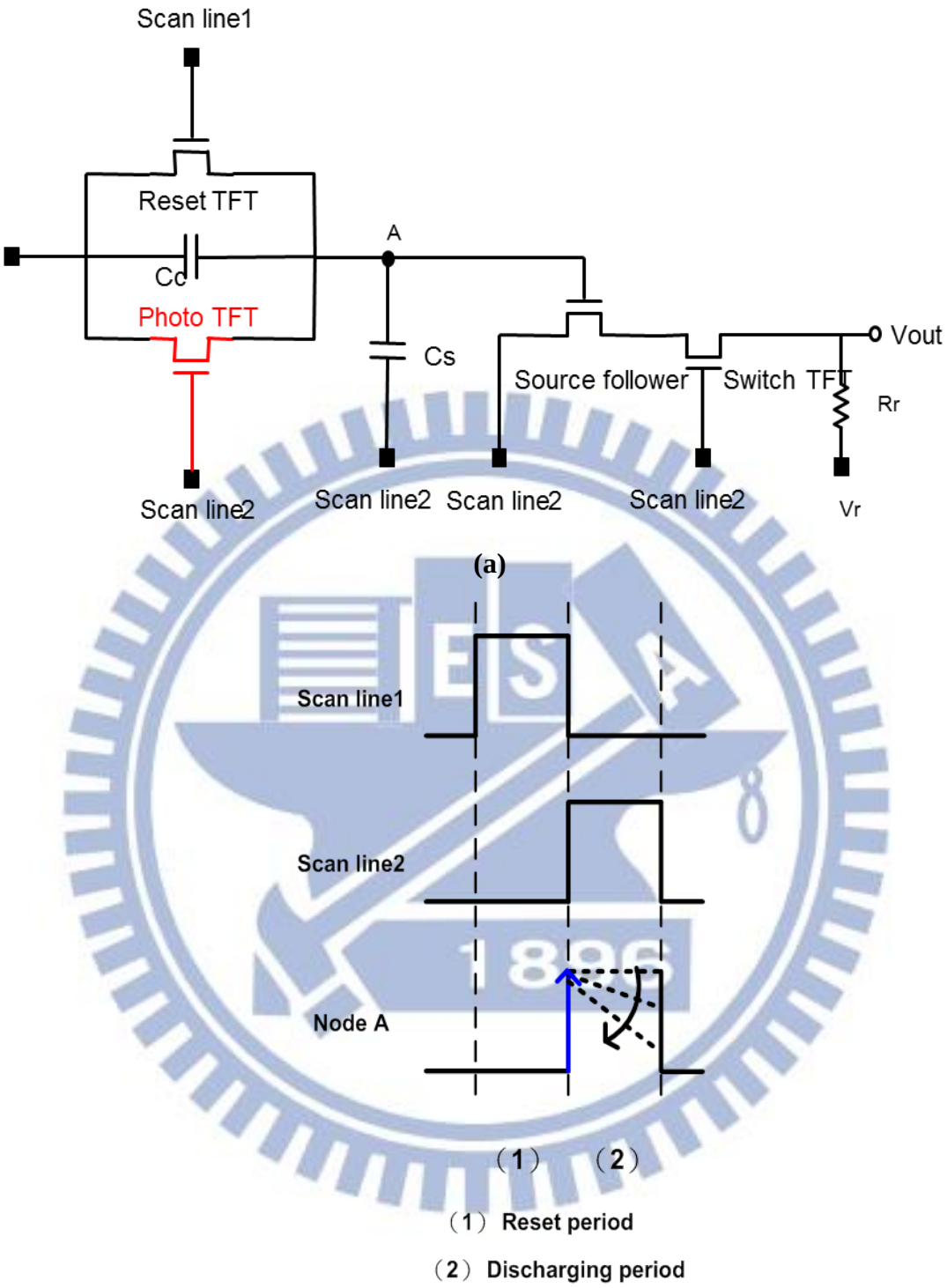

Fig. 3-18 (a) Proposed 4T2C light sensing circuit and (b) The time diagram

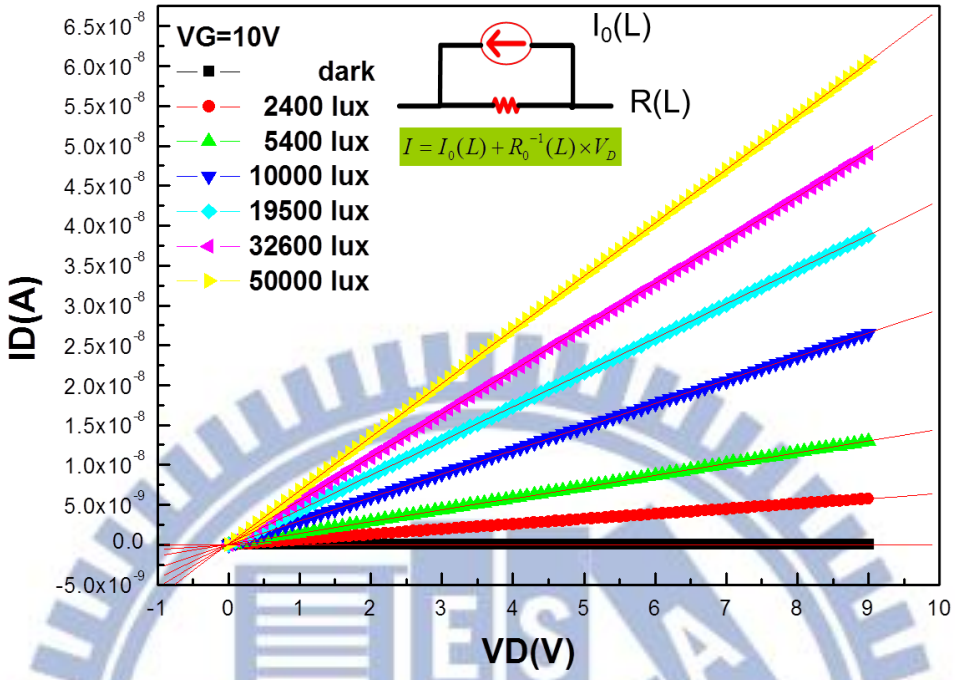

Fig. 3-19 ID-VD curve for photo current simulation

Brightness	$I_0(L)$ [A]	R=1/A(L) [Ω]
Dark	-2.85×10^{-13}	1.61×10^{12}
2400lx	2.22×10^{-11}	1.44×10^{9}
5400lx	3.15×10^{-11}	6.47×10^{8}
10000lx	6.30×10^{-11}	3.21×10^{8}
19500lx	8.01×10^{-11}	2.21×10^{8}
32600lx	7.95×10^{-11}	1.75×10^{8}
50000lx	7.44×10^{-11}	1.43×10^{8}

W/L=15/5

Table 3-1 $I_0(L)$ and $R_0 = 1/A_0(L)$ at V_{GS}= 10V with the illumination intensity variation

Feature	Specification
Operation region	ON. (V_{GS} = 10V)
Operation Period	16us
Illumination intensity	0~50000 lx
Scan line	-5V~15V
V_{com}	5V
C_{Sr}	0.012pF
C_c	0.016pF

Table 3-2 Circuit simulated conditions

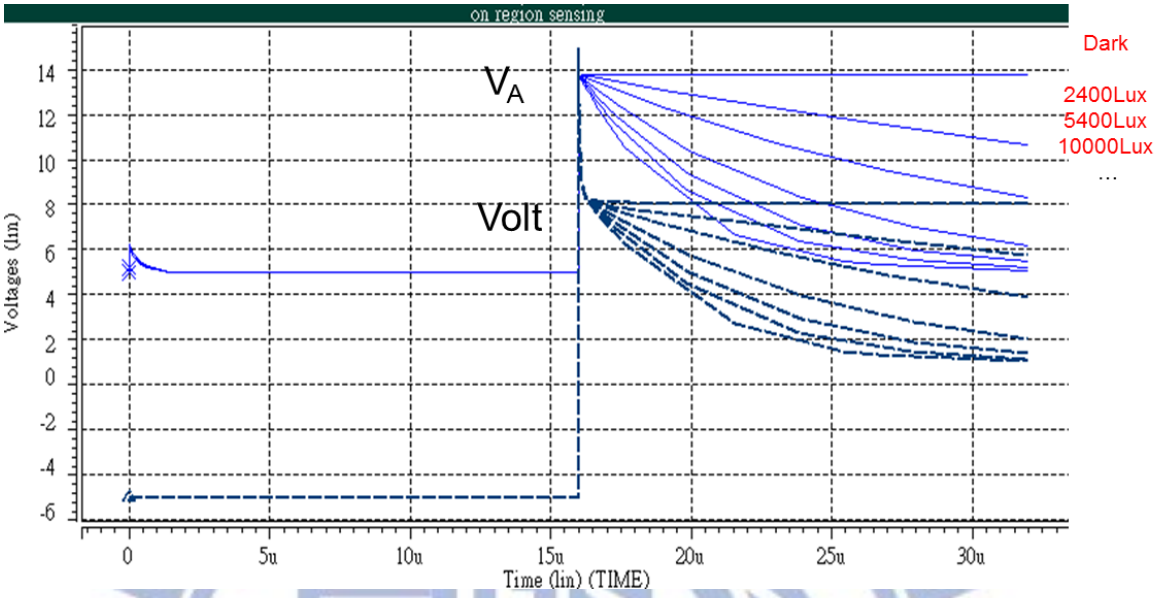

Fig. 3-20 Simulation results of light sensing circuit

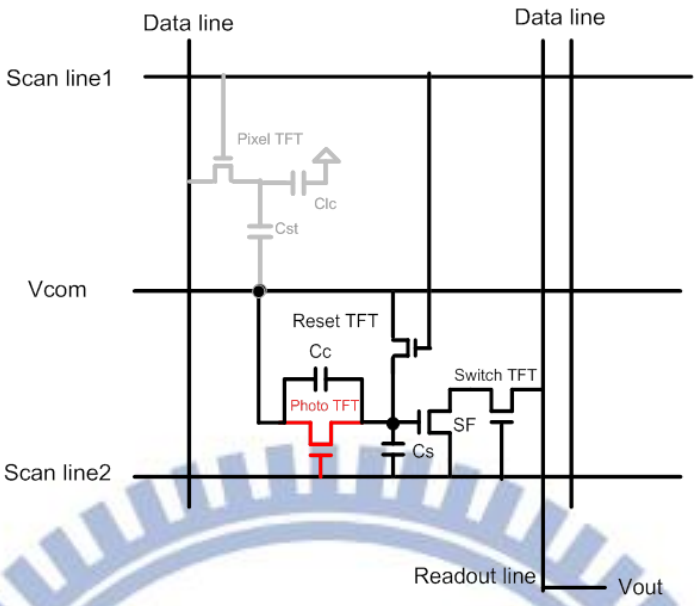

(a)

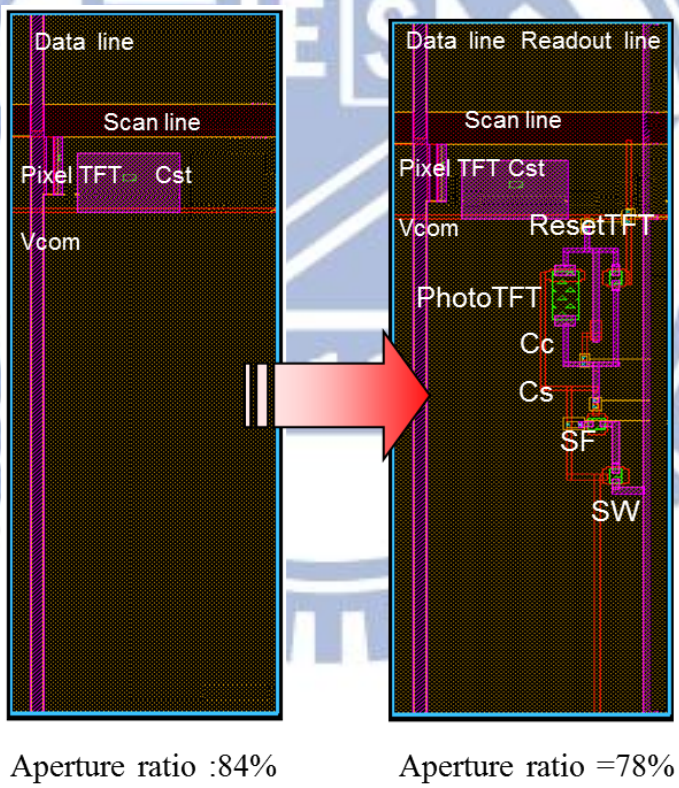

(b)

Fig. 3-21 (a) Equivalent circuit and (b) layout of the proposed sensor

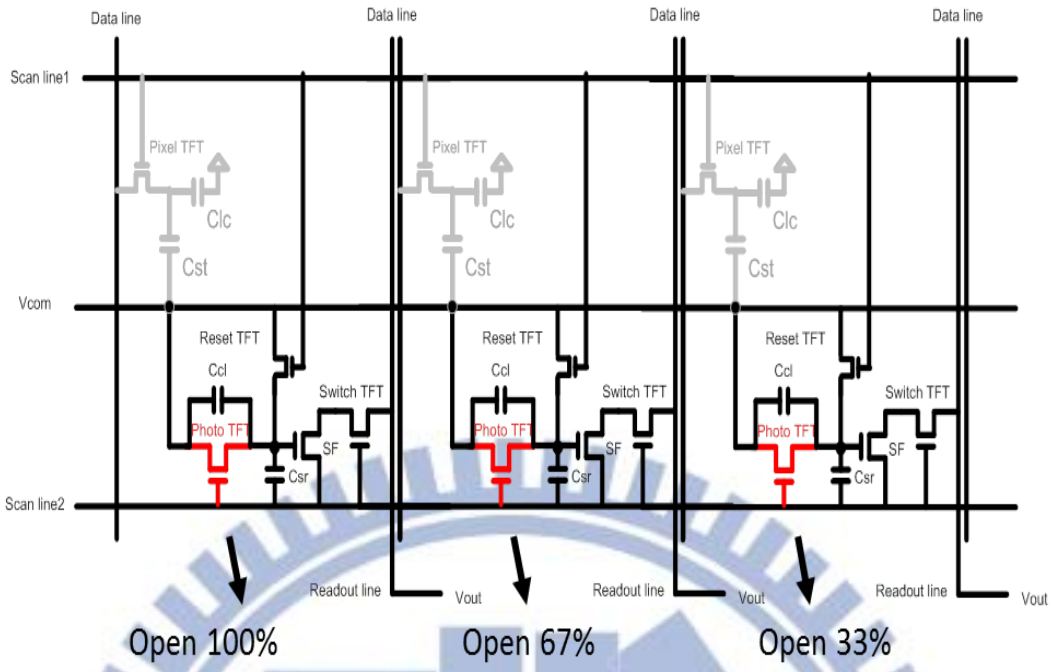

Fig. 3-22 A backlight sensing unit in panel

Fig. 3-23 Schematic diagram of sensor array embedded in panel

Chapter 4

Front-Light Sensing in Flat Panel Display

4.1 Introduction

The photo effect of the a-Si:H TFT has been studied to be used in imaging scanner, light sensor and touch panels, etc [40,46~47]. Currently discrete photo diodes are used for most ambient light sensing systems. However, normal environment illumination may contain over 3 orders of magnitude (60 dB or 10-bit) variation from the darkest to the brightest region. To cover such a wide range with linear photo detectors requires not only excessive output bandwidth but also high signal-to-noise ratio (SNR) of the sensor. This may impose the complexity and incidental power consumption on the system. Fig. 4-1 shows the structure of photodiode. In order to improve SNR for practical applications, it is necessary to increase the size of the photo detectors to resolve small difference [46]. However, large size photodiode may cause additional power consumption at high illumination levels and not suit with working in the pixel.

Integration of light sensors reduces module complexity, and location of the sensors close to the pixel array simplifies integration in products. There is an interest in integrating the sensors in the same TFT technology used to fabricate the display, so that the overall complexity of the module can be reduced. Since the sensors are fabricated on the glass substrate using the same fabrication processes as conventional TFTs, fabrication costs can be saved. In this chapter, we study the device performance under front light illumination and propose a feasible front light sensing circuit for flat panels.

4.2 Device Property

In this section, we examine the device properties under front light illumination as the similar study in chapter 3. Two different structures devices, conventional a-Si TFTs and gap-type a-Si TFTs, are discussed here and illustrated in Fig. 4-2 (a) and (b), respectively. The devices are identical as chapter 3, and the device process was revealed in section 3-2. To further analyze the effect of front illumination on the electrical performances of a-Si TFTs, we also evaluate the devices by considering the characteristics of current low dark current (I_{D_dark}), high illumination current (I_{D_illum}), and high $R_{L/D}$ (I_{D_illum} / I_{D_dark}).

Fig. 4-3 and Fig. 4-4 show the transfer characteristics of the conventional and the gap-type a-Si TFTs in the dark as well as irradiated at six different levels of halogen lamp illumination from the front side, respectively. It can be seen that the significant difference of the photosensitivity among them. Fig. 4-3 shows that the drain current is almost independent of illumination intensity when the conventional-gate TFT operates in the ON region. In OFF region, the photosensitivity is significantly higher than that in the ON-state. It means that the conventional a-Si TFT can be used as a front light sensor only in OFF region, which would easily influence by noise.

Fig. 4-4(a) shows the gap-type TFT operated as gate-near-drain mode, and Fig. 4-4(b) shows that operated as the gate-near-source mode. The $R_{L/D}$ of the gate-near-source one is not only larger than that of the other in OFF region (Vgs = -10V) but also in ON region (Vgs=10V). In aspect of application, the gate-near-source one has better photosensitivity to be the sensing device. From Fig. 4-4(b), we can see its $R_{L/D}$ can achieve to 4 orders both in OFF region and ON region. For further analysis, the gap region in the gap-gate TFT increases the total resistance between

source and drain, so that the ON current of gap-gate TFT is lower than the ON current of the conventional TFT. The total resistance R_{total} can be regarded as the sum of the resistance of the gate channel (R_{ch}) and gap channel (R_{gap}), namely, $R_{total}=R_{ch}+R_{gap}$. In the ON region, R_{ch} should be low in the on region, so that the R_{total} is dominated by R_{gap}. It is consistent with the observation that the illuminated ON current of gap-gate TFT differing from the conventional TFT is that it is not changed by the gate voltage.

Fig. 4-5(a) shows the relationships between photo current in the ON region and illumination intensity for several bias conditions. It can be seen that the increasing rate of the photo current under high illumination intensity is much less than that under weak light. In other words, it has poorer photosensitivity when device is operated under higher illumination. In Fig. 4-5(b), the photo current keeps almost linearity increasing rate with illumination.

To compare the current increasing rates in ON and OFF regions, we normalized the currents in Fig. 4-5 to their corresponding maximum currents. The normalized result, in ON and OFF regions at VD=10V are plotted together in Fig. 4-6(a). We further differentiate the curves of Fig. 4-6(a) to obtain the relative changing rate of photo current, namely, the relative photosensitivity versus illumination intensity and plot in Fig. 4-6(b). An intersection point at about 18860 lux is needed at the first sight. It means that sensing device operated in ON region has better relative photosensitivity below the illumination of 18860 lux, while OFF region offers better relative photosensitivity above 18860 lux. Consequently, we propose to operate the sensing device in ON region for weak illumination. Even very weak illumination, ON region operation can provide the ON current about 2 orders higher than OFF current. The higher current signal can reduce the effect of noise and be read easily. On the other hand, the OFF current is used for high illumination sensing to achieve better sensitivity with moderate current level. However, since the ambient light intensity in

an indoor environment is around 100~1000lux, the light sensing circuit operated in ON region is definitely enough for front light sensing. Thus, in the following discussion, we will focus on error factors of the devices in ON region.

4.3 Error Analysis

4.3.1 Uniformity

For any circuit needed to be manufacturable, it is clear that device-to-device uniformity must be controlled. Fig. 4-7 (a) shows the transfer characteristic curves of photo current versus of illumination intensity at V_{DS}=10V of four a-Si TFTs of gate-type structure for ON current operation. We average the four measured currents and take it as the reference standard. Next, we look up the original eight measured data according to the reference one to get the corresponding ambient light intensity, called measured light intensity ($Lux_{measured}$). Moreover, the error, which is defined as "$\frac{Lux_{measured} - Lux_{Real}}{Lux_{Real}}$", is shown in Fig 4-7(b) to illustrate the error from ON current variation. At 7547 lux illumination in the range of low illumination, it has a maximum error of 4.6%.

4.3.2 Temperature

In this section, we consider the temperature effect on device. As the same assumption in chapter 3, 40℃ is supposed to be the panel's normal operating temperature, and it varies within the range of ±5℃. Fig. 4-8 (a) shows the measured ON current of device-1 at 35℃、40℃ and 45℃. The error owing to temperature change can be calculated with the same method as that for uniformity. After calculating the errors for four devices, we plot them in Fig. 4-8(b) and find the maximum error exceeds 10% and up to 15.8% at low illumination level for ON region

operation. Because the influence from temperature cannot be neglected, we take further steps to understand the temperature effect on device.

Fig. 4-9(a) shows the ON current versus temperature at different illumination intensities. With the temperature increasing, the drain current also raises gradually. Then we try to fit these curves linearly and define the slopes as temperature coefficient (TC). Under different illumination intensities, we will get the different TCs. It means that the device does not have the identical response to temperature under different illumination intensities. Fig. 4-9(b) is the relation between TC and illumination intensity for four devices. Moreover, we find there is an obvious variation to temperature response from device to device. This phenomenon will cause more difficulty in calibration, since it is impossible to calibrate the sensor one by one in the panel. Therefore, we propose to add external control of the temperature to limit the temperature variation within ±3.5℃. In this case, the maximum error can be controlled to 10%.

4.3.3 Backlight Influence

If we plan to integrate the photo-sensor into the LCD pixel array, we should consider the photo effect of back light (BL) illumination to simulate its real situation on panel [48~49]. The illumination sources in our measurement include halogen lamp from front side and LED white light from back side as illustrated in Fig. 4-10.

To discuss on the photo effect of back light illumination, the ON current versus the front light (FL) intensity are plotted in Fig. 4-11(a). With a shift in the axis the FL, the corresponding curves for the case with BL are plotted again in the insets together with original curves for the case with BL. As can be seen, the pairs of the curves overlap perfectly. It depicts that when we illuminate the device with FL and BL at the same time, the BL intensity of 5070 lux can be equivalent as FL intensity 3624 lux in

ON region. If the BL intensity is fixed in application, we can calibrate the BL effect by the characteristic as mentioned above. Firstly, we take the curve (FL) of the current versus front light as the reference as shown in Fig. 4-11(a). Next, we use the originally measured current to look up the illumination intensity according to the reference. This corresponding front light intensity is called $Lux_{measured}$. It is different from the real light intensity (Lux_{real}), as shown by the solid circles in Fig. 4-11(b). Another measured intensity can be obtained by subtracting a constant quantity of illumination, which is called calibrated intensity $Lux_{calibration}$. The curves of $Lux_{calibration}$ versus Lux_{real} are also plotted by solid triangles in Fig. 4-11(b). We define the error to be "$\frac{Lux_{measured} - Lux_{real}}{Lux_{real}}$". Fig. 4-11(c) shows the case of ON current sensing. For low illumination, after calibration it has a maximum error 4.46% at 6683 lux illumination.

If backlight intensity is a constant, we can offset the BL effect during the sensing operation by substrate a constant light intensity. Therefore, this issue might not so important. In such a case, the photo effect of BL illumination on the current measurement can be subsided. However, BL induced instability will hinder the sensor operation with BL illumination. This issue will be discussed in next section.

4.3.4 Staebler-Wronski (SW) Effect

Fig.4-12 shows the curves of current versus illumination intensity for the gap-type TFT stressed for up to 4800 seconds by a halogen lamp of a continuous front illumination intensity of 13600 Lux. The drain current degradation under illumination stress is obviously observed. When the gap-type a-Si:H TFTs are used as sensing devices in TFT LCD, they are irradiated by backlight of display, too. Therefore, the influence of backlight illumination must also be considered. The degradation in the ON current of the gap-type a-Si:H TFT with time under backlight is shown in Fig.

4-13. For both of Fig.4-12 and Fig.4-13, they are observed that the degradation trend and level of the illuminated drain current are very similar.

Since the photo effect of gap-type TFT in the ON region is restricted by the high resistance of gap region, the same high resistance of gap length makes the current degradation with time, resulting in the same trend for the front and back illuminations. The different degradation levels are attributed to the different illuminated intensities and spectrums.

Fig.4-14 shows the ON current of the gap-type a-Si:H TFT measured under various front light intensities, with and without the illumination at a fixed backlight intensity of 5070 lux. The case with back light is marked as $I_{D(Fl+BL)}$ and that without backlight is named as $I_{D(FL)}$. These currents are measured at drain voltage of 10 V and gate voltage of 20 V after different illuminated stress time (Tst) of the front light illumination. It is observed that the curves of $I_{D(Fl+BL)}$ and $I_{D(FL)}$ exhibit parallel shift in the x-axis approximately, even for the different stress time. This shift is caused by the backlight of the fixed intensity. It is further observed that the degradation trends under the two conditions are similar.

A new parameter R, which is defined as the ratio of $I_{D(Fl+BL)}$ to $I_{D(FL)}$ is plotted against the front light intensity in Fig.4-15. As can be seen, the curves of R versus intensity of the front light coincide for various stress time. It implies that we can use this ratio R to be an index for the light sensing, even with the decay in the drain current after long-term illumination. A formula in the form of $y=1/(a+b*x^c)$ is used to best fit the curves in Fig.4-15. Using the fitting curve as a reference, the light intensity can be looked up from the ratio R and the extracted error can be calculated.

Fig.4-16 (a) shows the back traced light intensity $Lux_{measured}$ for various applied front light intensity Lux_{real}. The term Lux_{real} represents the identified illumination intensity measured by a photometer, and the term $Lux_{measured}$ represents the measured

result according to the correction concept in last paragraph. In ideal case, the slope of the curve in Fig.4-16 (a) is equal one. Meanwhile, the corresponding errors for those data extracted from R and the drain current after long-term illumination are presented in Fig.4-16 (b). The error is defined as ($Lux_{measured}$ - Lux_{real})/ Lux_{real}. In conventional case without calibration, the sensing result is calculated by the degraded illuminated current according to the initial illuminated characteristic of gap-type TFT. Therefore, the sensing error without calibration increases with the stress time, as shown in Fig.4-16(b). In the weak front illumination below 6000 Lux, the error of the calibrated case is less than 13%. The large error for the high-intensity light is attributed to the fast degradation during the measurement. Fortunately, such a high intensity is rarely the case in normal usage. The independence of stress time for the ratio R provides a way to get around the difficulty in application owing to SW effect, which is to be discussed in the next section.

4.4 Front-Light Sensing Circuit

4.4.1 Proposed Sensing Circuit

The proposed light sensing array circuit including the display and sensing parts is shown in Fig.4-17. Because the ON/OFF current ratio for the gap-type a-Si:H TFT is not significant, in order to restrain the leakage current from the unselected pixels on the same column, a conventional a-Si:H TFT with light shield is connected in series with the gap-type TFT. The shielded a-Si:H TFT limits the OFF current of unselected pixel. Meanwhile, the sensing signal is dominated by the dark or illuminated ON current of gap-type TFTs, since it is much smaller than the ON current of conventional a-Si:H TFTs.

The proposed circuit does not need the source follower circuit to buffer out the

signal because the ON current is used to extract the sensing signal [50]. Thus, it occupies less area and a lager aperture ratio can be obtained. Moreover, it avoids the sensing error arisen from the threshold voltage variation of the source follower TFT, since the drain currents of gap-type TFTs is independent of gate voltage in the ON region, as shown in Fig.4-4 (b). The error caused by the threshold voltage shift is no more an issue in the proposed circuit.

4.4.2 Operation in TFT LCD

In order to obtain the proposed ratio R, both $I_{D(FL+BL)}$ and $I_{D(FL)}$ must be acquired. In many advanced TFT LCDs, to eliminate the motion blur, black frames are inserted between normal frames [51~52]. These black frames can be implemented by turning of the back light. Taking advantages of this technique, we propose the operation method. The timing scheme for the proposed circuit is shown in Fig.4-18. Before each scan line N turning on, the reset switch is closed to reset the current integrator. In the black frame, $I_{D(FL)}$ for all the pixels in the array can be measured line by line and the values for the whole matrix can be stored in a frame memory. In the following normal frame, another matrix values of $I_{D(FlL+BL)}$ can be detected and stored with backlight on. Assuming that the front light does not change in these two successive frames, the ratio R for each corresponding pixel can be calculated and stored by the system. Consequently, the front light intensity can be determined by referring the calculated ratio R to the predetermined curve of R versus light intensity.

4.5 Summaries

It is firstly found that the ratio of the front light-induced currents of the gap-type a-Si:H TFT with and without backlight illumination is independent of the illumination stress time. This phenomenon gives a way to avoid the issue of SW effect when the

gap-gate a-Si:H TFT is used as the light sensor. We propose a simple sensing array circuit and its operation in an array. This method has merits of large signal current level, wide dynamic sensitivity, high pixel aperture ratio, and immunity to threshold voltage shift. It can be easily implemented in TFT LCD since it can be made by the same process with conventional display and the operation is compatible with the TFT LCD application.

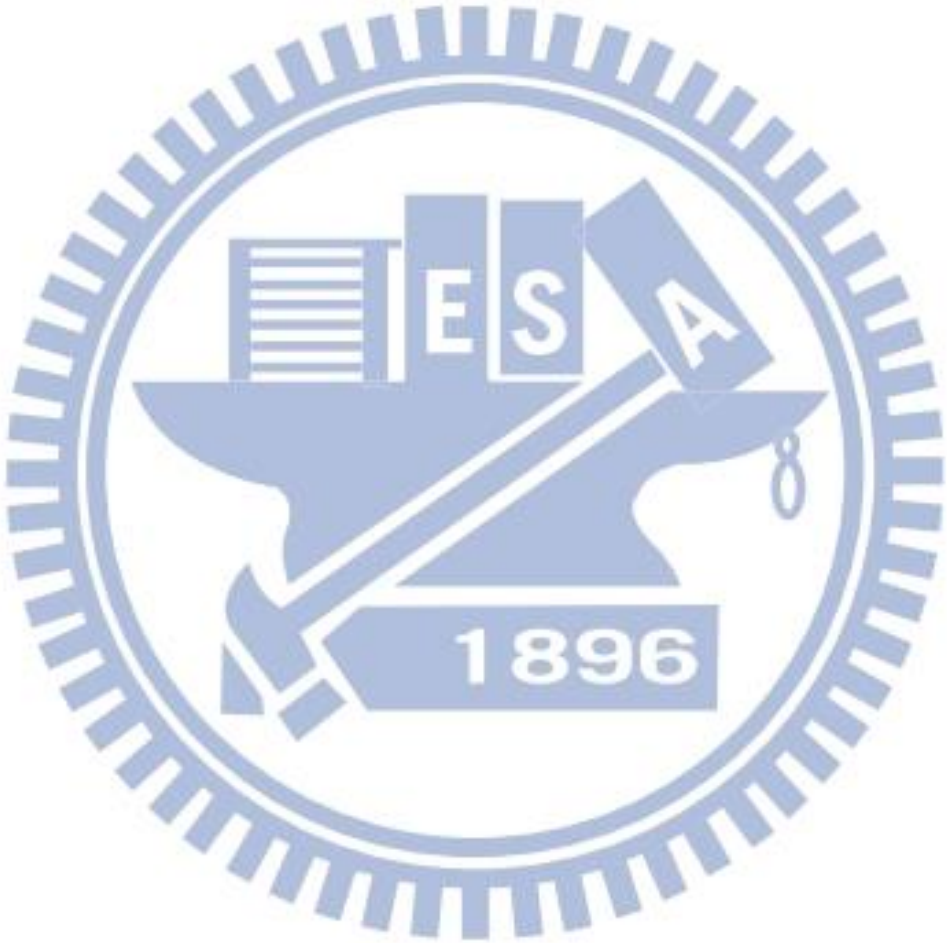

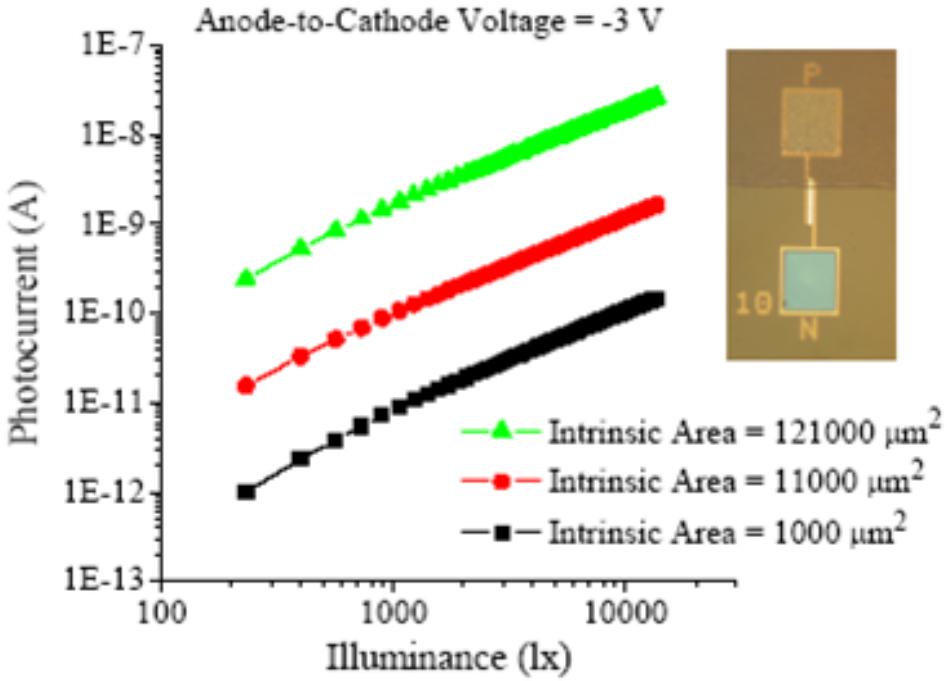

Fig. 4-1 The linearity between the illuminance and the photocurrent of lateral PIN photodiodes with area= 1000/11000/121000 μm^2

(Ref. Hyun-Sang Park et al., SID, Vol. 39, No. 1, 2008, pp. 716-719)

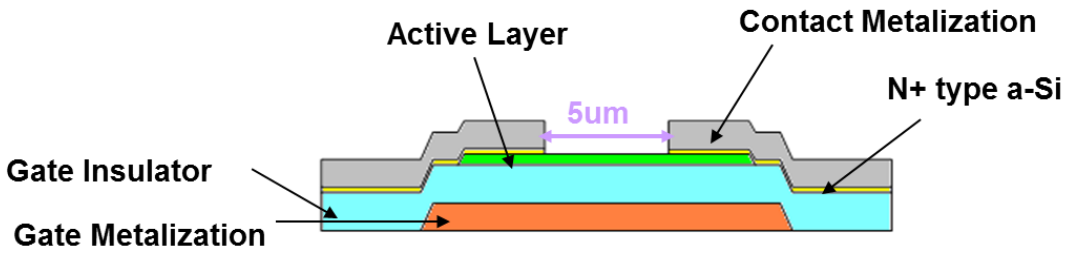

(a)

(b)

Fig. 4-2 The cross-section of (a) the conventional a-Si TFT (b) the gap-type a-Si TFT

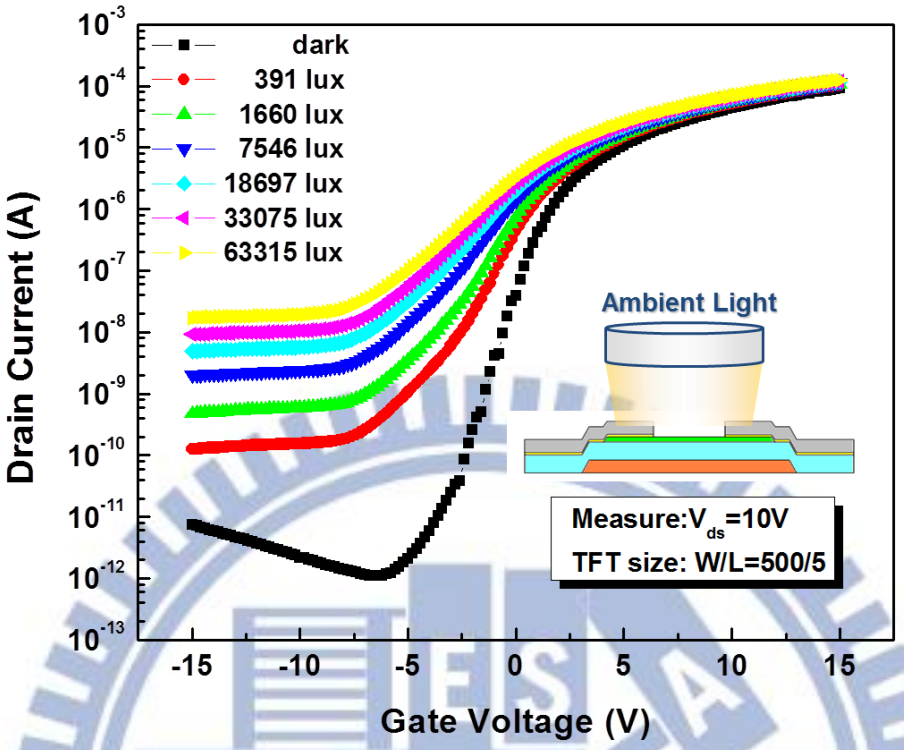

Fig. 4-3 The transfer curves of the conventional a-Si TFT with the front light illumination

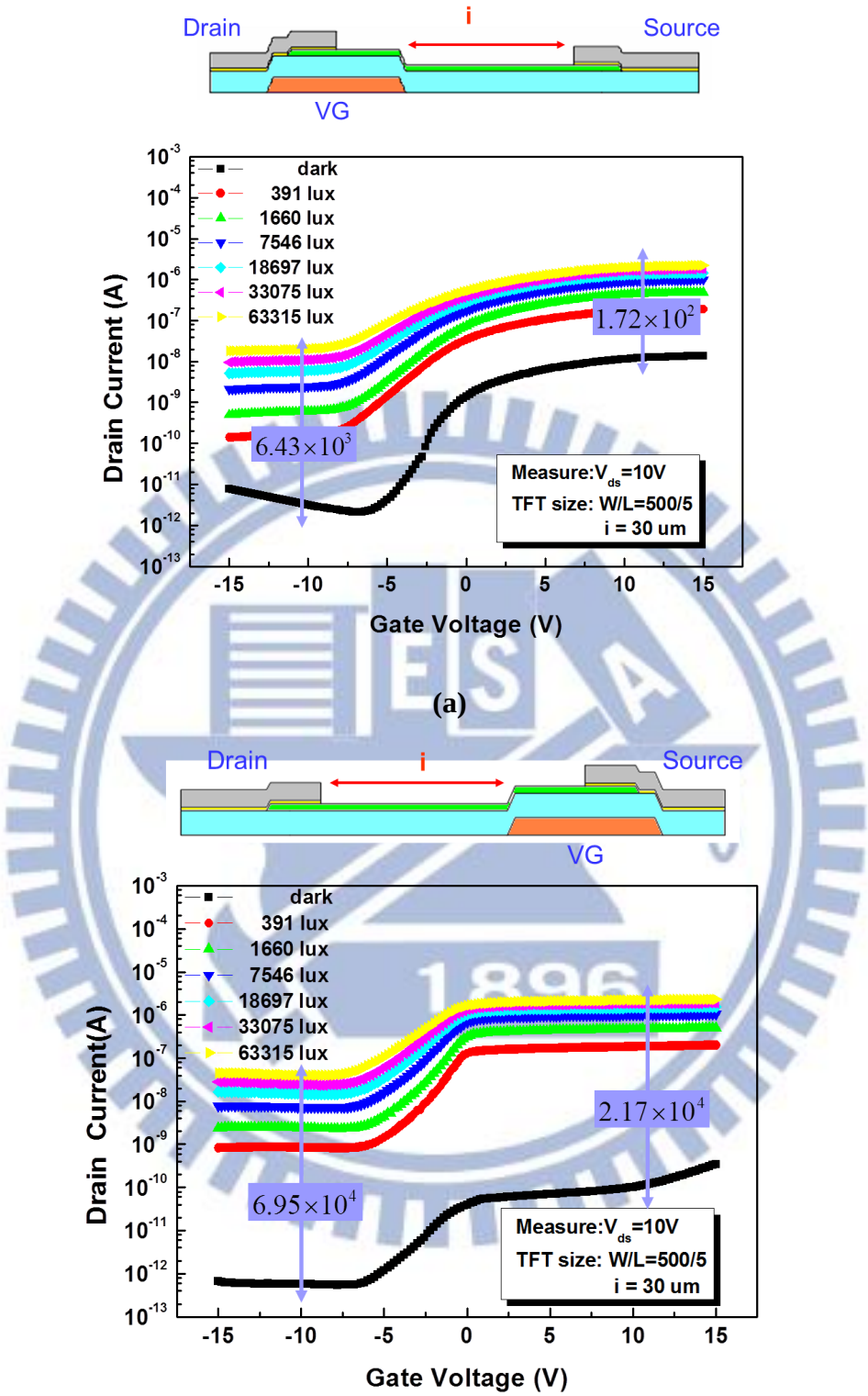

Fig. 4-4 The transfer curves of the front illuminated gap-type a-Si TFT operated in (a) gate-near-drain mode (b) gate-near-source mode

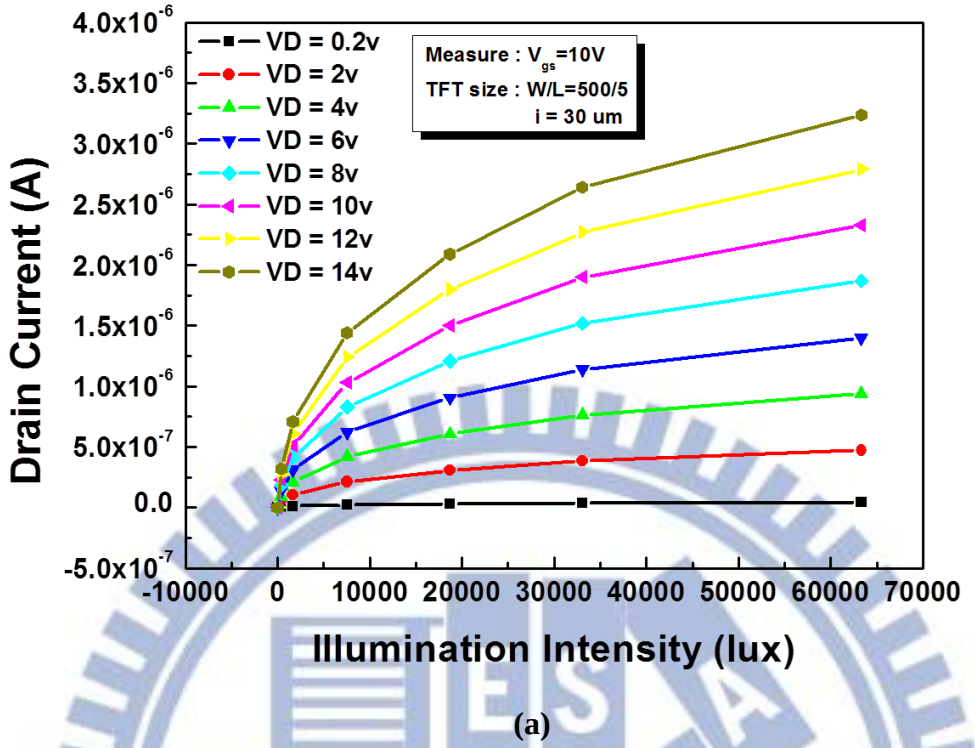

(a)

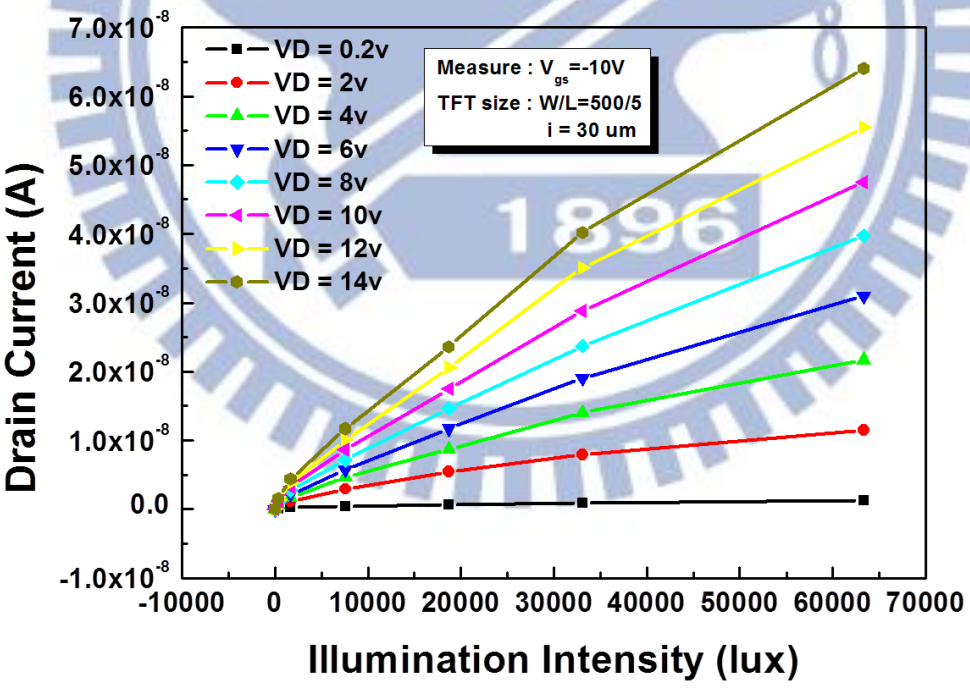

(b)

Fig. 4-5 The relationships between photocurrent and illumination intensity of gap-type TFTs for several bias conditions in (a) the ON region and (b) the OFF region

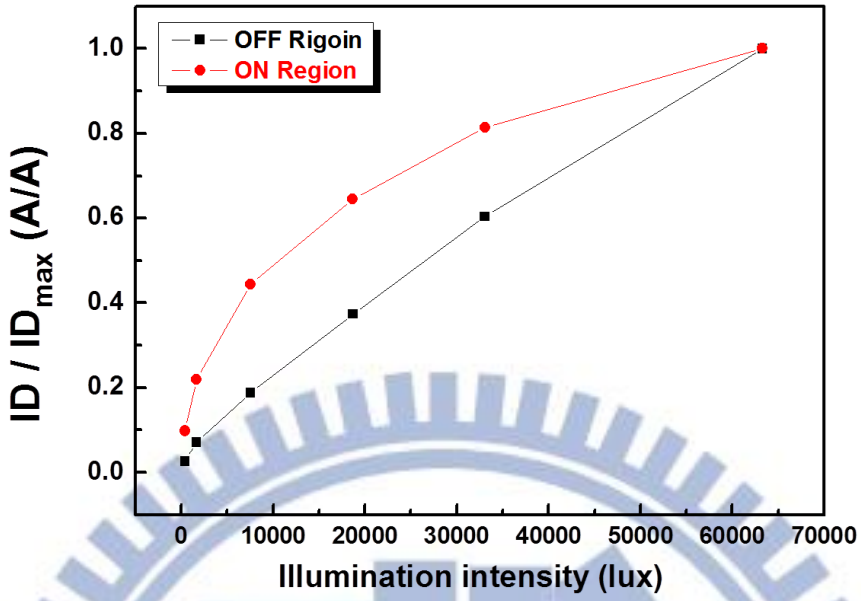

(a)

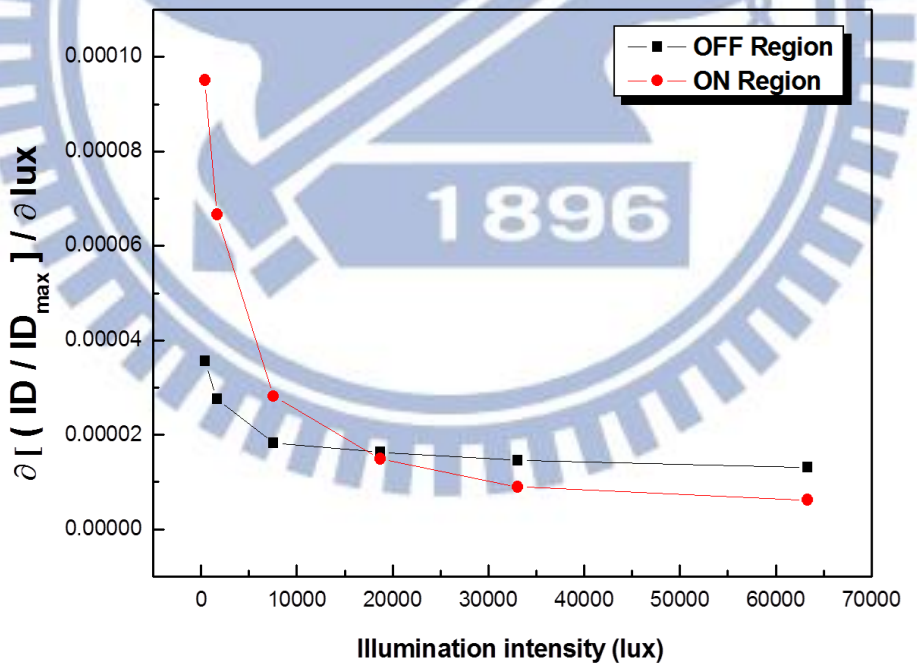

(b)

Fig. 4-6 The normalized drain current versus front light illumination intensity of ON and OFF region (b) The relative photosensitivity of ON region and OFF region

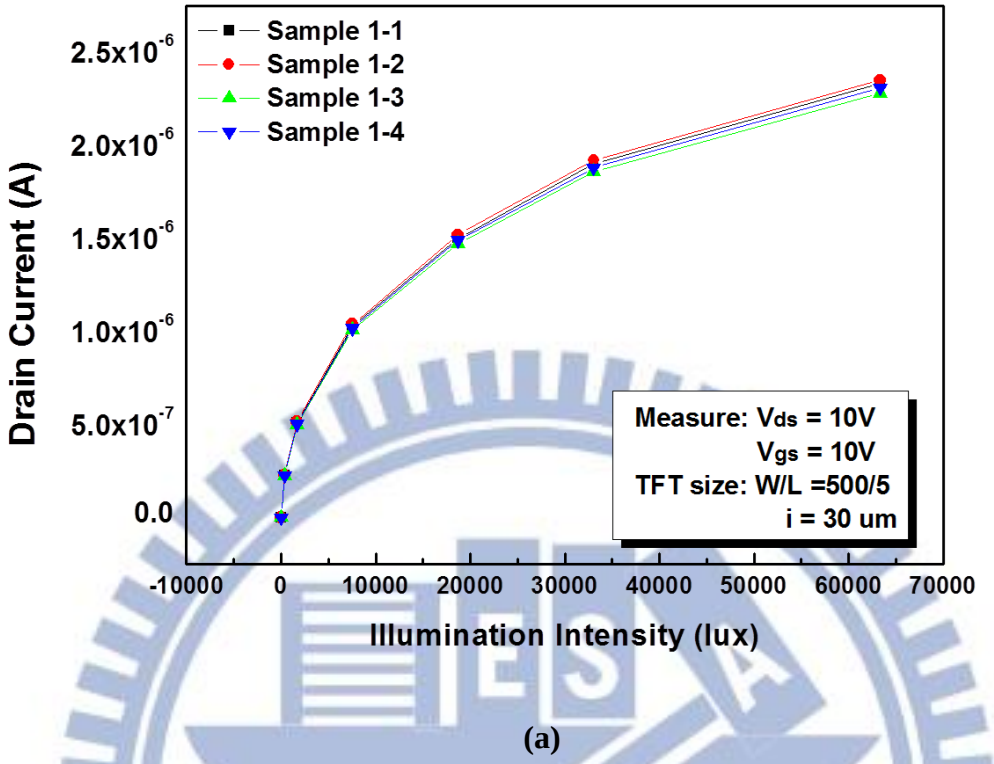

(a)

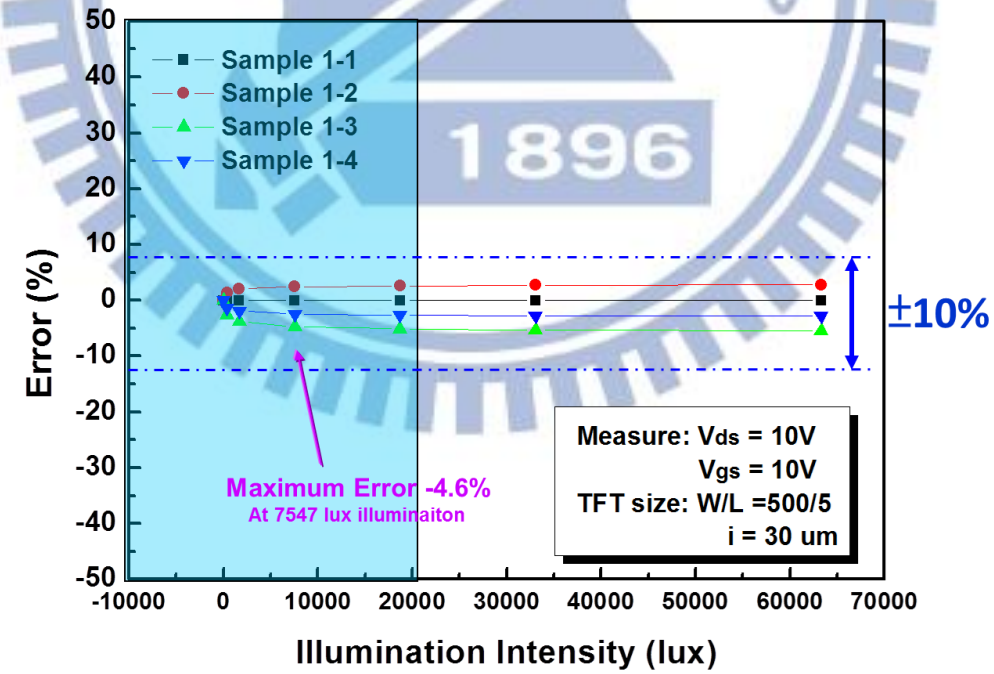

(b)

Fig. 4-7 (a) ON current variations of a-Si TFTs of 4 devices (b) Error analysis of ON current variation between the measured and the illuminated light intensities

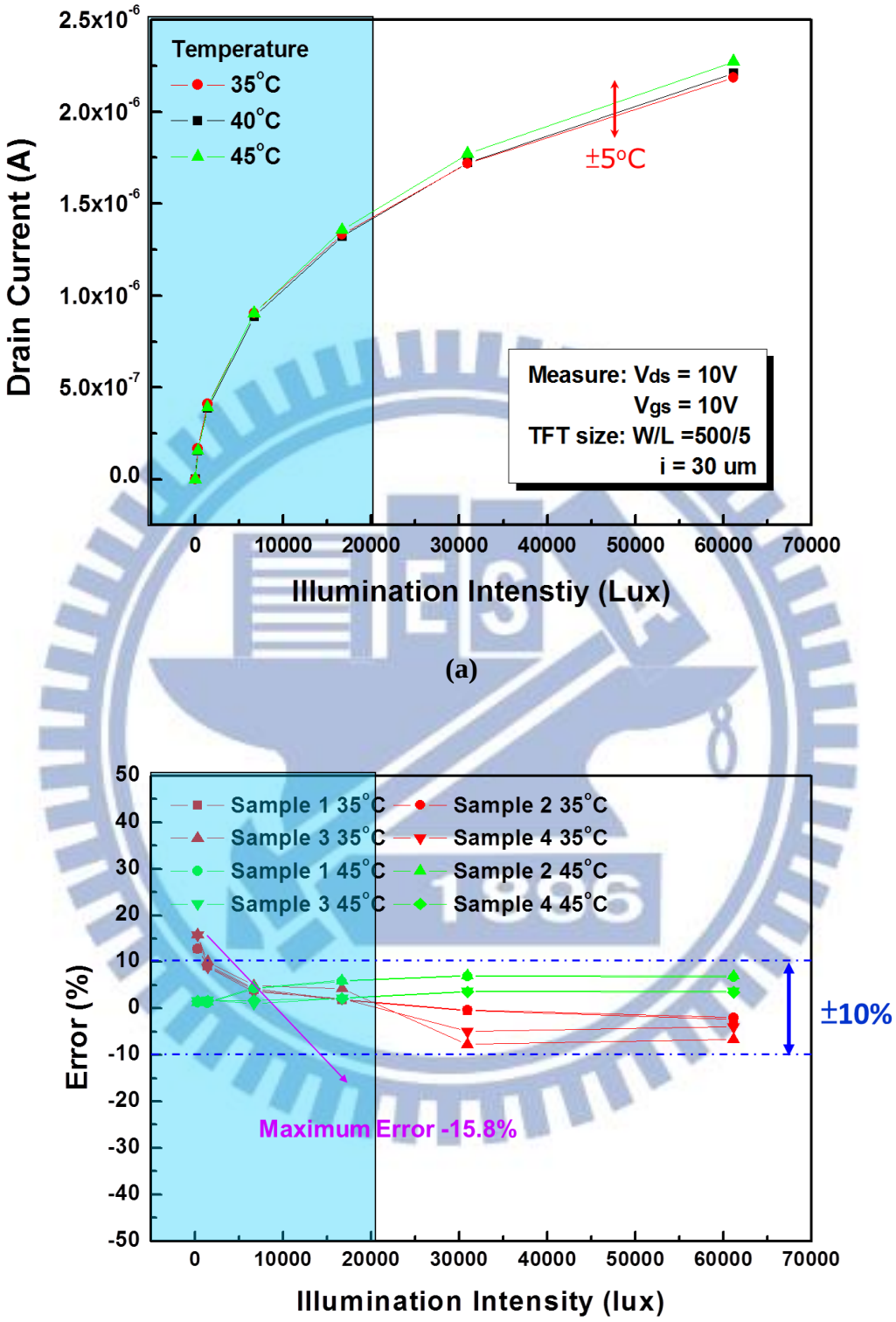

Fig. 4-8 (a) The ON current versus illumination intensity at 35°C, 40°C, and 45°C (b) Error analysis of temperature variation between the measured and the illuminated light intensity

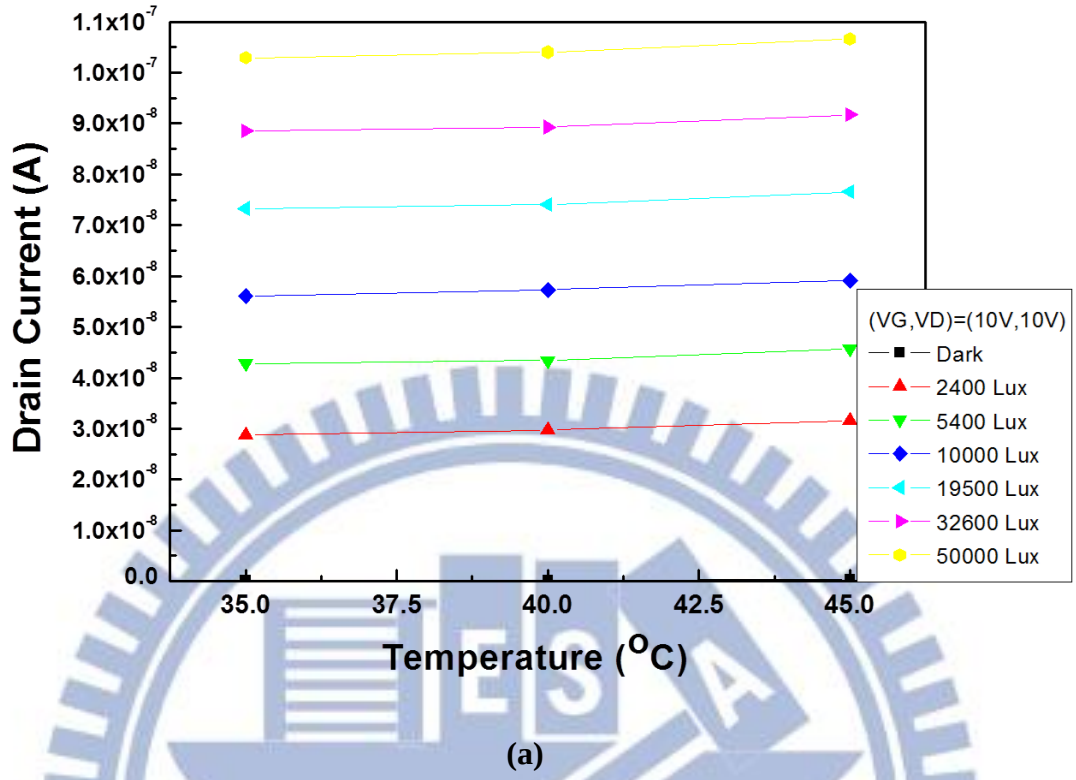
Drain Current (A)
1.1x10-7
1.0x10-7
9.0x10-8
8.0x10-8
7.0x10-8
6.0x10-8
5.0x10-8
4.0x10-8
3.0x10-8
2.0x10-8
1.0x10-8
0.0
35.0
37.5
40.0
42.5
45.0
Temperature (OC)
(VG,VD)=(10V,10V)
Dark
2400 Lux
5400 Lux
10000 Lux
19500 Lux
32600 Lux
50000 Lux

(a)

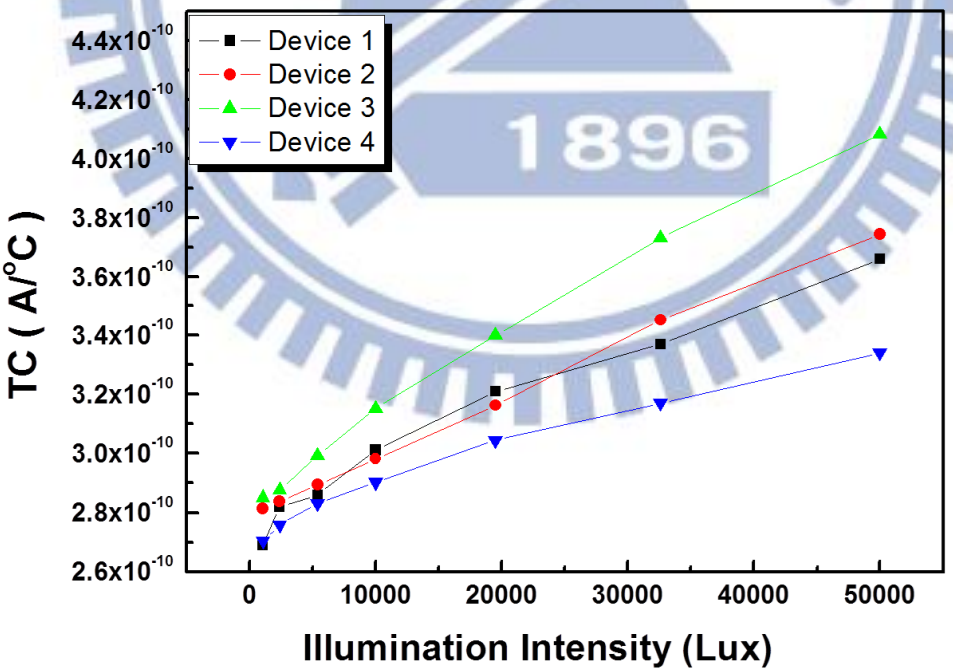
TC (A/OC)
4.4x10-10
4.2x10-10
4.0x10-10
3.8x10-10
3.6x10-10
3.4x10-10
3.2x10-10
3.0x10-10
2.8x10-10
2.6x10-10
0
10000
20000
30000
40000
50000
Illumination Intensity (Lux)
Device 1
Device 2
Device 3
Device 4

(b)

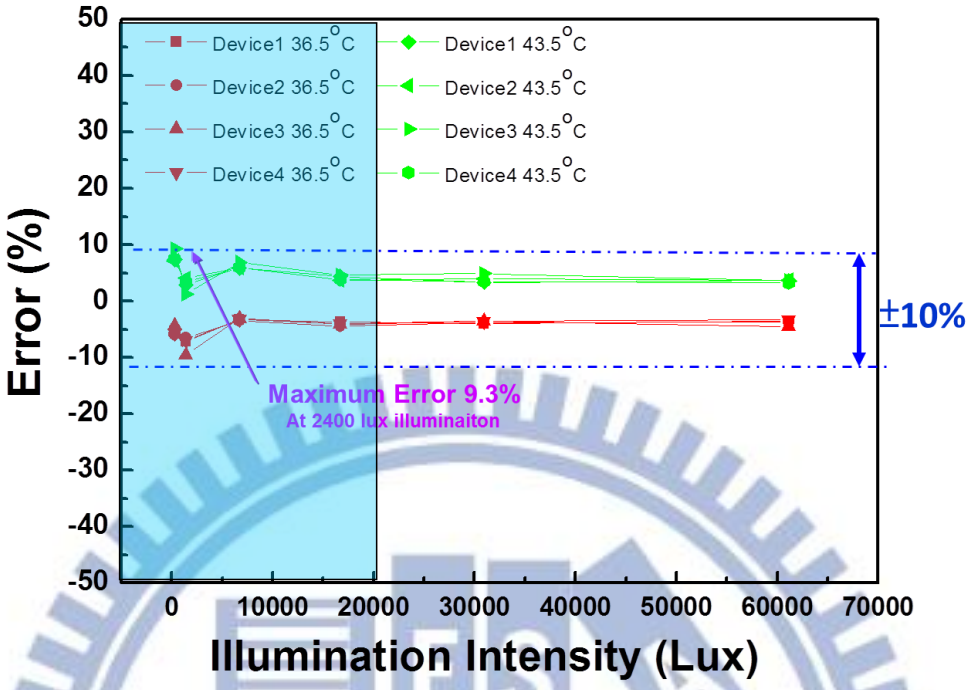

(c)

Fig. 4-9 (a) The ON current versus temperature at Vgs=10V, Vds=10V (b) The temperature coefficient versus temperature curves of 4 devices (c) Error analysis of temperature variation between the measured and the illuminated light intensity

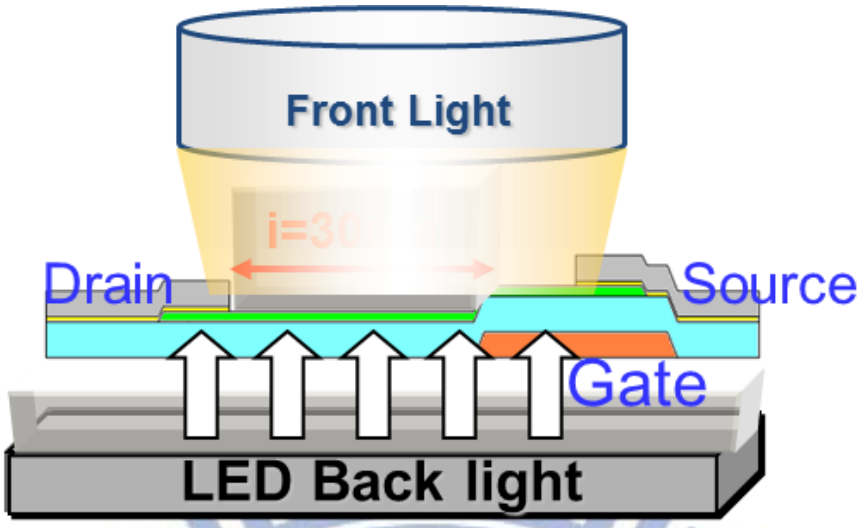

Fig. 4-10 Schematic diagram of the real situation of the a-Si TFT in panel

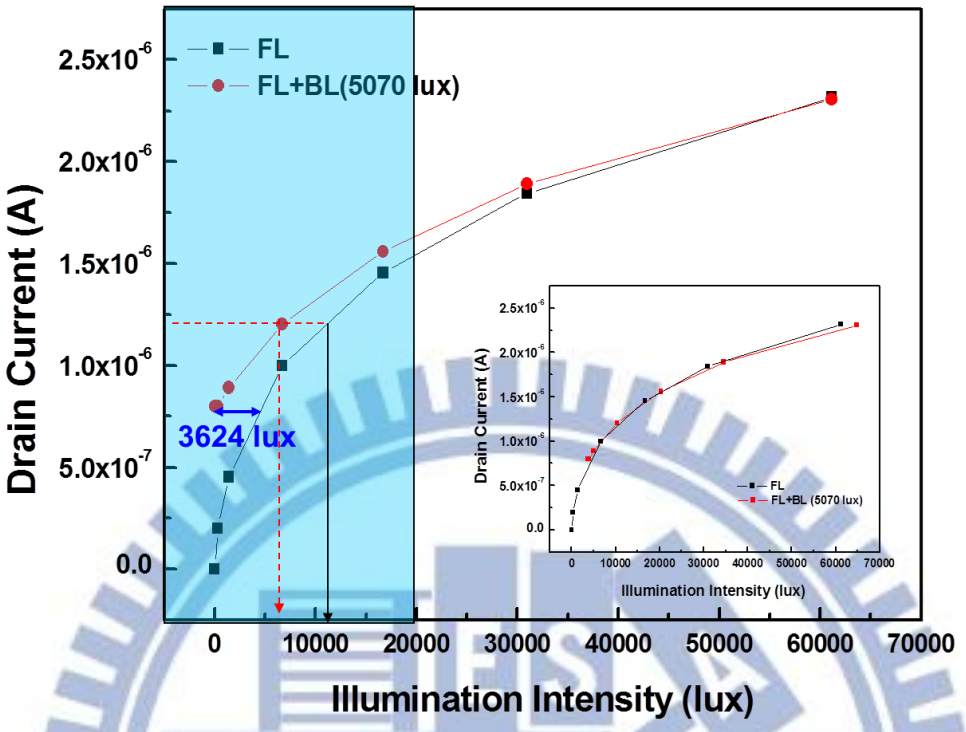
FL
FL+BL(5070 lux)
Drain Current (A)
2.5x10-6
2.0x10-6
1.5x10-6
1.0x10-6
5.0x10-7
0.0
3624 lux
0
10000
20000
30000
40000
50000
60000
70000
Illumination Intensity (lux)

(a)

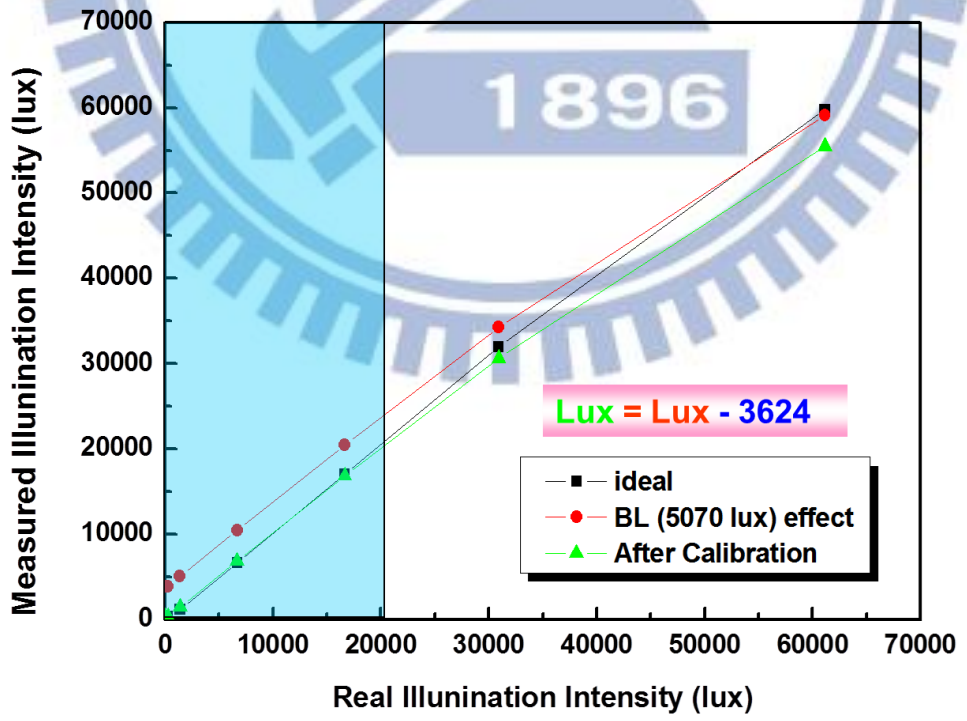
Measured Illunination Intensity (lux)
70000
60000
50000
40000
30000
20000
10000
0
Lux = Lux - 3624
ideal
BL (5070 lux) effect
After Calibration
Real Illunination Intensity (lux)

(b)

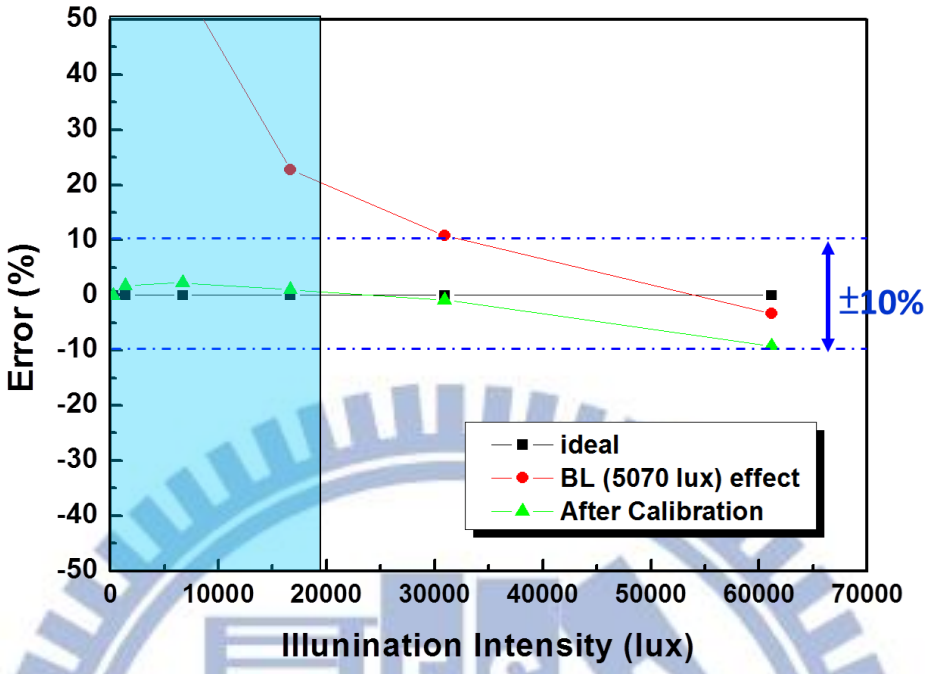

(c)

Fig. 4-11 (a) The ON current versus front light illumination intensity without backlight and with backlight (b) The relationship between the measured and the illuminated light intensity in ON region (c) Error analysis of backlight effect between the measured and the illuminated light intensity in ON region

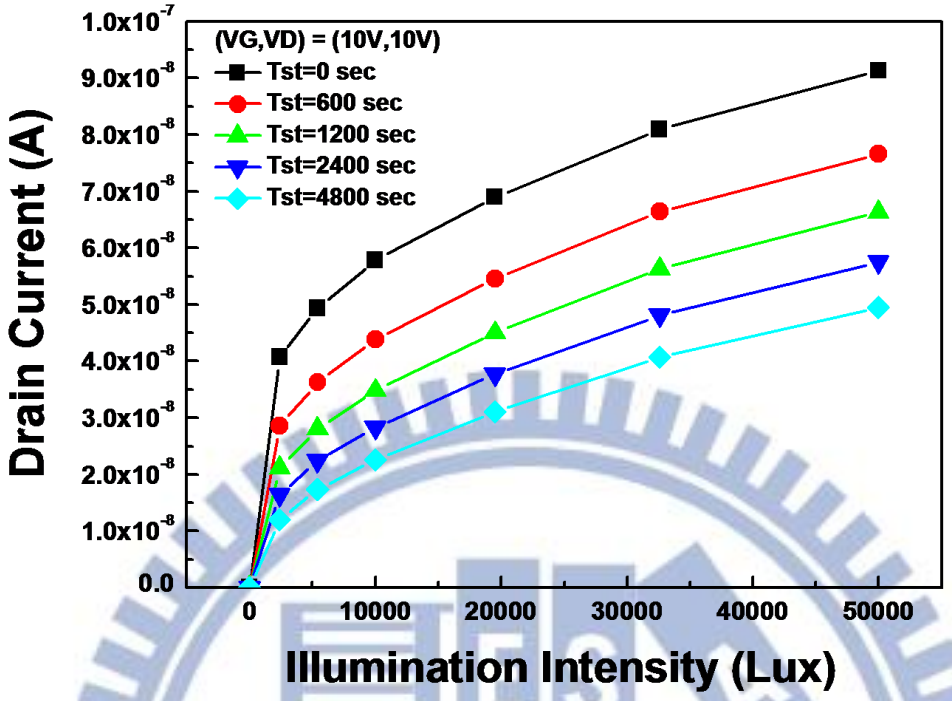

Fig. 4-12 The behavior of gap-gate a-Si:H TFTs under the stress of 16673 lux front light.

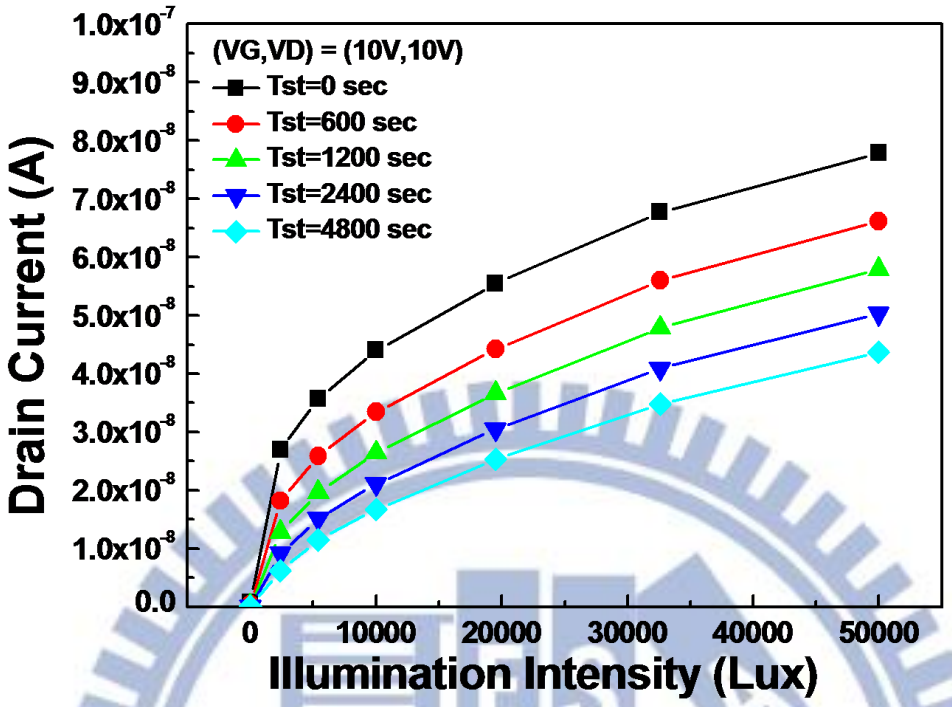

Fig. 4-13 Behavior of gap–gate a-Si:H TFTs under the stress of 19160 lux back light

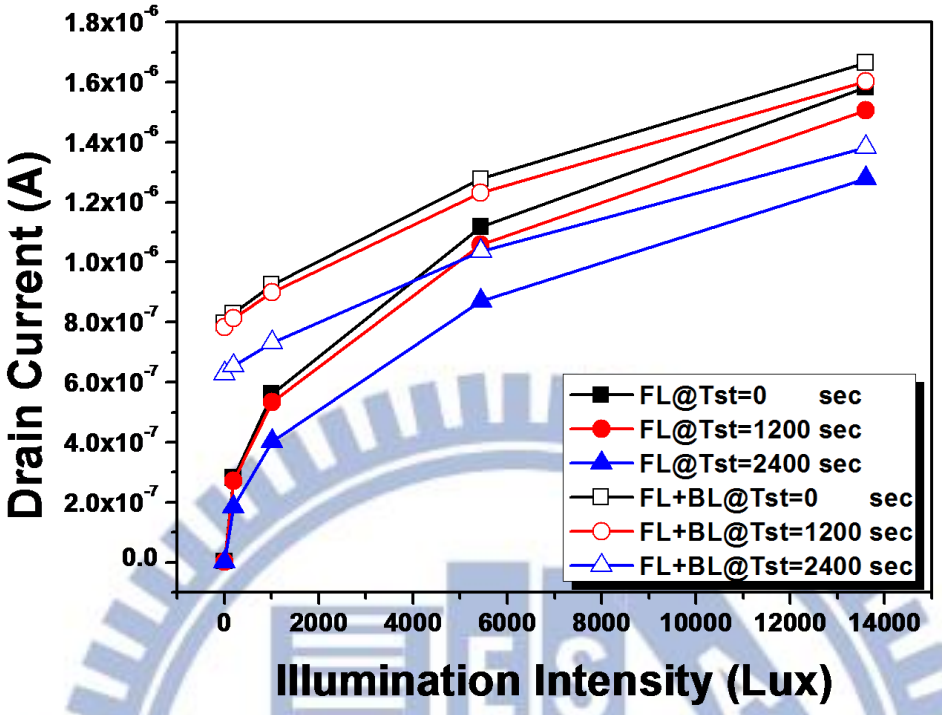

Fig. 4-14 Drain currents measured with and without backlight illumination after front light stress

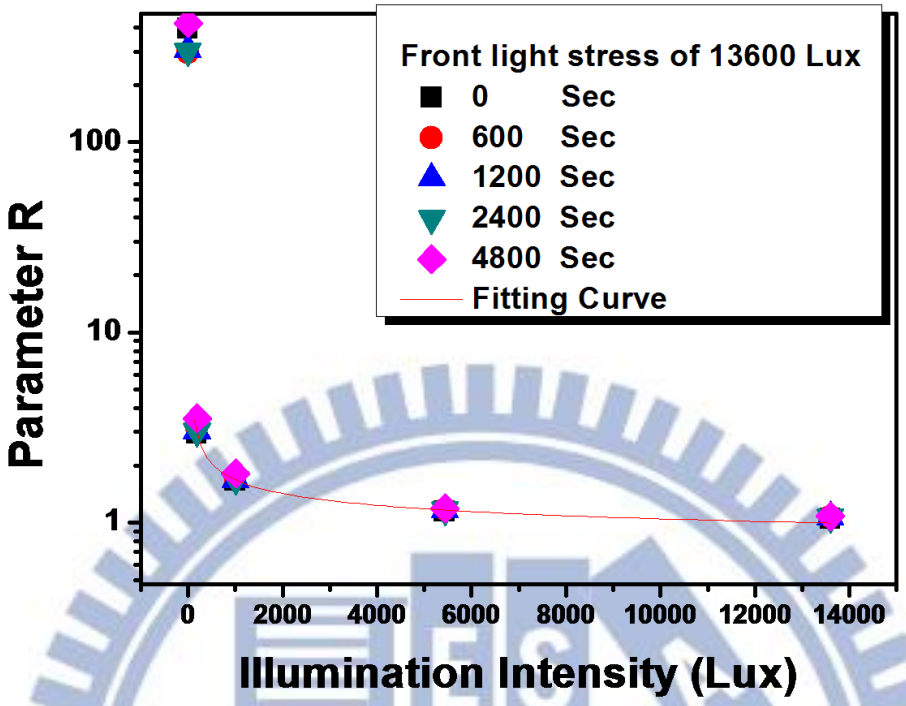

Fig. 4-15 Ratio R with respect to front illumination under front light of 13600 lux for different stress time

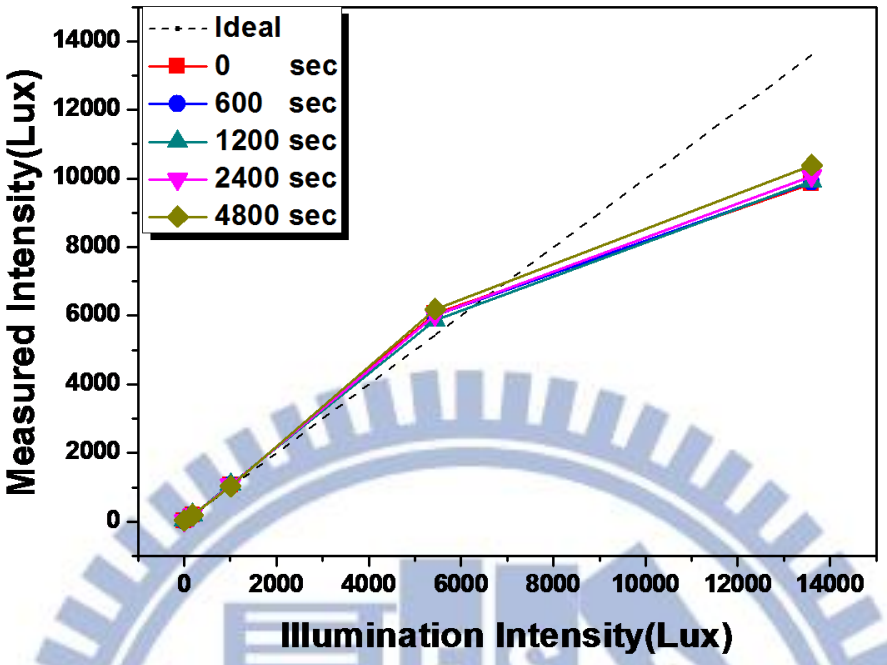

(a)

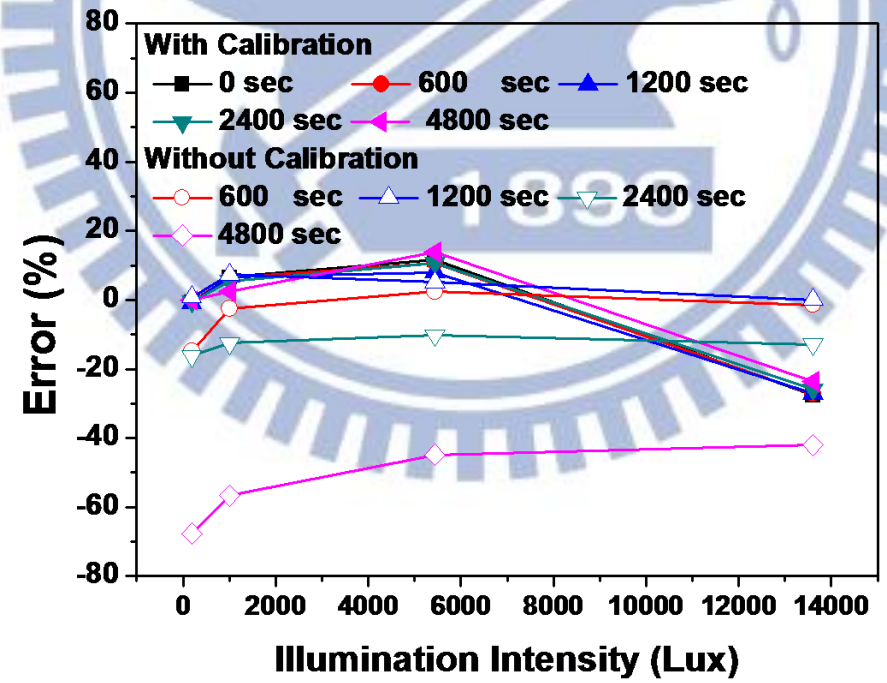

(b)

Fig. 4-16 (a) Measured intensity back traced by parameter R. (b) The error comparison of with and without calibration under different stress time of 13600 lux front light

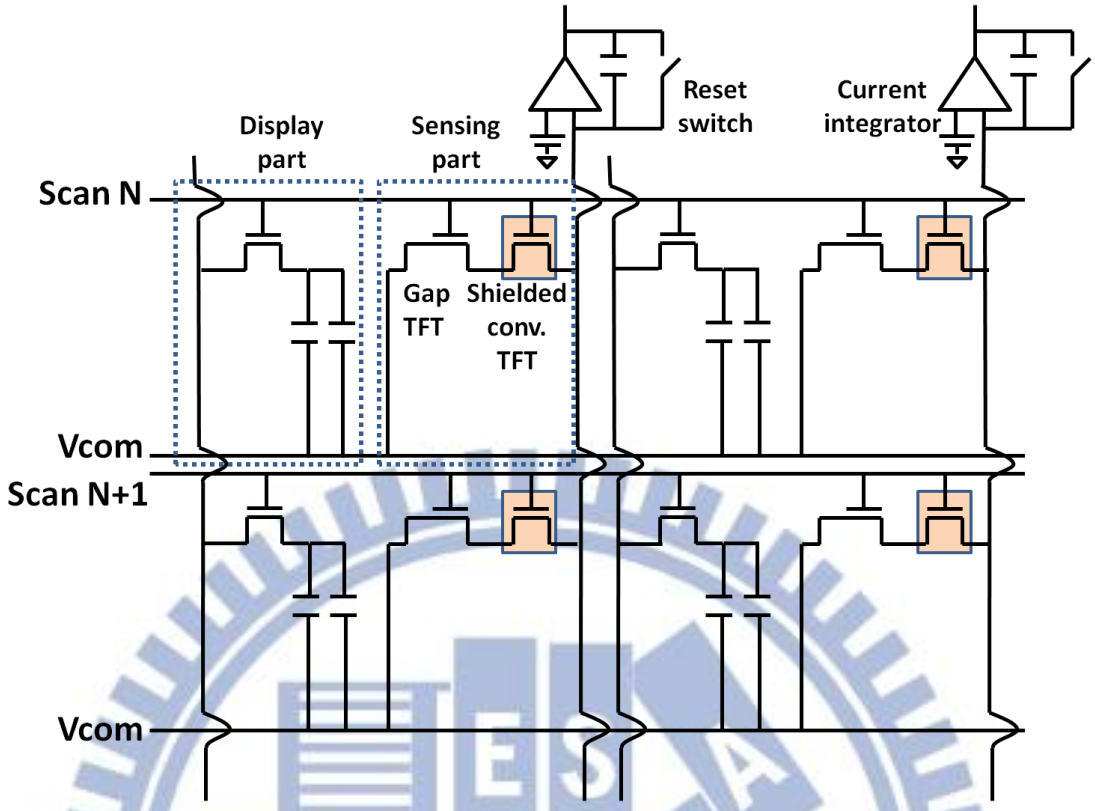

Fig. 4-17 The proposed front light sensing array circuit using gap-gate TFT

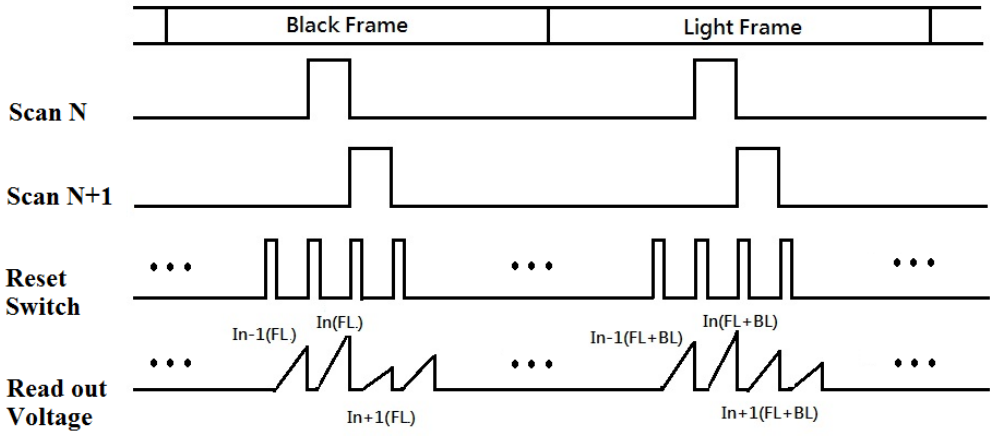

Fig. 4-18 The timing scheme of the proposed circuit

Chapter 5

Conclusion and Future Work

In previous chapters, the active matrix touch sensing and light sensing circuits are respectively studied. In chapter 2, the RC time delay concept is applied to the touch sensing circuit design. Based on the concept, the touch sensing circuit can be implemented by three different circuit configurations including two series single-gate TFTs type, one dual-gate TFT type, and one single-gate TFT type. We successfully verify their function in laboratory test and eventually fabricate a 2-inch touch panel to examine the issues in practical process. The advantages of the proposed circuit are revealed as large signal output and low standing state current. The large signal is easy to be read out and lower the cost on the readout IC, while the low standing-state current can effectively reduce the power consumption for whole panel operation. Since this sensing method can be made by the touch panels of different structures and different material TFTs, we discuss the difference between the key issues, such like the sensing capacitance, and propose a design procedure which can be followed by the manufacturers. This technology can break the barrier to the signal process of the conventional capacitive touch sensing technology, so that it is aimed to be used for the large-size touch panel. A model of a 42 inch touch panel is fully designed in this chapter. Besides, the problems in the large-size panel are discussed and simulated. According to the simulation result, the effect on the scan voltage drop is obvious but sustainable in our proposed circuit.

In chapter 3 and 4, we study the backlight and front light sensing applications of the gap-type a-Si TFT, respectively, which can replace the conventional a-Si TFT because of the photosensitivity in ON region. For the identical reason with the touch

sensing circuit in chapter 2, the ON current signal is excellent to acquire high signal-to-noise ratio. The asymmetric gap-type TFT has a gap region which can be used for light sensing between the bottom gate and one of the source and drain electrodes. After determining the proper device operation condition, we consider and analyze the possible error factors including the device uniformity, temperature effect, the reliability under illumination. The Staebler-Wronski effect means that the photo current of amorphous silicon will degrade under long-term illumination, which is the dominant error to make the sensing circuit fail. After a systematical study on the SW effect of gap-type TFT, we propose the backlight and front light sensing circuit in the end of chapter 3 and 4, respectively.

Although the a-Si TFT is still prevalent in current display products, the amorphous Indium-Gallium-Zinc-Oxide (a-IGZO) TFT rise sharply owing to its advantages of better mobility and transparent property. Hence, the sensing technologies for a-Si TFT are gradually required for a-IGZO TFT as well. Our proposed touch sensing circuit adapts to the process of different material TFTs. However, our proposed light sensing circuits are designed according to the device behavior of gap-type a-Si TFTs. The light sensing application using a-IGZO TFT is still an interesting subject and needed to be revealed. According to our preliminary experiments, the slow photo response time would also be another obstruction for light sensing application. To develop the light sensing application of IGZO TFTs, above issues should be carefully studied in future work.

Reference

[1]. M. Schadur and W. Helfrich, “ Voltage-dependent optical activity of a twisted nematic liquid crystal,” Appl. Phys. Lett., Vol. 18, No. 4, 1971, pp. 127-128.

[2]. T.J. Scheffer and J. Nehring,” A new, highly multiplexable liquid crystal display,” Appl. Phys. Lett., Vol. 45, No. 10, 1984, pp. 1021-1023.

[3]. E.P. Raynes and I.A. Shanks,” Fast-switching twisted nematic electro-optical shutter and colour filter,” Electronics Lett., Vol. 10, No. 7, 1974, pp. 114-115.

[4]. E.P. Raynes,” Improved contrast uniformity in twisted nematic liquid-crystal electro-optic display devices,” Electronics Lett., Vol. 10, No. 9, 1974, pp. 141-142.

[5]. Miyaji, M. Yamaguchi, A. Toda, H. Mada, and S. Kobayashi,” Control and elimination of disclinations in twisted nematic liquid-crystal displays,” IEEE Trans. on Electron Devices, Vol. 24, No. 7, 1977, pp. 811-815.

[6]. H. Fukuro and S. Kobayashi,” Newly synthesized polyimide for aligning nematic liquid crystals accompanying high pretilt angles,” Molecular Crystals and Liquid Crystals, Vol. 163, No.1, 1988, pp. 157-162.

[7]. T. P. Brody, J. A. Asars, and G. D. Dixon,” A 6x6 inch 20 lines-per-inch liquid-crystal display panel,” IEEE Trans. on Electron Devices, Vol. 20, No. 11, 1973, pp. 995-1001.

[8]. T. P. Brody,” The birth and early childhood of active matrix- A person memoir,” J. Society for Information Display, Vol. 4, No. 3, 1996, pp. 113-127.

[9]. K.H. Kim and J. K. Song,” Technical evolution of liquid crystal displays,” NPG Asia Meterial, Vol. 1, 2009, pp. 29-36.

[10]. Ming-Po Tien," Technical development of flat panel displays," Wu-Nan Book Inc., 2008

[11]. D. Lee," The State of the touch-screen panel market in 2011," Information Display, 2011.

[12]. Touch Panel Market Forecast and Cost/Issue/Industry Analysis 2013, Displaybank.

[13]. S. Tomita, T. Nakamura, T. Morita, T. Imai, T. Okada, H. Hayashi, Y. Saruhashi, M. Fuchi, M. Hashimoto, M. Tada, T. Endo, K. Saito, and H. Nakamura,"An In-Cell Capacitive Touch-Sensor Integrated in an LTPS WSVGA TFT-LCD," SID Symp. Dig. Technical paper, Vol. 42, No. 1, 2011, pp. 629-632.

[14]. B. H. You, B. J. Lee, K.-C. Lee, S. Y. Han, J. H. Koh, J. H. Lee, S. Takahashi, R. H. Berkeley, N. D. Kim, and S. S.Kim,"12.1-inch a-Si:H TFT LCD with Embeded Touch Screen Panel," SID Symp. Dig. Technical paper, Vol. 39, No. 1, 2008, pp. 830-833.

[15]. C. J. Brown, H. Kato, K. Maeda, and B. Hadwen," A continuous-grain silicon-system LCD with optical input function," IEEE J. Solid-State Circuits, Vol. 42, No. 12, 2007, pp. 2904-2912.

[16]. Y.-H. Tai, L.-S. Chou, and H.-L. Chiu, " Gap-type a-Si TFTs for front light sensing application," IEEE J. Display Tech., Vol. 7, No. 12, 2011, pp. 679-683.

[17]. J. Colegrove, "The state of the touch-screen market in 2010," Information Display, pp. 22-24, 2010.

[18]. W. C. Wang, T. Y. Chang, K. C. Su, C. F. Hsu, and C. C. Lai," The Structure and Driving Method of Multi-Touch Resistive Touch Panel," SID Symp. Dig. Technical paper, Vol. 41, No.1, 2010, pp. 541-543.

[19]. B. H. You, B. J. Lee, S. Y. Han, S. Takahashi, R. H. Berkeley, N. D. Kim, and S. S. Kim," Touch-screen panel integrated into 12.1-in. a-Si:H TFT-LCD," J. SID \,

Vol. 17, No. 2, 2009, pp. 87-94.

[20]. J. A. Destura1, J. T. M. Osenga, and S. J. van der Hoef," Novel Touch Sensitive In-Cell AMLCD," SID Symp. Dig. Technical paper, Vol. 35, No.1, 2004, pp. 22-23.

[21]. G. Barrett and R. Omote," Projected-capacitive Touch Technology," Information Display 2010, pp. 16-21.

[22]. S. S. Hwang, S. H. Bae, S. H. Cho, H. K. Kang, D. S. Lee, J. K. Shin, and I. J. Chung, " On-cell Projected Capacitive Type Touch Sensor for NBPC," SID Symp. Dig. Technical paper, Vol. 41, No.1, 2010, pp. 677-679.

[23]. H. S. Shim, S. K. Kim, Y. T. Chun, H. J. Kwon, I. S. Kee, W. Choi, and S. Y. Lee," Mutual Capacitance Touch Screen Integrated into Thin Film Encapsulated Active-Matrix OLED," SID Symp. Dig. Technical paper, Vol. 42, No.1, 2011, pp. 621-624.

[24]. S. Takahashi, D. H. Cho., H.-S. Moon, and N. De Kim," In-Cell Embedded Touch Screen Technology for Large Size LCD Applications," SID Symp. Dig. Technical paper, Vol. 41, No. 1, 2010, pp. 544-547.

[25]. H.-S. Park, Y.-J. Kim, and M.-K. Han," Touch-Sensitive Active-Matrix Display with Liquid-Crystal Capacitance Detector Arrays," Jpn. J. Appl. Phys., Vol. 49, No.3, p. 03CC01, 2010.

[26]. C. S. Kim, B. K. Kang, J. H. Jung, M. J. Lee, H. B. Kim, S. S. Oh, S. H. Jang, H. J. Lee, H. Kastuyoshi, and J. K. Shin, "Active Matrix Touch Sensor Perceiving Liquid Crystal Capacitance with Amorphous Silicon Thin Film Transistors," Jpn. J. Appl. Phys., Vol. 49, No.3, p. 03CC03, 2010.

[27]. K. Tanaka, H. Kato, Y. Sugita, N. Usukura, H. Kawamori, K. Maeda, and Y. Kubota," A System LCD with Optical Input Function using Infra-Red Backlight Subtraction Scheme," SID Symp. Dig. Technical paper, Vol. 41, No. 1, 2010, pp.

680-683.

[28]. O.-K. Kwong and H.-S. Lim,” Photo sensing circuit using low-temperature polycrystalline silicon TFTs and photo diode for smart functional display,” SID Symp. Dig. Technical paper, Vol. 41, No. 1, 2010, pp. 684-687.

[29]. H. Tamura, T. Hamada, T. Nakagawa, T. Aoki, M. Ikeda, M. Kozuma, Y. Kurokawa, T. Ikeda, K. Moriya, Y. Hirakata, N. Kamata, T. Murakawa, J. Koyama, and S. Yamazaki,” High reliable In-Ga-Zn-Oxide FET based electronic global shutter sensors for in-cell optical touchscreens and image sensors,” SID Symp. Dig. Technical paper, Vol. 42, No. 1, 2011, pp. 729-732.

[30]. K.-S. Son, J.-S. Jung, and K.-H. Lee,” Characteristics of double-gate GaInZnO thin-film transistor”, IEEE Electron Devices Letter, Vol. 31, No. 3, pp. 219-221, 2010.

[31]. K.-S. Son, J.-S. Jung, and K.-H. Lee,” Highly stable double-gate GaInZnO thin-film transistor”, IEEE Electron Devices Letter, Vol. 31, No. 8, pp. 812-814, 2010.

[32]. C. C. Lai and C. C. Tsai,” Backlight power reduction and image contrast enhancement using adaptive dimming for global backlight application,” IEEE Transactions on Consumer Electronics, Vol. 54, No. 2, pp. 669-674, 2008.

[33]. M. Anandan,” LED backlight: Enhancement of picture quality on LCD screen,” Proc.of ASID Symp, 2006, pp. 130-134.

[34]. J. Anderson, C. Schardt, J. Yang, B. Koehler, B. Ostlie, P. Watson, K. Ingham, S. Kienitz, and A. Ouderkirk, “ New back reflector and front film for improved efficiency of direct-lit LED backlights for LCD TV,” SID Symp. Dig. Technical paper, Vol. 38, No. 1, 2007, pp. 1236-1239.

[35]. C. Casale, D. D. Monte, L. Albani, and S. Bonfiglio,” LED Backlight System for Medical Imaging on LCD Monitors,” SID Symp. Dig. Technical paper, Vol. 38,

No. 1, 2007, pp. 306-307.

[36]. A. Masood, “Driving schemes for backlighting large-area LCD displays,” SID Symp. Dig. Technical paper, Vol. 38, No. 1, 2007, pp. 308-311.

[37]. W. Schwedler and F. Nguyen,” LED backlighting for LCD TVs,” SID Symp. Dig. Technical paper, Vol. 41, No. 1, 2010, pp. 1091-1096.

[38]. M. Zeiler, L. Plötz, W. Schwedler and H. Ott,” Highly efficient LED backlight solutions for large LCDs,” 1st Crystal Valley Conf. LCD Backlight, 2005, pp. 51-57.

[39]. T. Murai, K. Fujiwara, T. Masuda, Y. Ajichi, and T. Yamamoto,” Compensation Methods for Local-Dimming Backlights with RGB-LED,” SID Symp. Dig. Technical paper, Vol. 41, No. 1, 2010, pp. 1001-1004.

[40]. S. M. GadelRab, S. G. Chamberlain,” The source-gated amorphous silicon photo-transistor,” IEEE Trans. on Electron Devices, Vol. 44, No. 10, pp. 1789-1794, 2002.

[41]. J. D. Gallezot, S. Martin, J. Kanichi,” Photosensitivity of a-Si TFTs,” Proc. Of ASID Symp., 2001, pp. 407-410.

[42]. W.S. Lee, G.W. Neudeck, J. Choi, and S. Luan, “A Model for the temperature-dependent saturated I_D-V_D characteristics of an a-Si:H thin-film transistor” IEEE Trans. on Electron Devices, Vol. 38, No. 9, pp.2070-2074, 1991.

[43]. M. Vanecek, A. Poruba, A. Fejfar, and J. Kocka, “Direct measurement of the deep defect density in thin amorphous silicon films with the absolute constant photocurrent method,” Jap. Appl. Phys., Vol. 78, No. 10, pp.6203-6210, 1995.

[44]. T. Kruger, “On the origin of the Staebler-Wronski effect,” J. Appl. Phys., Vol. 99, No.6, p. 063509 , Mar. 2006.

[45]. L. Eglseer, S. Horvat, and H. Kroha, “Study of the long-term behavior of the

sensitivity of amorphous silicon photo detectors under illumination," European Sym. on Semiconductor Detectors, Vol.568, No. 1, Nov. 2006, pp. 18-21.

[46]. H.-S. Park, T.-J. Ha, M.-K. Han, D.-H. Woo, K.-S. Shin, and C.-W. Kim, "A new monolithic polysilicon ambient light sensor system with wide dynamic range for active-matrix displays by employing an adaptive sensitivity control method," SID Symp. Dig. Technical paper, Vol. 39, No. 1, 2008, pp. 716-719.

[47]. M. Hack, A. G. Lewis, R. H. Bruce, and R. Lujan, "Optically addressable input circuit for two-dimensional image sensing," in Proc. Mat. Res. Soc. Symp., vol. 219, 1991, pp. 167–172.

[48]. N. Tada, H. Hayashi, M. Yoshida, M. Ishikawa, T. Nakamura, T. Motai, T. Nishibe, "A touch panel function integrated LCD using LTPS technology," Proc. of IDW, 2004, pp.349-350.

[49]. H. Hayashi, T. Nakamura, N. Tada, T. Imai, M. Yoshida, and H. Nakamura, "Optical sensor embedded input display usable under high-ambient-light conditions," SID Symp. Dig. Technical paper, Vol. 38, No. 1, 2007, pp. 1105-1108.

[50]. M. Hack, A. G. Lewis, and R. H. Bruce, "Timing independent pixel-scale light sensing apparatus," U.S. Patent 5 153 420, Oct. 6, 1992.

[51]. H. Pan, X.-F. Feng, and S. Daly, "LCD motion blur modeling and analysis," in IEEE Int. Conf. on Image Process., Vol. 2, 2005, p. II-21-4.

[52]. S. Hong, B. H. Shin, T.-S. Kim, B. Berkeley, and S. S. Kim, "Advanced method for motion-blur reduction in LCDs," SID Symp. Dig. Technical paper, Vol. 36, No. 1, 2005, pp. 466-469.

簡 歷

姓名：周祿盛

性別：男

住址：高雄市三民區大順二路６４９號１４樓之１

學經歷：

國立中山大學物理系學士　　(92/9~97/6)

國立交通大學光電所碩士　　(97/9~98/7)

國立交通大學光電所博士　　(98/8~102/7)

博士論文題目：

主動陣列觸控面板與光感測器之畫素電路研究

Study on the Pixel Circuits of Active Matrix Touch Panel and Light Sensor

Publication List

1. International Journal

[1] Ya-Hsiang Tai, **Lu-Sheng Chou**, Yan-Fu Kuo, and Shao-Wen Yen, "Gap-type a-Si TFTs for backlight sensing application," IEEE J Display Tech., Vol. 7, No. 8, pp. 420-425, Aug. 2011.

[2] Ya-Hsiang Tai, **Lu-Sheng Chou**, and Hao-Lin Chiu, " Gap-type a-Si TFTs for front light sensing application," IEEE J Display Tech., Vol. 7, No. 12, pp. 679-683, Dec. 2011.

[3] Ya-Hsiang Tai, Hao-Lin Chiu, and **Lu-Sheng Chou**, " Active matrix touch sensor detecting time-constant change implemented by dual-gate IGZO TFTs," Solid-State Electronics, Vol. 72, No.15, pp. 67-72, 2012.

[4] Ya-Hsiang Tai, **Lu-Sheng Chou**, Hao-Lin Chiu, and Bo-Cheng Chen, " Three-transistor AMOLED pixel circuit with threshold voltage compensation function using dual-gate IGZO TFT," IEEE Electron Device Lett., Vol. 33, No. 3, pp. 393-395, Mar. 2012.

[5] Ya-Hsiang Tai, Hao-Lin Chiu, and **Lu-Sheng Chou**, " The deterioration of a-IGZO TFTs owing to the copper diffusion after the process of the source/drain metal formation," J Electrochemical Soc., Vol. 159, No. 5, pp. J200-J203, 2012.

[6] Ya-Hsiang Tai, Hao-Lin Chiu, **Lu-Sheng Chou**, and Chia-Hung Chang, "Boosted gain of the differential amplifier using the second gate of the dual-gate a-IGZO TFTs," IEEE Electron Device Letters, Vol. 33, No.12, Dec. 2012.

[7] Ya-Hsiang Tai, Hao-Lin Chiu, and **Lu-Sheng Chou**," Large-area capacitive active touch panel using the method of pulse overlapping detection," IEEE J Display Tech., Vol.9, No. 3, pp. 170-175, 2013

[8] Ya-Hsiang Tai, Hao-Lin Chiu, and **Lu-Sheng Chou**," Test and analysis of the

ESD robustness for the diode-connected a-IGZO thin film transistors," Accepted, IEEE J Display Tech., May 2013

2. International Conference

[1] Yan-Fu Kuo, Chin-Jung Lin, **Lu-Sheng Chou**, and Ya-Hsiang Tai," Using low temperature poly-silicon thin film transistor as oblique light sensors for 3D interaction display," *SID Symp. Dig. Technical paper*, 2010, pp. 1272-1275.

[2] **Lu-Sheng Chou**, Hao-Lin Chiu, Kuan-Ta Lin, and Ya-Hsiang Tai, "Active matrix touch sensor detecting time-constant change implemented by IGZO TFTs," *SID Symp. Dig. Technical paper*, 2011, pp. 1841-1844.

[3] **Lu-Sheng Chou**, Cheng-Ta Yang, Hao-Lin Chiu, Ya-Hsiang Tai, Isaac Chan, and Ming-Hua Yeh," Noise analysis for high resolution active matrix X-ray sensing array," *International Electron Devices and Materials Symposium (IEDMS)*, 2011, p. D2-5 **(ORAL accepted)**

[4] Ya-Hsiang Tai and **Lu-Sheng Chou**," Active matrix touch sensing pixel circuit of scan pulse overlapping detection," *International Display Manufacturing Conference (IDMC)*, 2011, p S8-04**. (ORAL accepted)**

[5] **Lu-Sheng Chou**, Hao-Lin Chiu, and Ya-Hsiang Tai," Light sensing application using gap-gate amorphous silicon TFTs," *International Photonics Conference (IPC)*, 2011 **(ORAL accepted)**

[6] **Lu-Sheng Chou**, Hao-Lin Chiu, Bo-Cheng Chen, and Ya-Hsiang Tai," Dual-gate IGZO TFT for threshold-voltage compensation in AMOLED pixel circuits," *SID Symp. Dig. Technical paper*, 2012, pp. 768-771. (**ORAL accepted)**

[7] Ya-Hsiang Tai, Hao-Lin Chiu, **Lu-Sheng Chou**, and Cheng Ming Li, "The I-V transfer characteristics of a-IGZO TFTs deteriorated owing to the copper diffusion in the process of the source/drain metal," *39th International Conference*

on Metallurgical Coatings and Thin Films (ICMCTF), 2012 (**ORAL accepted)**

[8] **Lu-Sheng Chou**, Huo-Moun Chen, Cheng-Ta Yang, Yung-Hsuan Yang, Ya-Hsiang Tai, and Ming-Hua Yeh, "High resolution active photo-sensing circuit using dual-scan compensation," *IDW/AD*, 2012, pp. 1623-1626 (**ORAL accepted**)

[9] **Lu-Sheng Chou**, Huo-Moun Chen, Bo-Cheng Chen, Jun-Yi Zhang, Ya-Hsiang Tai, Isaac Chan, and Ming-Hua Yeh, "Active photo-sensing array of thin film transistor with threshold voltage compensation," *IDW/AD*, 2012, pp. 829-832. (O**RAL accepted**)

[10] **Lu-Sheng Chou,** Chia-Hung Chang, Hua-Mao Chen, and Ya-Hsiang Tai," High input impedance active pixel sensing circuit with threshold voltage compensation implemented by dual-gate IGZO TFTs," *SID Symp. Dig. Technical paper*, 2013, pp. 1059-1061.

[11] **Lu-Sheng Chou**, Chia-Hung Chang, Chun-Yu Lin, Ya-Hsiang Tai, Bo-Wen Xiao, Heng-Yin Chen, and Ming-Hua Yeh," Two-TFT active pixel sensing circuits with threshold voltage compensating function," *International Display Manufacturing Conference (IDMC), 2013*

[12] **Lu-Sheng Chou**, Yung-Hsuan Yang, Chung-Lun Hsieh, Ya-Hsiang Tai, Bo-Wen Xiao, Heng-Yin Chen, and Ming-Hua Yeh," Noise analysis in the device and circuit levels for active matrix X-ray sensing application," *International Display Manufacturing Conference (IDMC), 2013*

3. Domestic Journal

[1] 周祿盛、戴亞翔,"應用於主動式平面顯示器之新式觸控感測技術," 電子月刊, July 2012.

4. Patent

[1] 戴亞翔、周祿盛、邱皓麟," An active touch sensing circuit apparatus," Korean Patent Application No. 10-2011-0052210